Explicit Circuit Parameter Design Methodology for Operational Amplifier Stability

JIANLONG WANG

PhD Dissertation

DIVISION OF ELECTRONICS&INFORMATICS

GRADUATE SCHOOL OF SCIENCE&TECHNOLOGY

GUNMA UNIVERSITY

JAPAN

January 2020

Explicit Circuit Parameter Design Methodology for Operational Amplifier Stability

DISSERTATION

Submitted by

JIANLONG WANG

In partial fulfillment of the requirements for the award of the degree of

DOCTOR OF PHILOSOPHY

IN

ELECTRONICS &INFORMATICS ENGINEERING

Under the guidance of

PROFESSOR HARUO KOBAYASHI, Ph. D. Eng.

DIVISION OF ELECTRONICS&INFORMATICS
GRADUATE SCHOOL OF SCIENCE&TECHNOLOGY
GUNMA UNIVERSITY
JAPAN

January 2020

Acknowledgement

I would like to express my deepest appreciation to all those who provided me the possibility to complete this dissertation. Special thanks to my supervisor Professor Dr. Haruo KOBAYASHI for his patient guidance and encouragement. Like an elder, he gave me care in life and guidance in study, and without his support, this study could not have been done properly. Not only in the study has affected me, in the outlook on life, values, the truth of life has deeply affected me, is my teacher, is also a wise man. I would like to express my gratitude to Dr. Yuji GENDAI. I was deeply impressed and respected by his profound knowledge and rigorous attitude towards research. His guidance and help to me made me deeply feel my shortcomings in professional study and encouraged me to improve and move forward. I would also like to thank my review committee members, Professors Seiji HASHIMOTO, Yusaku FUJII, Yasushi YUMINAKA and Toshiki TAKAHASHI.

I am thankful to the members of our Laboratory. Thanks to Nobukazu TSUKIJI, Kosuke MACHIDA for their valuable discussion and advice. Thanks to Junya KOJIMA, Nene KUSHITA, Yuto SASAKI, Shotaro SAKURAI, for their help in terms of adapting to Japanese life and my Japanese communication. I would also like to thank Keita KURIHARA, Yuki OZAWA as my Japanese tutor, and Mr. Nobuyoshi ISHIKAWA. They teach me Japanese language and culture.

Additionally, I would like to thank Assistant Professor Anna KUWANA for her kind assistance. Not just academically, but also for her help in procuring lab equipment. I would like to thank Kumiko TAURA and Nami SAKAGUCHI who are staffs at human resources cultivation center of Gunma University for their guidance and help in the workplace.

I also want to thank the younger Chinese in the lab for their spiritual encouragement. By helping them, I also grew.

Furthermore, I would like to thank Professor Decheng YUAN who is my master degree supervisor at Shenyang University of Chemical Technology. Under his advice, I chose to study abroad, learned advanced knowledge and broadened my horizon. So to speak, his opinion changed my life. Thanks to all the people who have helped me during my study abroad, either in study or in life no matter how much, let me feel warm in a foreign country, encourage me to continue to move forward. I would like to thank those who have given me guidance and help during my internship in various companies.

Finally, sincerely thank to my parent Yuhui WANG and Qingfang SUN, and my sisters. Thanks for their endless love that give me courage, Thanks for their patience and support during the tenure of research work.

Declaration

I hereby declare about this submission is my own work and that, to the best of my knowledge and belief, it contains no material previously or written by another person, nor material which has been accepted for the award of any other degree of the university or other institute of higher learning, except where due acknowledge has been made in the text.

Signature:
Name: JIANLONG WANG
Student NO.: T15808004
Date:

Table of content

List of Figures

List of Tables

Abbreviations

ADC	Analog-digital converter
DAC	Digital-analog converter
Opamp	Operational amplifier
R-H	Routh-Hurwitz
LPF	Low pass filter
PM	Phase margin
GM	Gain margin
MOS	Complementary Metal-Oxide-Semiconductor
LTspice	Linear Technology Simulation Program with Integrated Circuit Emphasis

Abstract

This dissertation proposes a method to derive explicit circuit parameter conditions for stability and phase margin of the operational amplifier circuit with various circuit topology. Based on the derived conditions, the circuit designer knows which parameter value should be increased and which one should be decreased to obtain its stability with enough margin. First, the small signal equivalent circuit model of the operational amplifier is derived and its transfer function is obtained. Then the Routh-Hurwitz stability criterion is applied and the explicit circuit parameter conditions for the stability are obtained, which were not obtained before. In the theoretical part, the equivalence between Nyquist and Routh-Hurwitz stability criteria under some conditions is shown. Next the relationship between parameters of Routh-Hurwitz stability criterion and phase margin of the operational amplifier are deduced. Then explicit circuit parameter conditions for the operational amplifier stability with enough margin are obtained, which are useful for operational amplifier analysis and design, and which could not have been obtained with the conventional methods. In the verification part, the above statement is confirmed with SPICE simulations at transistor level operational amplifier circuits.

In the later part of this dissertation, an additional method is proposed to obtain the open loop characteristics directly without opening up loop and not need to insert any extra circuit element. This operation is called as a closed-open conversion method to obtain the open loop characteristics with corresponding closed loop measurement. Its principle is introduced and simulation verification is shown. When this method reveals that the phase margin is not sufficient for the designed operational amplifier, some parameter values are increased or decreased based on the results obtained by the above-mentioned Routh-Hurwitz method so that its enough phase margin should be gained. In addition, we discuss the application of Nyquist plot for judging the stability which is not often used by circuit designer, including discussion on its advantages and disadvantages.

Chapter 1 introduces the research background and research objective, and the outline of this dissertation. Chapter 2 reviews control theory and introduces Nyquist stability criterion and Routh-Hurwitz stability criterion. At first, we introduce the concept of feedback control system through

practical examples, and then the transfer function and Laplace transform are also introduced in detail. Chapter 3 briefly introduces transistor circuit and small signal model of the operational amplifier. In this chapter we present detailed derivation process of the proposed criterion with application to the small signal models of the three selected amplifiers. Chapter 4 deduces respective mathematical foundations of these criteria, and the equivalency is demonstrated, and then, we deduce the relationship between Routh-Hurwitz stability criterion parameters with PM (phase margin). In Chapter 5, we select some amplifiers to verify our proposed method with theoretical analysis and SPICE simulations. In Chapter 6, we introduce an idea for obtaining the open loop characteristics from the closed loop measurement of the operational amplifier. We explain its principle and our simulations have verified the effectiveness of the proposed method by compared with the conventional methods. Chapter 7 presents some discussions, and also provides the future work. Chapter 8 summarizes conclusions obtained through this research.

CHAPTER Ⅰ INTRODUCTION

1.1 Research background and Research objective

The operational amplifier is an important circuit that plays a crucial role in analog signal conditioning. Examining the stability of operational amplifier circuits has been a concern since the negative feedback circuit was invented. The purpose of this dissertation is to use the Routh-Hurwitz stability criterion for operational amplifier stability analysis and design, to obtain explicit stability conditions for operational amplifier circuit parameters [1-4]; this has not been described in any operational design book/paper, to the best of our knowledge [5-13]. In this dissertation, we demonstrate that the respective mathematical foundations of Nyquist and Routh-Hurwitz stability criteria are equivalent, and we deduce the relationship between Routh-Hurwitz stability criterion parameter with phase margin of the operational amplifier as theoretical support and perfection for the proposed method. Then, we verify our proposed method with some amplifier models. Our SPICE simulation results show good agreements with our theoretical analysis based on the proposed method.

In the control theory field, there are many criteria for judging the stability of the feedback system [13]. For example, Nyquist stability criterion and Routh-Hurwitz (R-H) stability criterion are widely utilized. The Nyquist stability criterion is a graphical technique for determining the stability of a dynamical system, and the Bode plot and Nyquist plot which are well known and used in all application examples based on the principle of Nyquist stability criterion. In the electronic circuit design field, Bode plot for the open-loop frequency characteristic is the most frequently used by circuit designers [5-12], while Nyquist plot is occasionally used [14]. However, strangely enough, according to our survey of the related texts about analog electronic circuits [1-9], the Routh-Hurwitz method [12-14] is rarely mentioned in analysis and design of the operational amplifier stability. It seems that even some mature analog designers are not familiar with the R-H stability criterion. On this account, we have made attempts to introduce the R-H stability criterion into electronic circuit design field and begin with usage for judging stability of operational amplifier.

1.2 Outline of this dissertation

The outline of this dissertation is as follows:

Chapter1

This chapter introduces the research background and research objective in detail, and the outline of this dissertation.

Chapter 2

This chapter reviews control theory and introduces Nyquist stability criterion and Routh-Hurwitz stability criterion. At first, we introduce the concept of feedback control system through practical examples, and then the transfer function and Laplace transform are also introduced in detail.

Chapter 3

This chapter briefly introduces transistor and small signal model of the operational amplifier. In this chapter we present detailed derivation process of the proposed criterion with application to the small signal models of the three selected amplifiers.

Chapter 4

This chapter deduces respective mathematical foundations of these criteria, and the equivalency is demonstrated. We also deduce the relationship between Routh-Hurwitz stability criterion parameters with PM (phase margin).

Chapter 5

In this chapter we select some amplifiers to verify our proposed method with theoretical analysis and SPICE simulations.

Chapter 6

In this chapter we introduce a closed-open conversion method to obtain the open loop characteristics from the closed loop measurement of the operational amplifier without opening up the loop.

Chapter 7

This chapter presents discussions and also provides the future work.

Chapter 8

This chapter summarizes conclusions.

CHAPTER Ⅱ
CONTROL THEORY

Control system exists in every corner of our life, not only the automatic production line in practical industry, but also including individual human, collectivity even more the operation of the whole human society. All these can be viewed as control system. For example, our brains are constantly controlling our bodies to do what we want to do, from getting up in the morning to going to bed at night to rest.

Control system is divided into feedback control system and feed forward control system. This chapter introduces the fundamental structure, principle and classification of the feedback control system, which are extensively applied to every aspect of modern industrial society, and the stability criteria which are often used in control theory field are also introduced. Before knowing these stability criteria, related mathematical derivation is necessary so that we preparatory study transfer function and Laplace transform and so on.

2.1 Feedback control system

2.1.1 Principle and structure

Car driving is often used as an example to explain the definition of a control system. When we want to go to destination by driving a car, we will operate gear, steering wheel, throttle and brake. In this case, gear operation, brake operation and throttle operation are necessary control operations for arriving at the destination by driving the car. As one control system, the car is an object manipulated by our operation; the speed and position are physical quantities in the target which we want to change and adjust.

In the control theory field, the target is called as controlled system and the physical quantity is called as controlled variable, while the necessary operations are called as manipulated variables. While driving, we will encounter many disturbing factors, for example, traffic coming from the opposite direction, animals and pedestrians which cross the street, and wind and snow in bad weather; all of these will influence our driving, influence the control system, and these disturbing factors are called disturbance. The control system used in equipment and machinery without manual labor is called as automatic control, contrast to the manual control.

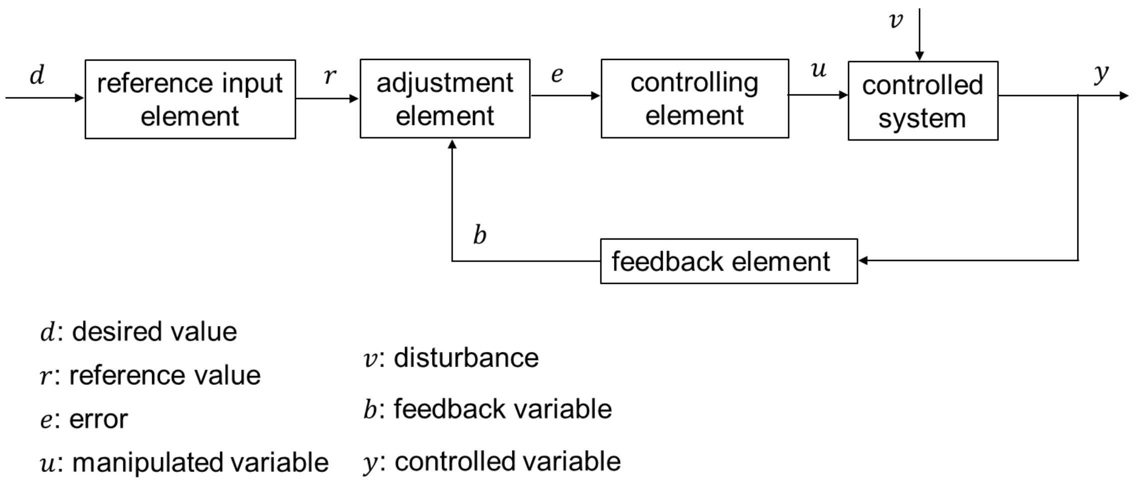

Fig. 2.1 Feedback control system

The block diagram of the feedback system which can express the relation of each element and the procession is shown in Fig. 2.1. The controlled variable that we hoped at first is called as desired value; in the driving case, it is the definition. When we want to arrive somewhere, we will plan a route whether it can be obtained by electronic navigation using internet or our memories of the past and this route is the reference value. Then the consciousness will be produced by our brain that can control our limbs to make a series of operations that are called as manipulated variable, our brain and our body is called as adjustment element and controlling element respectively. If we go the wrong way, electronic navigation or our nervous system will sense this mistake, and these perceptual actions are called detecting element which is to be included at feedback element in Fig. 2.1[15].

Based on the feedback information, our brain or electronic navigation will make a series of calculations and judgments, and at this moment error will be produced:

$$e = r - b \tag{2.1}$$

This error will be as basis for new manipulated variable production. Above consideration is the feedback control system. The corresponding relationship between driving control system and human is shown as Table. 2.1.

Table. 2.1 Corresponding relationship between driving control system and human

Control System	Human
adjustment element	brain
controlling element	limbs
detecting element	sense organ

2.1.2 Classification

At first, positive feedback and negative feedback are the most basic classification. We introduce this classification by using the feedback circuit that can amplify a voltage signal as shown in Fig. 2.2. Output voltage signal v_2 of amplifier A through attenuation F, obtains feedback signal Fv_2. Then, the sum or difference of signal Fv_2 with input voltage signal v_1 again inputs to the amplifier. This transformation can be expressed using the following equations:

$$\begin{aligned} v_2 &= Av_1 \\ v_i &= v_1 \pm Fv_2 \end{aligned} \tag{2.2}$$

Erase v_i and obtain the voltage gain:

$$G = \frac{v_2}{v_1} = \frac{A}{1 \mp AF} \tag{2.3}$$

Plus or minus sign in Eq. (2.3) is in the same order as Fig. 2.2. The condition of plus and minus shown in Fig. 2.2 is regarded as positive feedback and negative feedback respectively.

Under the positive feedback condition, the circuit will be unstable when $AF \geq 1$, so the positive feedback is not much used except for oscillator and latch circuit, whereas the negative feedback is often used in amplifier circuit. By using the negative feedback technology, many performance improvements can be made in amplifiers, such as suppression of gain fluctuation, expansion of frequency band and reduction of noise and distortion.

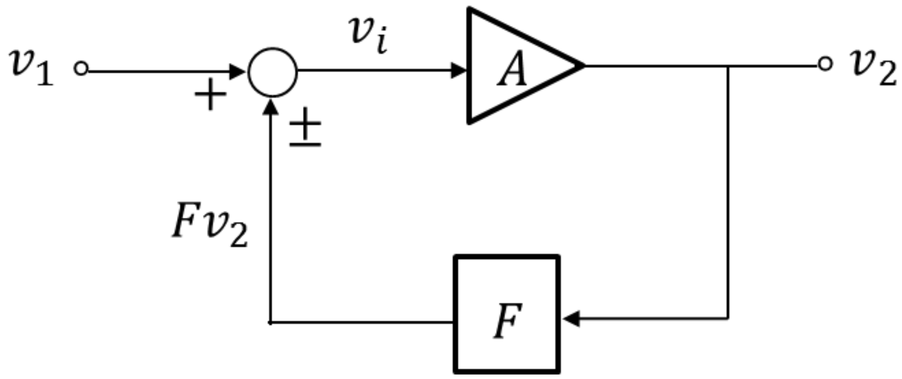

Fig. 2.2 Feedback circuit

In the control system, adjustment element corresponds to the human brain, and in this element, analog mode calculation or digital mode calculation is processed. Based on the process mode, the control system can be classified into analog control and digital control. As we know, only finite word length operation such as 16 bits can be processed in the microprocessor of digital control, so we must use an analog-digital-converter (ADC) for transforming analog quantity into digital quantity at digital control. Conversely, the digital quantity must be transformed into analog quantity by a digital- analog-converter (DAC) for being used as manipulated variable [16].

Before 1960 year, the control theory which is called as classical control theory mainly based on the transfer function method. In the classical control, we make Laplace transform to a linear differential equation which expresses the characteristics of the control system, and the one input-one output form the linear time-invariant system where system parameters are invariable regardless of time as the control system. The control element focuses only on the input and output of the control object, but it does not consider the internal state, and regards it as a black box. Frequency response method is well used in the classical control.

Since 1960, in order to control an artificial satellite with high precision and following the appearance of movement which can be expressed by a dynamic system using a state vector, new control theory which is called as modern control theory appeared. The modern control theory based on the state section that departs from expressing by a state equation and an output equation, and can correspond to multiple input multiple output form multivariable system. Not only linear time-invariant system, but also time-variant system and nonlinear system can be handled. In addition to the input and output of the system, the control element also includes state variables that represent the internal state of the system at each time, and it is possible to perform an evaluation analysis on the internal state of the system.

Table. 2.2 Main differences between classical control and modern control

Item	Classic control	Modern control
Controlled object	One input-one output form Linear time-invariant system	Multiple input-multiple output form Linear time-invariant system Time-variant system Nonlinear system
Design & analysis domain	Frequency domain	Time domain
Mathematical model	Transfer function	State function
Control element	Only input and output of control target	Multi-input and Multi-output of control target, Internal state

Classical control theory and modern control theory own their respective advantages; the former has rapidity and easy to operate or calculate, whereas the later can statement and dispose the complex system. Furthermore, due to the rapid spread of microcomputers in recent years, the theory is further developing greatly. The main differences between classical control and modern control are shown as in Table. 2.2.

In later chapters, we will talk about Routh-Hurwitz stability criterion and Nyquist stability criterion which belongs to the classical control theory.

2.2 Transfer function

2.2.1 Composition of block diagram

The composition of block diagram includes signal, block, calculation and branch. We will introduce these composition elements in turn.

- Signal and block

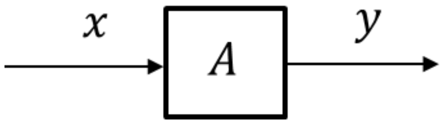

Fig. 2.3 Signal and block

The variables are shown in Fig. 2.3, where x is input signal, y is output signal, and the output signal is the input signal's A multiples. In other words, this symbol can be express relation as the following:

$$y = Ax \tag{2.4}$$

Signal is expressed as arrow, the relation between two signals is expressed as a box. In comparison with Eq. (2.4), Fig. 2.3 can clearly express the relation between input signal and output signal, and which is the input signal and which is output signal also can be identified obviously.

- Calculation

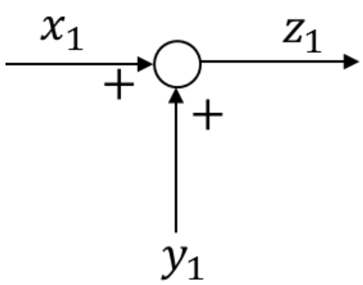

Fig. 2.4 Addition symbol

The addition symbol as shown in Fig. 2.4, can express the processing, or two signals addition into one signal and output, and this relationship also can be expressed as the following equation:

$$x_1 + y_1 = z_1 \tag{2.5}$$

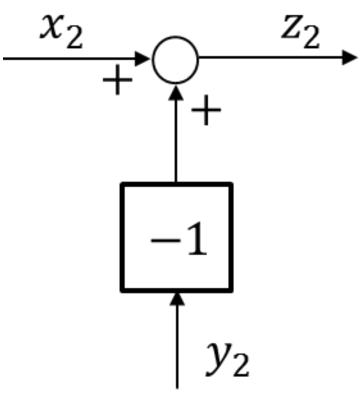

Fig. 2.5 Block diagram of Eq. (2.4)

Using the addition symbol as shown in Fig. 2.5, we can also express the processing that two signals is transformed into one signal by subtraction calculation, and the corresponding expression equation is shown as following:

$$x_2 - y_2 = z_2 \tag{2.6}$$

But in practical applications, we usually use the subtraction symbol to express the subtraction calculation directly as shown in Fig. 2.6 after simplification.

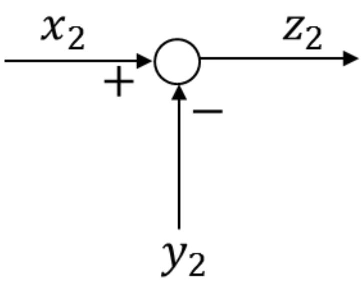

Fig. 2.6 Subtraction symbol

- Branch

As shown in Fig. 2.7 (a), when the signal is needed into two-addition point, or the condition in Fig. 2.7 (b), signal need into branch for other process such as observation. These symbols are called as a branch symbol.

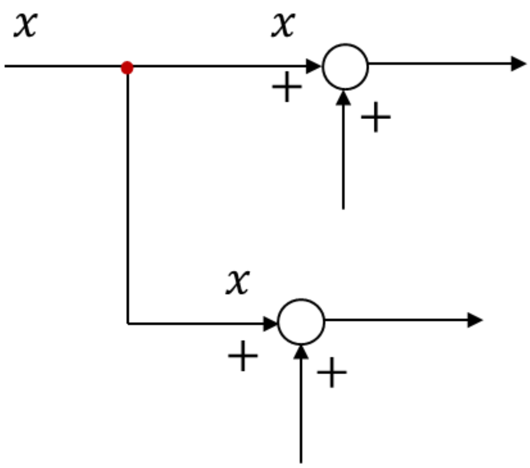

(a)

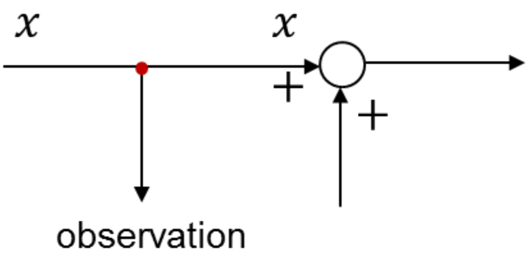

(b)

Fig. 2.7 Branch symbol

The diagram which combines above introduced signals, blocks, calculations and branches, is called as a block diagram.

2.2.2 Differential equation and transfer function

The operation of each system in the electrical circuit, mechanical system, and thermal system is a phenomenon that is completely different from each other, and there is no relation between them. However, if we abstract the various quantities that appear in these and view it as a mere signal conversion process, these phenomena are all expressed by differential equations of the same form. Take a first-order transfer element for example, which can describe rotating motion, thermal system and electric circuit. Its differential equation of the first transfer element is given by:

$$\frac{dy(t)}{dt} = ay(t) + bx(t) \tag{2.7}$$

In Eq. 2.7, $x(t)$is the input applied to the system from the outside, and $y(t)$ is the resulting system state. If we want to directly solve differential equation that like Eq. (2.7), complex procedure is required and the general solution is:

$$y(t) = y(0)e^{at} + \int_0^t be^{a(t-\tau)}x(\tau)d\tau \tag{2.8}$$

The second term of the equation is the convolution integral. All the inputs $x(\tau)(0 \leq \tau \leq t)$ from the past to the current time are involved in the state $y(t)$ at the current time t. However, a weight corresponding to the elapsed time $t - \tau$ from that time is applied to $u(\tau)$ at the past time τ.

Input sine wave $x(t)$ into the first-order transfer element as shown in Eq.2.7 can be expressed as follows:

$$x(t) = |X|\sin(\omega t + \varphi) = \frac{1}{2}\left\{Xe^{j\omega t} + \bar{X}e^{-j\omega t}\right\} \tag{2.9}$$

Here, $X = |X|e^{j\varphi}$ is a complex quantity that can express amplitude and phase, $\bar{X}$ is conjugate complex quantity of X.

After enough time, the output signal will only include sine wave which has the same angular frequency with the input signal:

$$y(t) = \frac{1}{2}\left\{Ye^{j\omega t} + \bar{Y}e^{-j\omega t}\right\} \tag{2.10}$$

Substitute Eq. (2.9) and Eq. (2.10) into Eq. (2.7) and we have as follows:

$$j\omega Ye^{j\omega t} - j\omega\bar{Y}e^{-j\omega t} = a\left(Ye^{j\omega t} + \bar{Y}e^{-j\omega t}\right) + b\left(Xe^{j\omega t} + \bar{X}e^{-j\omega t}\right) \tag{2.11}$$

Because they are equal on both sides, we can obtain:

$$j\omega Y = aY + bX \tag{2.12}$$

Organize Eq. (2.12), and we can obtain expression function of the element as follows:

$$Y = \frac{b}{j\omega - a} X \tag{2.13}$$

As shown in Fig. 2.8, the input signal $x(t)$ into this transfer element and the output signal $y(t)$, frequency transfer function is as follows:

$$G(j\omega) = \frac{b}{j\omega - a} \tag{2.14}$$

At the dynamic system, $G(j\omega)$ is the complex quantity and various following with the input signal, and in general it is function of $j\omega$. About the calculation method of the frequency transfer function, used the function which can express the characteristic of the system, and mechanically instead of d/dt into $j\omega$ is satisfied. Not only the first-order linear stationary system, the high order system also can use this thinking method about frequency transfer function.

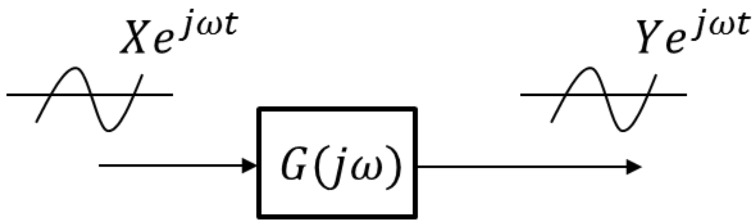

Fig. 2.8 Frequency response

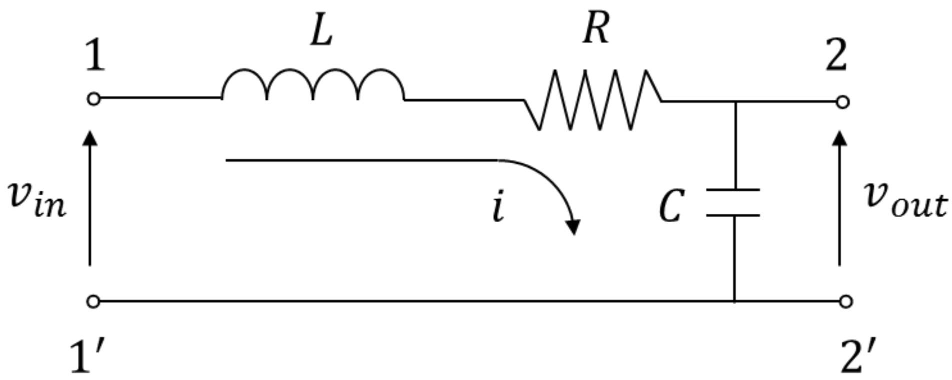

Fig. 2.9 Four-terminal network

As a specific example, Fig. 2.9 shows the four-terminal network, the input any voltage v_{in} to the terminal $11'$ and the output voltage v_{out}, the following differential equations setup:

$$v_{out} = L\frac{di}{dt} + Ri + \frac{1}{C}\int idi$$

$$v_{in} = \frac{1}{C}\int idi \tag{2.15}$$

If the input voltage is a sine wave and its angular frequency is ω, we have

$$v_{out} = j\omega Li + Ri + \frac{1}{j\omega C}i$$

$$v_{in} = \frac{1}{j\omega C}i \tag{2.16}$$

Therefore,

$$\frac{v_{out}}{v_{in}} = \frac{1}{1+j\omega RC-\omega^2 LC} \tag{2.17}$$

Eq. (2.17) can express the voltage transformation characteristic of this four-terminal network. In general control system, not only voltage and current signal can be handled, there are many other type control systems, for example, temperature, pressure, speed and displacement control system.

Different types of transformation characteristics are also very much, the input side and the output side, that is, the dimensions are often different. In these conditions, the transformation characteristic generic name is given as transfer function. In Fig. 2.9, the transfer function of voltage to voltage is:

$$G(j\omega) = \frac{v_{out}}{v_{in}} = \frac{1}{1 + j\omega RC - \omega^2 LC} \tag{2.18}$$

The first term of Eq. (2.8) shows the influence of the initial value $y(0)$ of the state quantity y on the subsequent time. The second term means the change that the input $x(t)$ gives to x. If $a < 0$, the first term decays with time, and only the second term remains after sufficient time. If the influence of the initial value can be ignored, Eq. (2.7) can be written as:

$$Y(s) = \frac{b}{s-a} U(s) \tag{2.19}$$

Focusing on only the component of the output $y(t)$ that is directly influenced by the input $x(t)$, the ratio of both Laplace transforms is taken and defined as the transfer function of this element.

$$G(s) = \frac{Y(s)}{X(s)} = \frac{b}{s-a} \tag{2.20}$$

This transfer function can be obtained only set s in place of d/dt in the original differential equation. Moreover, the frequency transfer function $G(j\omega)$ can be obtained by setting $j\omega$ instead of s in $G(s)$.

For example, let the input voltage be $x(t)$ and the output voltage be $y(t)$ in the circuit of Fig.2.9. Then, since the current flowing through the capacitor becomes $i = C\, dy(t)/dt$ and also the current flowing through the capacitor, the back electromotive force of the capacitor becomes $L\, di/dt = LC\, d^2y(t)/dt^2$. Therefore,

$$LC \frac{d^2y(t)}{dt^2} + RC \frac{dy(t)}{dt} + y(t) = x(t) \tag{2.21}$$

Here, under the initial condition y (residual voltage of the capacitor) and $y^{(1)}(0)$, if both sides are Laplace transformed and arranged in the same manner as the previous item, the following equation can be obtained:

$$Y(s) = \frac{(sLC + RC)y(0) + LC\, y^{(1)}(0)}{LCs^2 + RCs + 1} + \frac{1}{LCs^2 + RCs + 1}X(s) \tag{2.22}$$

The first term in the above equation affects the output of the initial value, and the second term represents the portion where the input affects the output, and it can be seen that the superposition theory holds for both. Especially when the initial values are all zero, we have the following:

$$Y(s) = \frac{1}{LCs^2+RCs+1}X(s) \tag{2.23}$$

The input / output relationship is represented by the block diagram of Fig. 2.10. Therefore, it can be said that the block diagram shows the input / output ratio in the Laplace transform region when all the initial values in the system are considered to be zero.

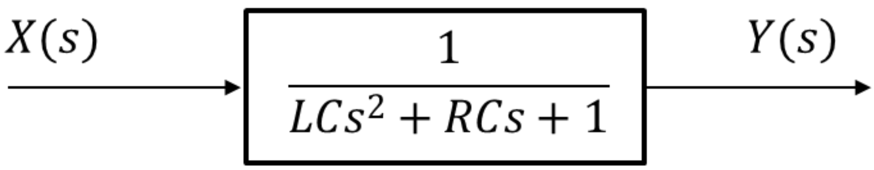

Fig. 2.10 Block diagram of $\boldsymbol{LCR}$ circuit

In a circuit using a capacitor or an inductor, the voltage-current characteristic is expressed by a differential equation. Therefore, in order to obtain the response of the circuit, it is necessary to solve the differential equation. The Laplace transform converts a time domain function into a complex frequency domain function, and the Laplace transform converts the differential equation into an algebraic equation. Once Laplace transform is performed, not only the time response but also the frequency response can be easily obtained. It is also possible to determine the stability of the system from the position of the poles of the transfer function.

2.2.3 Laplace transform

As described in the previous section, the solving differential equation requires complicated calculation. However, if it is limited only to the steady state response to the sinusoidal input as described in the previous section, it can be easily solved by the method of AC theory regardless of any frequency value.

Input for any waveform, and without solving the differential equation, whether the method that finds out the solution of differential equation is not? If $x(t)$ only has one frequency, we can use Fourier transform to expand $x(t)$. It can be decomposed into fundamental wave and each high harmonic component, and then calculate the corresponding output of each high harmonic with the frequency transfer function, and at last synthesize these outputs. But when we use the Fourier transform, depending on the waveform of x, it may be difficult to determine the integral value.

To overcome above trouble and question, we select to use Laplace transform for applying to wider range of input signal wave. Laplace transform is also an integral transform named after its discoverer Pierre-Simon Laplace. It takes a function of a real variable t (often time) to a function of a complex variable s (complex frequency). The Laplace transform is very similar to the Fourier transform, but the former is more complicated than the later. While the Fourier transform of a function is a complex function of a real variable (frequency), the Laplace transform of a function is a complex function of a complex variable. Laplace transforms are usually restricted to functions of t with $t \geq 0$. A consequence of this restriction is that the Laplace transform of a function is a holomorphic function of the variable s.

The Laplace transform is invertible on a large class of functions. The inverse Laplace transform takes a function of a complex variable s (often frequency) and yields a function of a real variable t (time). Given a simple mathematical or functional description of an input or output to a system, the Laplace transform provides an alternative functional description that often simplifies the process of analyzing the behavior of the system, or in synthesizing a new system based on a set of specifications [17]. So, for example, Laplace transformation from the time domain to the frequency domain transforms differential equations into algebraic equations and convolution into multiplication [18].

Laplace transform has many applications in the sciences and technology. At electronic circuit design field, since the voltage-current characteristics are represented by differential equations in circuits using capacitors and inductors, so it is necessary to solve the beautiful sentence equation in order to obtain the response of the circuit. Once Laplace transform is performed, not only the time response but also the frequency response can be easily obtained. It is also possible to judge the stability of the system from the position of the pole of the transfer function. The Routh-Hurwitz method is based on the characteristics equation of transfer function that in s field.

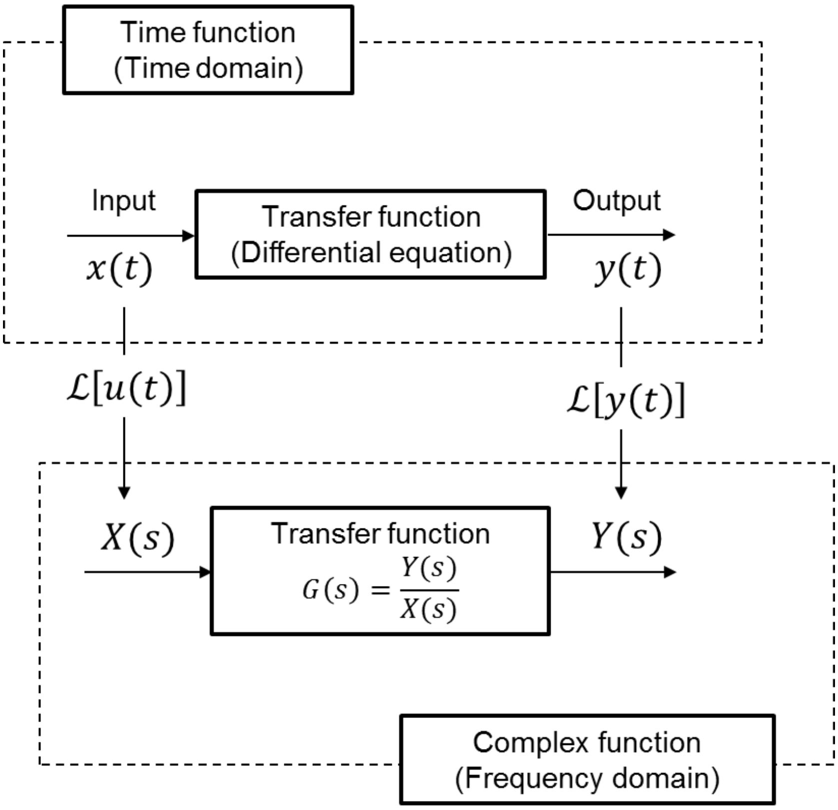

Fig. 2.11 Input / output relationship by transfer function

From frequency transfer function Eq. (2.14), Laplace transform uses s, instead of $j\omega$, which is not limited to pure imaginary numbers and extends it to multiple general areas.

$f(t)$ is one function of time t, using complex number s as operator, and rewrite as follows:

$$F(s) = \int_0^\infty f(t)e^{-st}dt \tag{2.24}$$

$F(s) = \mathcal{L}[f(t)]$ is called as Laplace transform of $f(t)$, and is written as:

$$F(s) = \mathcal{L}[f(t)] \tag{2.25}$$

Inverse Laplace transform returns $F(s)$ into time function:

$$f(t) = \mathcal{L}^{-1}[F(t)] = \frac{1}{2\pi j}\int_{c-\infty}^{c+\infty} F(s)e^{st}ds \tag{2.26}$$

The condition of Laplace transform existence is that $f(t)$ must be a monovalent function at $t \geq 0$ area. That is to say, there is a real number σ_0 that makes the following formula true:

$$\int_0^\infty |f(t)|e^{-\sigma_0 t}dt < \infty \tag{2.27}$$

However, this condition is always satisfied whichever control system that physically exists. The parameter c in Eq. (2.26) is one real number which is much bigger than σ_0.

1. Unit step function

The unit step function $u(t)$ which is shown as in Fig. 2.12, is always used when closing the switch in a certain circuit system for applying a constant voltage at electronic circuit filed.

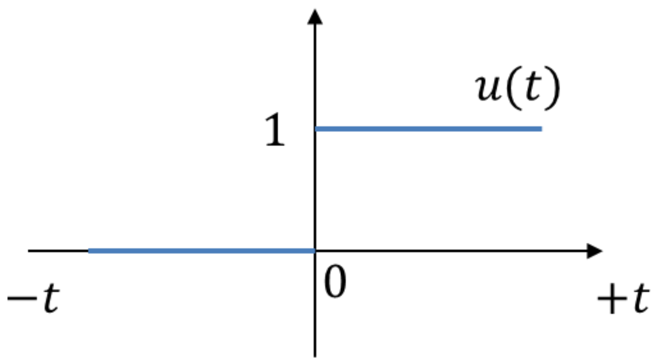

Fig. 2.12 Unit step function

Unit step function is defined as follows:

$$u(t) = \begin{cases} 1, & t \geq 0 \\ 0, & t < 0 \end{cases} \tag{2.28}$$

The corresponding Laplace transform is as follows:

$$U(s) = \mathcal{L}[u(t)] = \int_0^\infty u(t)e^{-st}dt = \int_0^\infty 1 \cdot e^{-st}dt = [-\frac{1}{s}e^{-st}]_0^\infty =$$

$$= \lim_{t\to\infty}\left(-\frac{1}{s}e^{-st}\right) + \frac{1}{s} = \frac{1}{s} \tag{2.29}$$

2. Unit impulse function

Unit impulse function $\delta(t)$ is always used for solving system's function that can express the inherent properties of the system.

$$\delta(t) = \begin{cases} \infty, & t = 0 \\ 0, & t \neq 0 \end{cases}, \qquad \int_0^\infty \delta(t)dt = 1 \tag{2.30}$$

Use Eq. (2.24):

$$\delta(s) = \mathcal{L}[\delta(t)] = \int_0^\infty \delta(t)e^{-st}dt = 1 \tag{2.31}$$

3. Exponential function

Using Eq. (2.24) for the Laplace transform of exponential function e^{at}:

$$F(s) = \mathcal{L}[e^{\alpha t}]$$

$$= \int_0^\infty e^{\alpha t} e^{-st} dt \quad = \int_0^\infty e^{-(s-\alpha)t} dt = [-\frac{1}{s-\alpha} e^{-(s-\alpha)t}]_0^\infty = \frac{1}{s-\alpha} \quad (2.32)$$

Laplace transform of exponential function is important and used to find solutions to differential equations. At the processing of sine wave or cosine wave Laplace transform, Laplace transform of the exponential function is also used after using Euler's formula to transform the sine wave or cosine wave.

4. Sine wave function and cosine wave function.
   Using Euler's formula to transform the cosine wave function and sine wave function.

$$e^{\pm j\omega t} = cos\omega t \pm jsin\omega t \quad (2.33)$$

$$cos\omega t = \frac{e^{j\omega t} + e^{-j\omega t}}{2}, sin\omega t = \frac{e^{j\omega t} - e^{-j\omega t}}{2j} \quad (2.34)$$

So, we can obtain the Laplace transform of cosine wave and sine wave:

$$\cos(s) = \mathcal{L}[cos\omega t] = \frac{1}{2}\left(\frac{1}{s-j\omega} + \frac{1}{s+j\omega}\right) = \frac{s}{s^2+\omega^2} \quad (2.35)$$

$$\sin(s) = \mathcal{L}[sin\omega t] = \frac{1}{2j}\left(\frac{1}{s-j\omega} - \frac{1}{s+j\omega}\right) = \frac{\omega}{s^2+\omega^2} \quad (2.36)$$

5. Integral
   Laplace transform of first order integral:

$$K(s) = \mathcal{L}\left[\frac{df(t)}{dt}\right] = sF(s) - f(0) \quad (2.37)$$

Laplace transform of second-order integral and third-order integral:

$$\mathcal{L}\left[\frac{d^2f(t)}{dt^2}\right] = s^2F(s) - sf(0) - f'(0) \quad (2.38)$$

$$\mathcal{L}\left[\frac{d^3 f(t)}{dt^3}\right] = s^3F(s) - s^2 f(0) - sf'(0) - f''(0) \qquad (2.39)$$

Laplace transform of nth-order integral:

$$\mathcal{L}\left[\frac{d^n f(t)}{dt^n}\right] = s^nF(s) - \sum_{k=1}^{n} s^{n-k}\, f^{n-k} \qquad (2.40)$$

6. Differential
   Laplace transform of differential:

$$K(s) = \mathcal{L}\left[\int_{-\infty}^{t} f(t)dt\right] = \frac{F(s)}{s} + \frac{q(0)}{s} \qquad (2.41)$$

Here, $q(0) \equiv [\int_{-\infty}^{t} f(t)dt]_{t=0}$.

7. Time delay wave
   $k(t)$ is the one time wave that from wave $f(t)$ after T time delay:

$$k(t) = g(t-T)u(t-T) \qquad (2.42)$$

The Laplace transform of $k(t)$ is as the following:

$$K(s) = \mathcal{L}[k(t)] = \int_{0}^{\infty} g(t-T)u(t-T)e^{-st}dt = e^{-sT}F(s) \qquad (2.43)$$

This transform is the connection bridge between time continuous analog signal with time discretion digital signal, so its applicability is very important.

Table. 2.3 Laplace transform of typical functions

Function name	$f(t)$ $f(t) = 0, \text{at } t < 0$	$F(s) = \mathcal{L}[f(t)]$
Unit step function	$u(t)$	$\frac{1}{s}$
Unit impulse function	$\delta(t)$	1
Exponential function	$e^{\mp\alpha t}$	$\frac{1}{s \pm \alpha}$
	$te^{-\alpha t}$	$\frac{1}{(s+\alpha)^2}$
Sine wave function	$sin\omega t$	$\frac{\omega}{s^2+\omega^2}$
Cosine wave function	$cos\omega t$	$\frac{s}{s^2+\omega^2}$
	$e^{-\alpha t}sin\omega t$	$\frac{\omega}{(s+\alpha)^2+\omega^2}$
	$e^{-\alpha t}cos\omega t$	$\frac{s+\alpha}{(s+\alpha)^2+\omega^2}$

2.2.4 Basic element transfer characteristics

Simply loop block diagram of feedback linear system is shown as Fig. 2.13. $G(j\omega)$ and $H(j\omega)$ are transfer functions of transfer element and feedback element respectively.

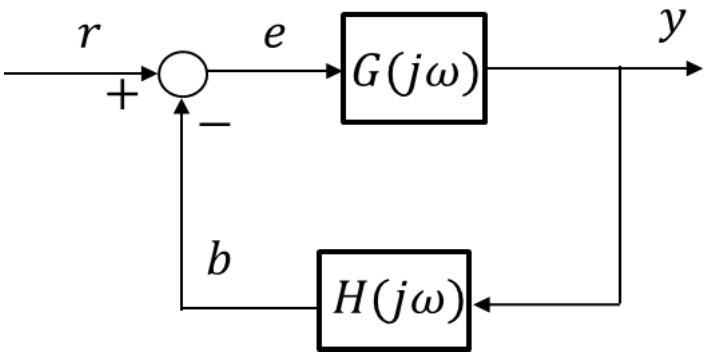

Fig. 2.13 First-order lag element

In the feedback amplifier condition, the transfer function is as follows:

$$\frac{Y(j\omega)}{R(j\omega)} = \frac{G(j\omega)}{1+G(j\omega)H(j\omega)} \tag{2.44}$$

Here, $G(j\omega)$ and $H(j\omega)$ are frequency spectrum of the controlled variable $y(t)$ and the reference value $r(t)$ respectively.

In the feedback control system, there are proportional element, integral element, differential element, first-order lag element, second-order lag element and dead time element as shown in Table. 2.4.

Table. 2.4 Basic elements of transfer function

Transfer function element name	Transfer function
Proportional element	$G(s) = K$
Differential element	$G(s) = T_D s$
Integral element	$G(s) = \dfrac{1}{T_I s}$
First order lag element	$G(s) = \dfrac{K}{1 + Ts}$
Second order lag element	$G(s) = \dfrac{K'}{s^2 + as + b}$
(Standard type)	$G(s) = \dfrac{K\omega_n^2}{s^2 + 2\zeta\omega_n + \omega_n^2}$
Dead time element	$G(s) = e^{-sL}$

In automatic control and negative feedback circuits, responses to step wave and impulse wave are important. These responses are called unit step response and impulse response. The unit step response is sometimes called the indicial response. In this section, we will introduce first-order lag element, second-order lag element and dead time element, and their response for corresponding input signal.

1, First-order lag element

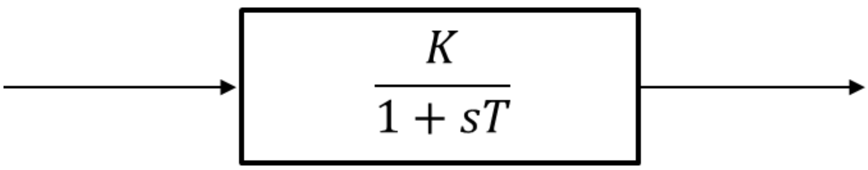

Fig. 2.14 First-order lag element

As shown in Fig. 2.14, an element having a transfer function whose denominator is a linear expression with respect to s is referred to as a first-order lag element. This transfer function itself is called a first-order lag transfer function. When the first-order lag transfer function is expressed in the form shown in Fig.2.14, K is called a gain constant and T is called a time constant.

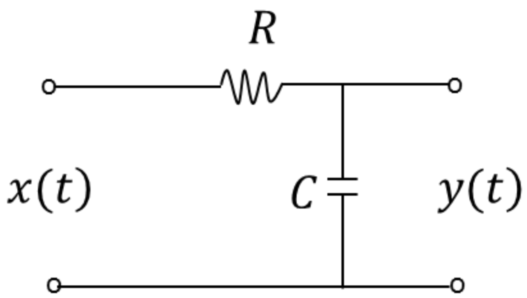

Fig. 2.15 $\boldsymbol{RC}$ integration circuit

As shown in Fig.2.15, a circuit that includes only a resistor and a capacitor or a resistor and an inductor, and does not include the capacitor and the inductor at the same time is a first-order lag system. The unit step response of this circuit is:

$$y(t) = \mathcal{L}^{-1}\left[\frac{1}{s} * G(s)\right] = \mathcal{L}^{-1}\left\{\frac{K}{s(1+Ts)}\right\} = K\left(1 - e^{-\frac{t}{T}}\right) \qquad (2.45)$$

The waveform of step response and impulse response are shown in Fig.2.16. The time constant T is a parameter indicating the speed of response. At step response, a time constant is given by extending the slope of the response waveform at time zero as it is and intersecting the final value. The response waveform at this time is becoming $1 - 1/e = 0.63$, which is the final value. In the circuit shown in Fig.2.16 (a) T is equal to RC. At the first-order lag system, there are no vibration components generated.

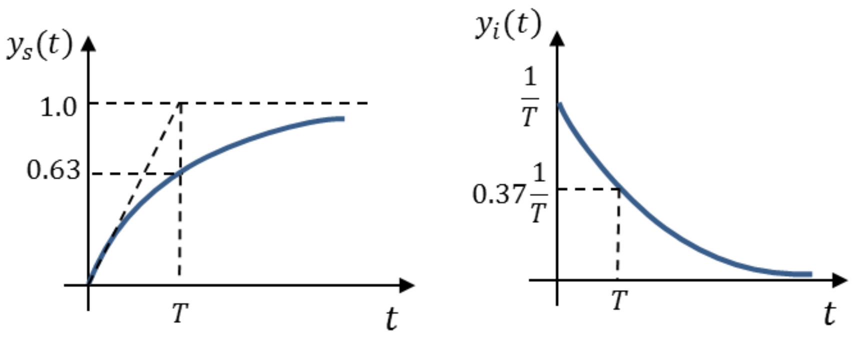

(a) Step response (b) Impulse response

Fig. 2.16 Transient response of first-order lag element

2， Second-order lag element

As mentioned in the previous section, the circuit as shown in Fig. 2.9 is one second-order lag element, and its frequency transfer function and transfer function be expressed as Eq. (2.18) and Eq. (2.23) respectively. In general, the transfer function of the quadratic element can be written as:

$$G(s) = \frac{K\omega_n^2}{s^2+2\zeta\omega_n+\omega_n^2} \tag{2.46}$$

Here, $\omega_n$is called natural frequency, and ζ is called damping factor. Its characteristic equation is $s^2 + 2\zeta\omega_n + \omega_n^2 = 0$, and its roots are $p_1 = p_2 = \left(-\zeta \pm \sqrt{\zeta^2 - 1}\right)\omega_n$. Therefor the unit step response is given by

$$y(t) = \mathcal{L}^{-1}\left\{\frac{K\omega_n^2}{s(s-p_1)(s-p_2)}\right\} \tag{2.47}$$

Calculated as Laplace inverse transform, and the unit step response is classified as follows, according to the damping factor ζ:

- $\zeta > 1$ (p_1 and p_2 are different real roots)

$$y(t) = 1 - e^{-\zeta\omega_n t}\frac{\sinh(\sqrt{\zeta^2 - 1}\omega_n t + \gamma)}{\sqrt{\zeta^2 - 1}}$$

$$\gamma = tanhh^{-1}\frac{\sqrt{\zeta^2-1}}{\zeta} \tag{2.48}$$

- $\zeta = 1$ (p_1 and p_2 are double roots)

$$y(t) = 1 - (1 + \omega_n t)e^{-\omega_n t} \tag{2.49}$$

- $\zeta < 1$ (p_1 and p_2 are complex conjugate roots)

$$y(t) = 1 - e^{-\zeta\omega_n t}\frac{\sinh(\sqrt{\zeta^2 - 1}\omega_n t + \phi)}{\sqrt{\zeta^2 - 1}}$$

$$\phi = tan^{-1}\frac{\sqrt{\zeta^2-1}}{\zeta} \tag{2.50}$$

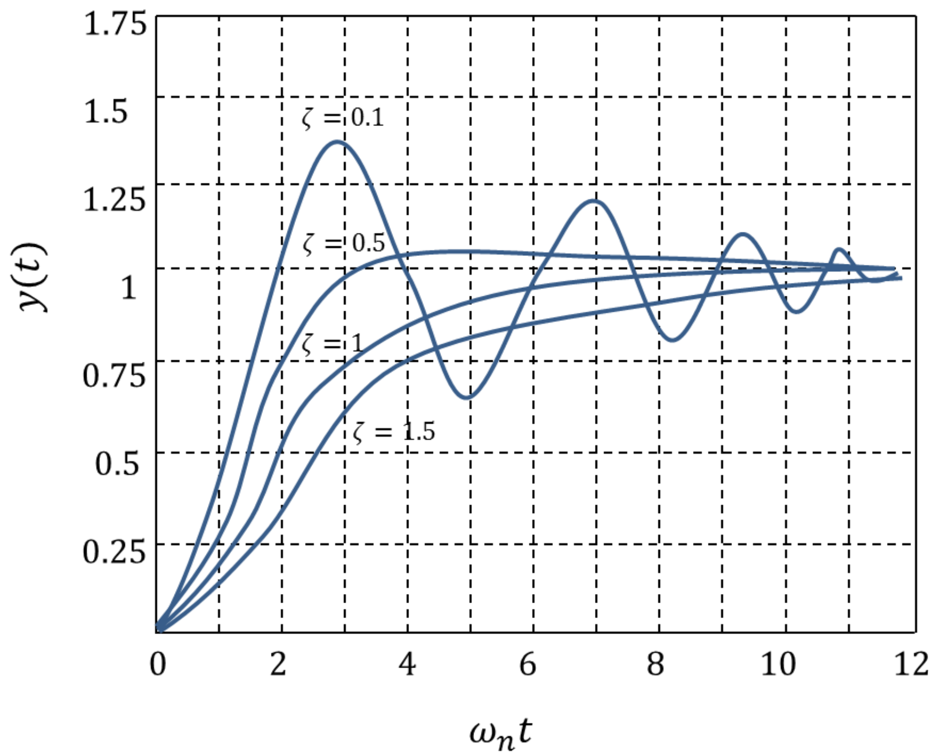

Fig. 2.17 Unit step response waveform of the second-order lag system

Fig.2.17 shows the response waveform when $\omega_n t$ is the horizontal axis and the damping factor ζ is a parameter. If the value of ζ is small, the waveform shows oscillation which is difficult to converge. On the other hand, if it is too large, the response becomes slow and it takes time to converge. Therefore, it can be seen that the attenuation coefficient is an important parameter in designing the system. Generally, in order to improve settling it is often set to about $\zeta \approx 0.7$.

3. Dead time element

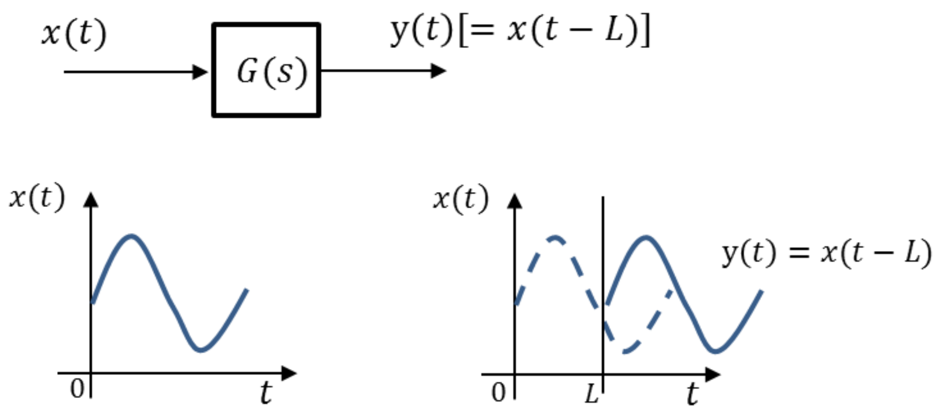

Fig. 2.18 Dead time element

As shown in Fig.2.18, an element that generates $y(t) = e(t - L)$ as an output signal when $x(t)$ is added as an input signal is referred to as a dead time element. Let us find the transfer function $G(s)$ of the dead time element. If the Laplace transform $X(s)$ of the input signal $x(t)$ is:

$$X(s) = \int_0^{\infty} e(t)e^{-st}dt \tag{2.51}$$

Then the Laplace transform $Y(s)$ of the output signal $y(t)$ is obtained as follows:

$$Y(s) = \int_0^{\infty} y(t)e^{-st}dt = e^{-sL}X(s) \tag{2.52}$$

Here, taking the ratio of the input and output signals, the transfer function

$G(s)$ is obtained as follows:

$$G(s) = e^{-sL} \tag{2.53}$$

2.3 Stability criterion

2.3.1 Conditions for stability

It is effective to have a closed loop as shown in Fig.2.1 in order to reduce the influence of fluctuations in parameters of the control target and control device or various disturbances entering each part and to reduce the control deviation. When the initial values of all integral elements included in such a feedback control system may be regarded as 0, it is convenient to analyze using a transfer function. Consider a system in Fig.2.19.

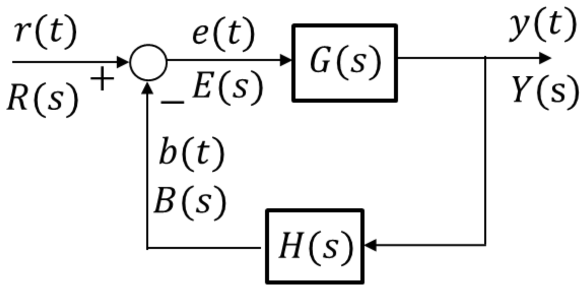

Fig. 2.19 Unit step function

If the transfer function of the forward transfer path is $G(s)$, the transfer function of the feedback circuit is $H(s)$, and the Laplace transform of the reference amount $r(t)$, the control amount $y(t)$, the deviation $e(t)$, and the feedback amount $b(t)$ are $R(s), Y(s), E(s),$ and $B(s)$ respectively. Then the following relational expression is obtained:

$$Y(s) = G(s)E(s) \tag{2.54}$$
$$E(s) = R(s) - B(s) \tag{2.55}$$
$$B(s) = H(s)Y(s) \tag{2.56}$$

Substituting Eq. (2.55) and Eq. (2.56) into Eq. (2.54), we have

$$Y(s) = G(s)R(s) - G(s)H(s)Y(s) \tag{2.57}$$

Therefore,

$$Y(s) = \frac{G(s)}{1+G(s)H(s)} R(s) \tag{2.58}$$

And then set:

$$W(s) = \frac{G(s)}{1+G(s)H(s)} \tag{2.59}$$

Then we have:

$$Y(s) = W(s)R(s) \tag{2.60}$$

$W(s)$ is the combined transfer function for the closed loop, and it is called the closed loop transfer function. On the other hand, $G(s)H(s)$ is a transfer function along the loop from one end of the cut to the other end when it is assumed that the cut is made somewhere in the loop, and $G(s)H(s)$ is called open loop transfer function.

When a finite arbitrary input is added to the control system, this system is said to be stable if its output is always rooted. If the inverse transformation of the closed-loop transfer function $W(s)$ expressed by Eq. (2.60) is $\omega(t)$, then the necessary and sufficient condition for $y(t)$ to be finite for any finite $r(t)$ is:

$$\int_0^\infty |y(t)| dt = finite \tag{2.61}$$

Let us consider this condition in the s region. In Eq. (2.60), assuming that the poles of $W(s)$ and $R(s)$ are all different from each other and if we put them into $p_1, p_1, \cdots\cdots, p_n$ and $q_1, q_2, \cdots\cdots, q_n$, then it can be expanded into the following form:

$$Y(s) = K_0 + \sum_{i=1}^{n} \frac{K_i}{s-p_i} + \sum_{j=1}^{r} \frac{K_j'}{s-q_j} \tag{2.62}$$

Apply inverse Laplace transform and return to the time domain:

$$y(t) = K_0\delta(t) + \sum_{i=1}^{n} K_i e^{p_i t} + \sum_{i=1}^{r} K_j' e^{q_j t} \tag{2.63}$$

When p_i or q_j is a real number, and if these are positive, $e^{p_i t}$ or $e^{q_j t}$ increases with time and eventually becomes infinite as shown in Fig. 2.20. If it is negative, it gradually decreases with time and eventually approaches zero.

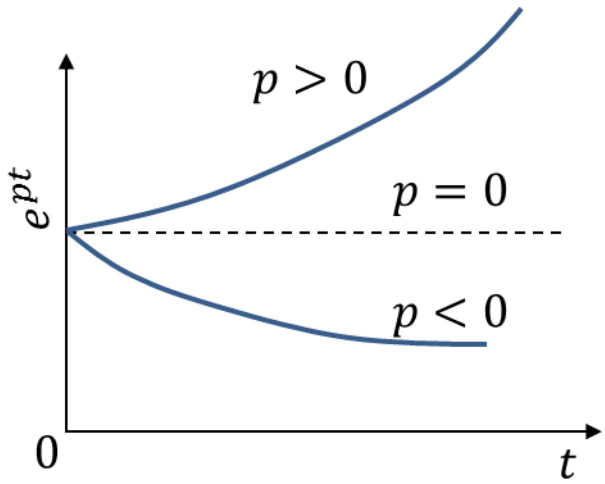

Fig. 2.20 Case of with real number pole $\boldsymbol{p}$

When p_i or q_j is a complex number, and if it is divided into a real part and an imaginary part and set to $\alpha + j\beta$, since the complex pole must be a conjugate pair, $\alpha - j\beta$ is another pole. A combination of the terms $\alpha + j\beta$ and $\alpha - j\beta$ makes the system oscillatory as shown in Fig. 2.20, and if the real part α is positive, the amplitude gradually increases with time as shown in Fig. 2.21 (a), whereas if α becomes negative, it gradually attenuates as shown in Fig. 2.21 (b).

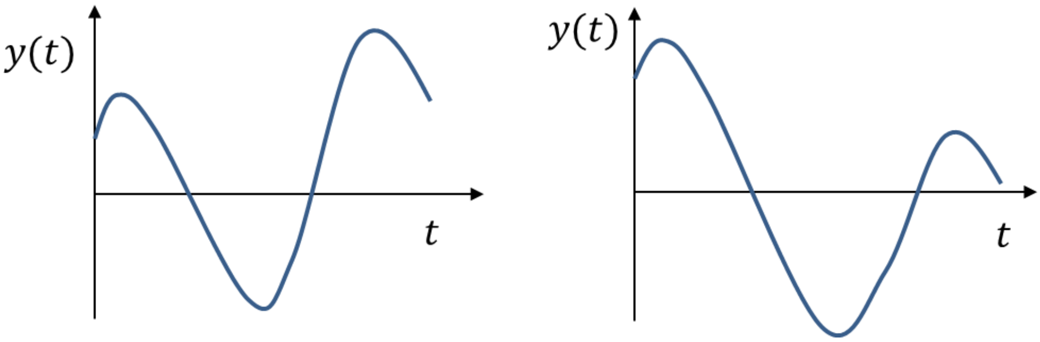

(a) $\alpha > 0$ (b) $\alpha < 0$

Fig. 2.21 Case of with conjugate complex number poles $\boldsymbol{\alpha \pm j\beta}$

From the above considerations, it can be seen that if at least one of p_i and q_j has a non-negative real part, $\int_0^\infty |y(t)|dt$ is no longer finite. Since the input $r(t)$ is considered as a finite arbitrary input, none of the poles $q_1, q_2, \cdots\cdots, q_n$ of $R(s)$ has a non-negative real part. Therefore, the condition for $y(t)$ to be finite is that the real parts of the poles $p_1, p_1, \cdots\cdots, p_n$ of $W(s)$ are all negative. Therefore, the condition for the control system to be stable is that all the poles of $W(s)$ are negative in the real part.

As is clear from Eq. (2.59), the pole of $W(s)$ is the root of the characteristic equation:

$$1 + G(s)H(s) = 0 \tag{2.64}$$

Now, when these roots are drawn on the complex plane representing s as shown in Fig. 2.22, the system is stable if all the roots exist only in the left half plane of the imaginary axis. If there is even one root on the right half, it becomes unstable. Also, if the root is just above the imaginary axis, it continues to vibrate with a certain amplitude, so it is difficult to say that it is stable.

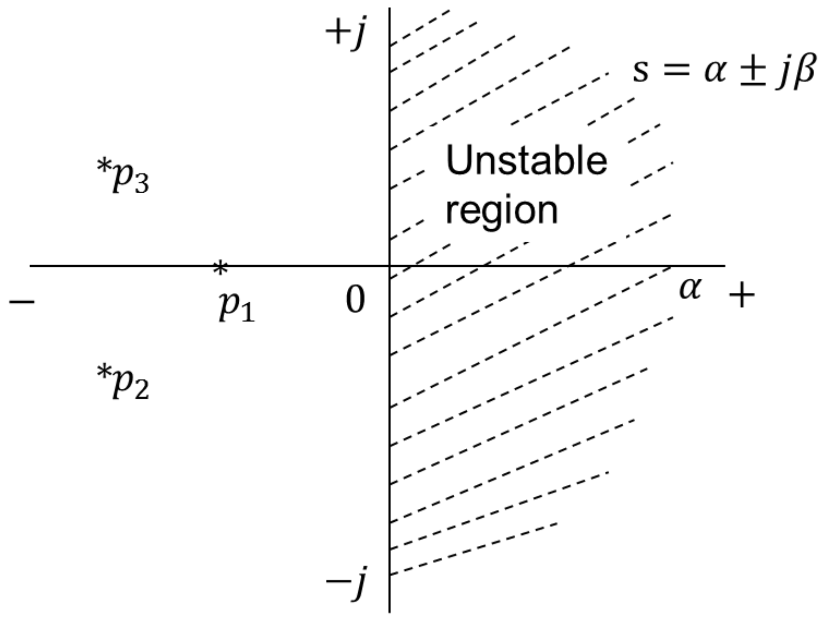

Fig. 2.22 Position of the pole on the s plane

A special case where the transfer function $H(s)$ of the feedback path becomes 1 in the feedback system of Fig. 2.23 is called a unity feedback system. Such a configuration is called a voltage follower in the electrical and electronic circuit area.

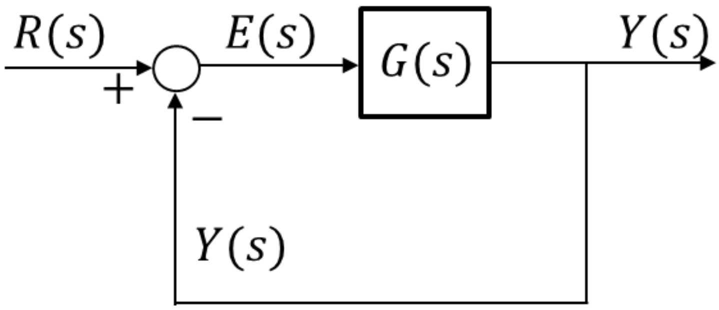

Fig. 2.23 Unity feedback system

In the unity feedback system as shown in Fig. 2.23, its transfer function is:

$$W(s) = \frac{G(s)}{1+G(s)} \tag{2.65}$$

Then its characteristic equation is:

$$1 + G(s) = 0 \tag{2.66}$$

2.3.1 Routh-Hurwitz stability criterion

When designing a feedback control system, the first requirement is that the system should be stable. If it is likely to become unstable, it is a predecessor to take some measures to stabilize it. In the time domain analysis of the control system theory, the Routh–Hurwitz stability criterion is a mathematical test that is the necessary and sufficient condition for the stability of a linear time invariant control system [13]. It uses the ideas above to determine whether a given polynomial has roots in the right half-plane.

If the control system is made up of a finite number of lumped elements, $G(s)$ is expressed by a rational function with respect to s. Therefore, the denominator of the closed-loop transfer function $W(s)$ can generally be expressed by the following real coefficient polynomial:

$$D(s) = \alpha_n s^n + \alpha_{n-1} s^{n-1} + \cdots + \alpha_1 s + \alpha_0 = 0 \tag{2.67}$$

Therefore, determining the stability can be attributed to the problem of finding out whether the real part of the root of the characteristic equation $D(s) = 0$ is positive or negative. When the order n is 2^{nd}, 3^{rd} or 4^{th} order, it is sufficient to actually solve the characteristic equation and examine the real part of the root. However, as the order becomes higher, it is troublesome to find the root. Therefore, the existence of a root whose real part is not negative may be determined by the following method.

For convenience, the coefficient in the first term is considered to be positive. If it is negative, each term of $D(s)$ multiplied by -1 can be considered as a characteristic equation. If any one of the coefficients $\alpha_{n-1}, \alpha_{n-2}, \dots \dots, \alpha_1, \alpha_0$ is negative or zero, some of the roots of the characteristic equation have a non-negative real part. Therefore, a necessary condition for the system to be stable is that the coefficients of all terms of the characteristic equation are present and all are positive. However, this is not a sufficient condition for stability. According to Hurwitz's stability determination, in addition to this, it is a necessary and sufficient condition for stability that all of the Hurwitz determinants described below are positive.

The coefficients of Eq. 2.67 are arranged as Fig. 2.24, first row first column, second row second column, third row third column, in order from the upper left corner of this sequence. The $n-1$ determinants made by taking the above are called Hurwitz determinants. However, in some higher-order determinants, the subscript α_k of k is negative, but these are all set to zero.

$$
\begin{array}{cccccccc}
\alpha_{n-1} & \alpha_n & 0 & 0 & 0 & 0 & \cdots\cdots & \\
\alpha_{n-3} & \alpha_{n-2} & \alpha_{n-1} & \alpha_n & 0 & 0 & \cdots\cdots & \\
\alpha_{n-5} & \alpha_{n-4} & \alpha_{n-3} & \alpha_{n-2} & \alpha_{n-1} & \alpha_n & 0 & \cdots\cdots \\
\alpha_{n-7} & \alpha_{n-6} & \cdots\cdots & & & & & \\
\vdots & \vdots & \vdots & \vdots & \vdots & & &
\end{array}
$$

Fig. 2.24 Coefficient of characteristic equation

$$
D_1 = \alpha_{n-1} \qquad D_2 = \begin{vmatrix} \alpha_{n-1} & \alpha_n \\ \alpha_{n-3} & \alpha_{n-2} \end{vmatrix} \qquad D_3 = \begin{vmatrix} \alpha_{n-1} & \alpha_n & 0 \\ \alpha_{n-3} & \alpha_{n-2} & \alpha_{n-1} \\ \alpha_{n-5} & \alpha_{n-4} & \alpha_{n-3} \end{vmatrix}
$$

$$
D_{n-1} = \begin{vmatrix} \alpha_{n-1} & \alpha_n & 0 & \cdots\cdots & & 0 \\ \alpha_{n-3} & \alpha_{n-2} & \alpha_{n-1} & \alpha_n & \cdots\cdots & 0 \\ \vdots & & & & & \vdots \\ 0 & \cdots\cdots & 0 & & \alpha_0 & \alpha_1 \end{vmatrix}
$$

Fig. 2.25 Hurwitz determinant

The necessary and sufficient condition for all roots of the characteristic equation $p(s)$ to be real parts is that all of $\alpha_{n-1}, \alpha_{n-2}, \ldots\ldots, \alpha_1, \alpha_0$ and $D_2, D_3, \ldots\ldots, D_{\mathrm{n}-1}$ are positive.

Routh's discriminant method is equivalent to the Hurwitz method, but is convenient for actual calculations and has the advantage of knowing the number of unstable roots. Necessary and sufficient condition of the stability is that all real parts of the solutions of characteristic equation are negative, which is equivalent to the following:

$\alpha_i > 0$ for i=0, 1, ... , n, and all values of the first column parameters in Routh table (Table. 2.5) are positive.

Table. 2.5 Routh table

s^n	α_n	α_{n-2}	α_{n-4}	α_{n-6}	$\cdots$
s^{n-1}	α_{n-1}	α_{n-3}	α_{n-5}	α_{n-7}	$\cdots$
s^{n-2}	$\beta_1 = \dfrac{\alpha_{n-1}\alpha_{n-2} - \alpha_n\alpha_{n-3}}{\alpha_{n-1}}$	$\beta_2 = \dfrac{\alpha_{n-1}\alpha_{n-4} - \alpha_n\alpha_{n-5}}{\alpha_{n-1}}$	β_3	β_4	$\cdots$
s^{n-3}	$\gamma_1 = \dfrac{\beta_1\alpha_{n-3} - \alpha_{n-1}\beta_2}{\beta_1}$	$\gamma_2 = \dfrac{\beta_1\alpha_{n-5} - \alpha_{n-1}\beta_3}{\beta_1}$	γ_3	γ_4	$\cdots$
$\vdots$	$\vdots$	$\vdots$	$\vdots$	$\vdots$	$\vdots$
s^0	α_0				

In the first column of the Routh table, the number of times for the coefficients sign changes is equal to the number of the system characteristic equation solutions with the positive real part.

2.3.2 Nyquist stability criterion

Routh discriminant method and Hurwitz discriminant method can be used only when the characteristic equation is given by a polynomial of s. It cannot be applied if the coefficient value is not mathematically clear or the characteristic equation includes a transcendental function. On the other hand, the Nyquist stability discriminant has a feature that can be determined graphically based on the frequency characteristic of the round transfer function $G(s)$.

In the feedback system, if the transfer function is $G(s)$, the value of s satisfying the characteristic equation as $1 + G(s) = 0$ is stable if there is no value on the right half or imaginary axis of the s plane. Therefore, as shown by Γ in Fig. 2.26(a), consider a trajectory that makes a round on the s plane. In other words, starting from the original point 0, proceeding upward on the imaginary axis and reaching $+j\infty$, from there, going to $-j\infty$ around the right side along the semicircle of infinity radius, and further upward on the imaginary axis. Let Γ be the closed path that returns to zero. The system is stable if there is no root of $1 + G(s) = 0$ inside the Γ. Now, as shown in Fig. 2.26(b), consider a plane in which the real part of the round transfer function $G(s)$ is represented on the horizontal axis and the imaginary part is represented on the vertical axis. If the value of s is moved along the trajectory Γ on the s plane, the corresponding $G(s)$ value also draws a closed path Γ' on the $G(s)$ plane.

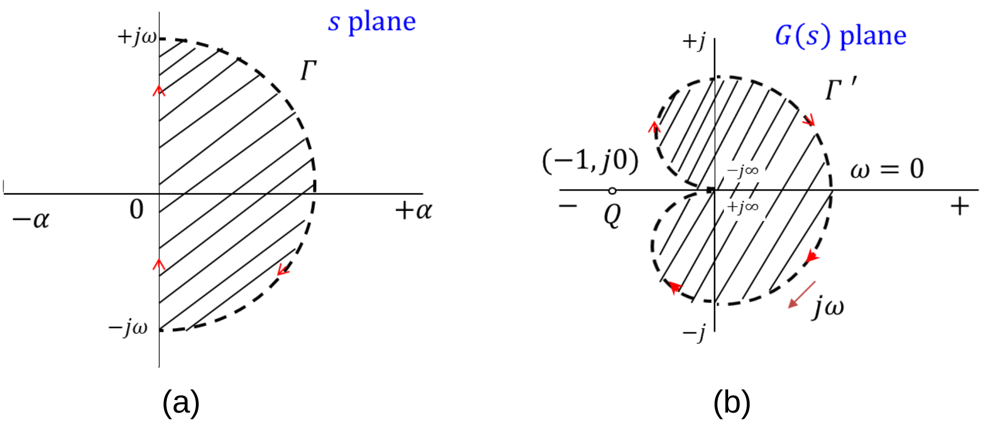

Fig. 2.26 Correspondence between s plane and $\boldsymbol{G(s)}$ plane

In other words, Γ' is the conformal mapping of the trajectory Γ on the s plane by the mapping function $G(s)$. The part surrounded by Γ on the s plane is always on the right side of the orbital direction. Therefore, the portion of the $G(s)$ plane that is wrapped to the right in the direction of travel of Γ' corresponds to the right half of the s plane.

In Fig. 2.26(b), Q is a point on the negative real axis at a distance of 1 from the original point. The value of $G(s)$ matches the point Q. It means that the value of s is the root of characteristic equation $1 + G(s) = 0$. From the above considerations, it can be said that the system is stable if the trajectory of Γ' does not wrap around point Q.

Nyquist plot: The Nyquist plot is a frequency response plot in

Gaussian plane, widely used in automatic control and signal processing (Fig. 2.27(a)) [14]. The most common usage of the Nyquist plot is for assessing the stability of the system with feedback.

Necessary and sufficient condition for the closed-loop system stability is given as follows:

$$\text{when}, \omega = 0 \to \infty, \ \ \mathrm{N} = \frac{P}{2}$$

Here, N is the number of Nyquist plot anti-clockwise encircle point (-1, j0), and P is the number of positive roots of the open-loop characteristic equation.

As shown in Fig. 2.27(a), if the vector locus of $G(j\omega)$ passes through the left side of the point $(-1, \mathrm{j}0)$ when ω changes from 0 to ∞, it is stable, whereas it is unstable if it passes on the right side. In many cases, this inference is sufficient.

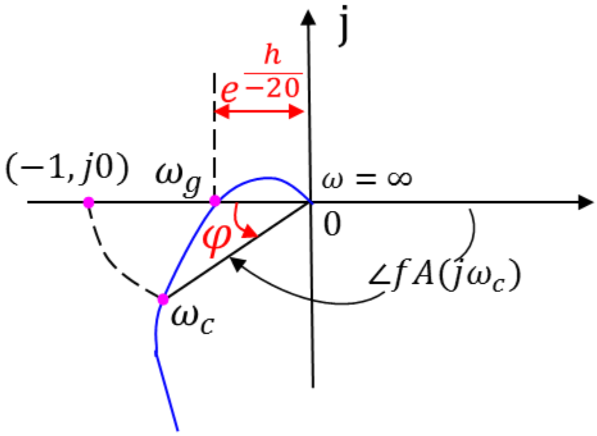

(a) Nyquist plot of an open-loop system

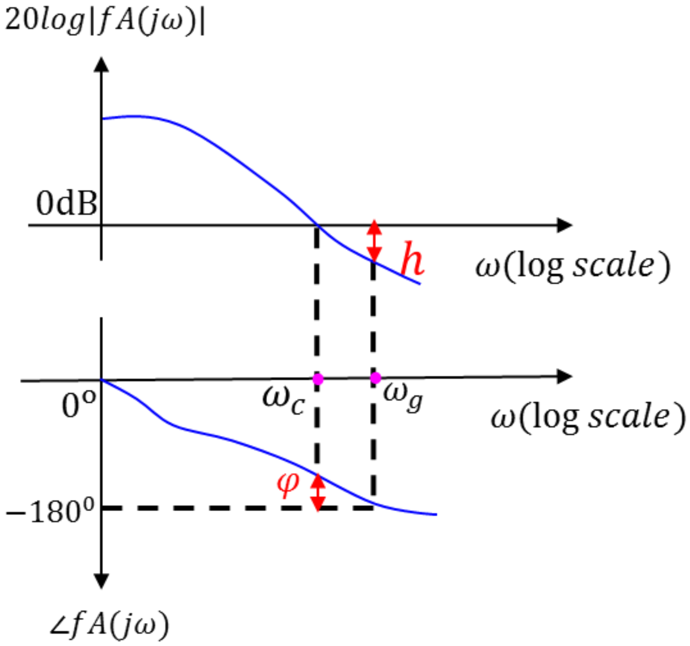

(b) Bode plots of the loop gain for stable system

Fig. 2.27 Nyquist plot and Bode plot

Bode plot: In electrical engineering and control theory, the Bode plots are graphs of the frequency responses (gain and phase) of the open-loop characteristics of the feedback system, and they can show gain margin and phase margin (Fig.2.27(b)) required to maintain feedback system stability under variations in circuit characteristics [5-13]. Also they provide visual representations of the operational amplifier transfer response and its potential stability, and they can be obtained by measurements as well as the mathematical model (small signal model) of the operational amplifier. This principle has been widely applied to design many feedback control systems. Circuit designers can routinely use the Bode plots to determine the bandwidth and frequency stability of the operational amplifier circuits. We can see from Fig. 2.27, that we can also obtain the gain margin and phase margin from Nyquist plot.

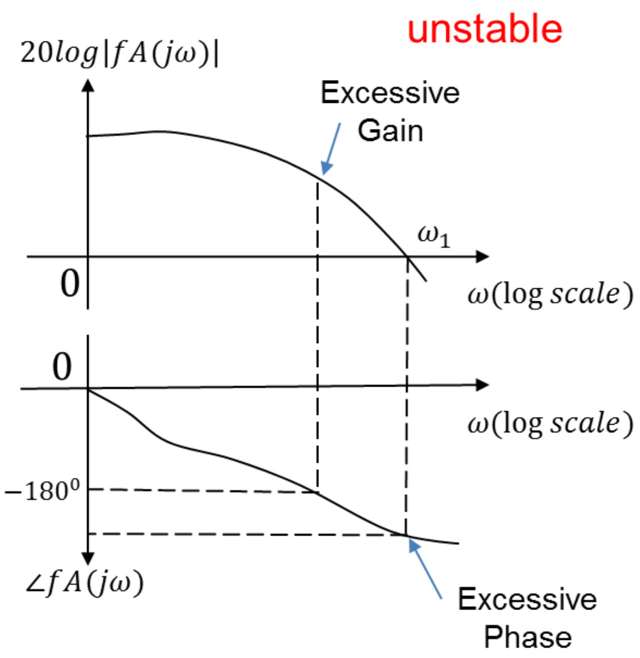

Fig. 2.28 Bode plots of the loop gain for unstable system

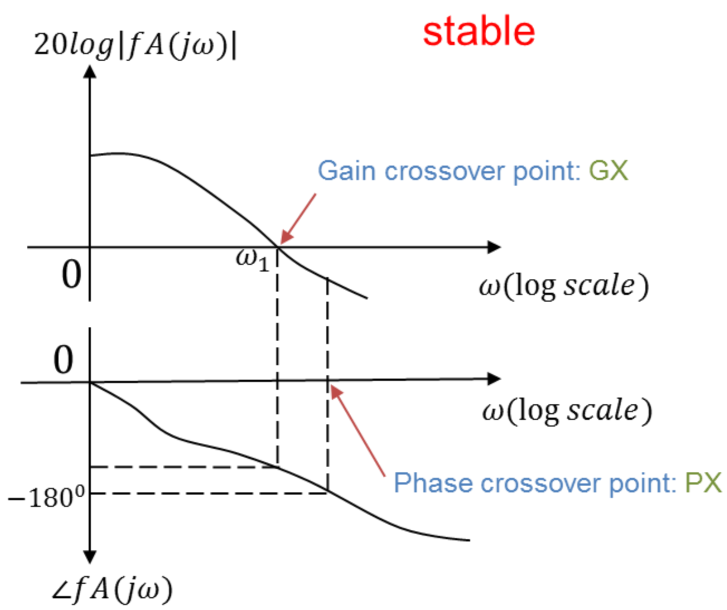

Fig. 2.29 Bode plots of the loop gain for stable system

The frequencies at which the magnitude and phase of the loop gain are equal to unity and -180^{o}, respectively, play a crucial role in the stability and they are called the "gain crossover point" (GX) and the "phase crossover point” (PX) respectively. In a stable system, the gain crossover must occur well-before the phase crossover. As shown in Fig 2.29, if the magnitude plots are shifted down, the gain crossover moves closer to the origin which makes the feedback system more stable.

To ensure stability, $|fA(j\omega)|$ must drop to unity before $\angle fA(j\omega)$ crosses -180^{o}. As shown in Fig. 2.30(a), GX is only slightly below PX, and in Fig.2.30 (b), GX precedes PX with a greater margin. Therefore, the greater the spacing between GX and PX (while GX remains below PX), the more stable the feedback system is.

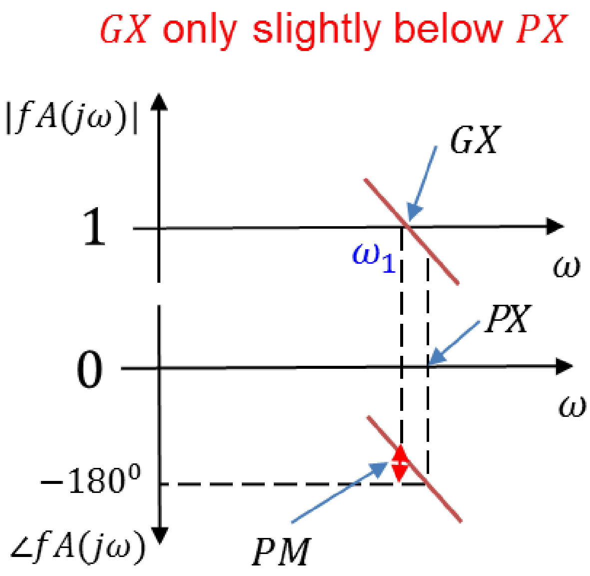

(a) Small margins

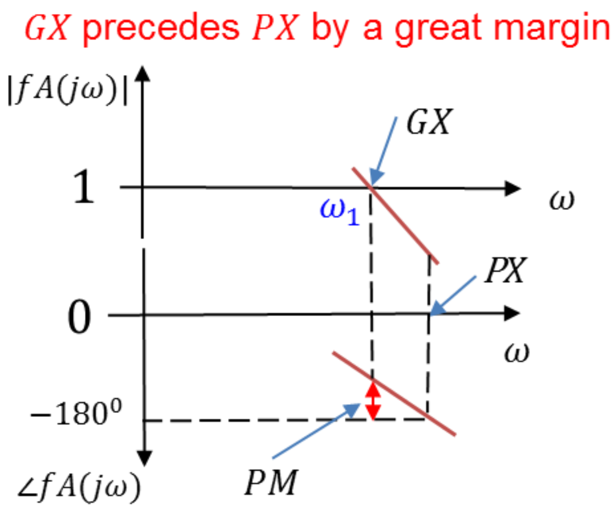

(b) Large margins

Fig. 2.30 Open-loop frequency responses for various margins between gain and phase crossover points. $\boldsymbol{GX}$= gain crossover point, $\boldsymbol{PX}$= phase crossover point.

Alternatively, the phase of $fA(j\omega)$ at the gain crossover frequency can serve as a measure of stability: the smaller $|fA(j\omega)|$ at this point, the more stable the system. This observation leads us to the concept of "phase margin" (PM), defined as:

$$\mathrm{PM} = 180^{\mathrm{o}} + \angle fA(\omega = \omega_1) \tag{2.68}$$

Here, ω_1 is the gain crossover frequency.

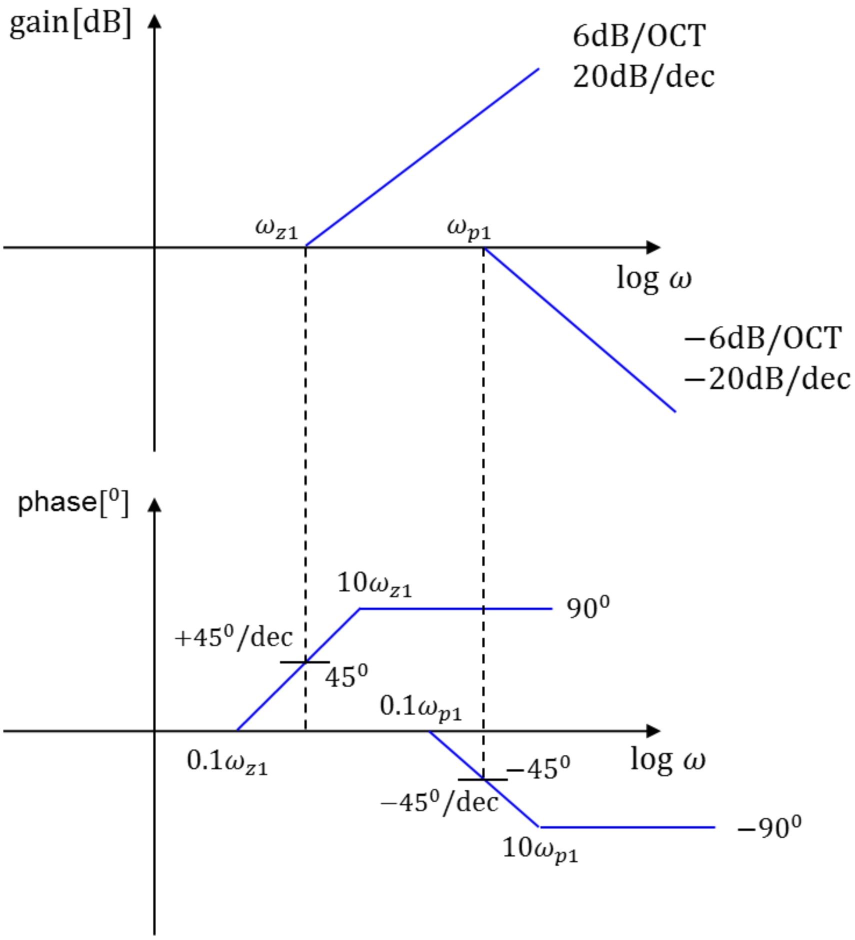

Fig. 2.31 Skeleton Bode plot

The skeleton Bode plot which is shown as in Fig. 2.31 is an approximation of the Bode plot by a straight line when the board or zero is a real number. By using the skeleton Bode plot, drawing is becoming easier for circuit design and analyses. 6dB/oct is means gain 6dB increase when frequency doubles, and 20dB/dec is means gain 20dB increase when frequency is 10 times. Drawing the phase is a little complicated than drawing the gain: in the case of zero point, it approximates linearly to 45^0at $\omega = \omega_z$, 0^0at $\omega = 0.1\omega_z$, 90^0at $\omega = 10\omega_z$; in the case of pole point, it approximates linearly to-45^0at $\omega = \omega_z$, 0^0at $\omega = 0.1\omega_z$,-90^0at $\omega = 10\omega_z$. Fig. 2.31 shows how to create a skeleton Bode plot of gain and phase when there is one zero point and one pole point.

Stability and many response characteristics are mutually restricted. For example, in relation to response seed, if there is a good phase margin in the frequency analysis, the speed will be slower in the response of the feedback system. On the contrary, if the speed of response is increased, the phase margin is hard to guarantee and the system will perform poorly in terms of stability.

2.4 Summary

In this chapter, we have introduced the stability criterion, including Routh-Hurwitz stability which is unpopular in electronic field, and Nyquist stability criterion which is widely used for judging stability by circuit designer. Before doing this, we first introduced the principle, composition and classification of the feedback control system in details. And then, we introduced the related knowledge that is needed when we derive the transfer function, including differential equation and Laplace transform. All of those are basic theoretical knowledge, but are very important and indispensable for carrying out research and learning in many subjects.

CHAPTER III
OPERATIONAL AMPLIFIER AND SMALL SIGANAL MODEL

Electronic circuits are configured using semiconductor devices such as diodes, bipolar transistors, and MOS transistors. In the former section of this chapter, we talk about the basic knowledge of electronics, including the constructions and principles as well as the voltage-current characteristic of transistors and its small signal equivalent circuit. In the later of transistor, we duce the small signal model of several examples of operational amplifiers.

3.1 Transistor and amplifier circuit

The most important purpose of electronic circuits is the amplification of electrical signals. Resistors, capacitors, and coils are called passive elements and do not function to amplify electrical signals. Active elements are required to amplify electrical signals. Until around 1960s, vacuum tubes were mainly used as active elements, but small and lightweight active elements called transistors later became the mainstream, and at present, vacuum tubes are used only in very special cases. This section describes the basic concept of what amplification is, focusing on the transistor operating principle and its equivalent circuit.

3.1.1 Bipolar transistor and MOS transistor

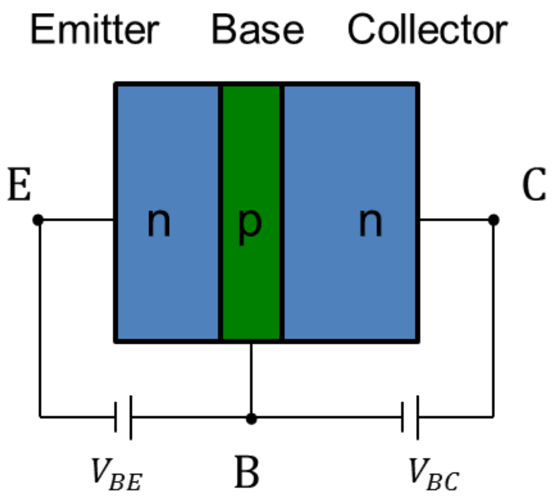

Fig. 3.1 npn transistor

As shown in Fig. 3.1, bipolar transistors are formed by sandwiching PN junctions, and there are two types, npn transistors using npn junctions and pnp transistors using pnp junctions. Fig. 3.1 shows an npn transistor.

The collector current I_C varies exponentially with the base-emitter voltage V_{BE}:

$$I_C = I_S e^{\frac{qV_{BE}}{kT}} \tag{3.1}$$

Since the base current I_B also varies exponentially with base-emitter voltage V_{BE}, so the relationship between collector current I_C and base current I_B is given by:

$$I_B = \frac{I_C}{\beta_F} \tag{3.2}$$

Here, $\beta_F$is called forward current gain. Since the emitter current is the sum of the base current and the collector current, and considering the polarity, we have the following:

$$I_E = -(I_B + I_C) = -\left(I_C + \frac{I_C}{\beta_F}\right) = -\frac{I_C}{\partial_F} \tag{3.3}$$

Here, ∂_F is called forward current transfer rate. The collector current I_C of the bipolar transistor is determined by the base-emitter voltage V_{BE} and varies exponentially with respect to the base-emitter voltage V_{BE}. It is basically independent of the collector voltage.

Fig. 3.2 is a plot of the collector current I_C against the collector-emitter voltage Vce using the base current I_B as a parameter. The collector current I_C has little dependency on the collector-emitter voltage V_{CE}, and is mostly determined by the base current I_B or the base-emitter voltage V_{BE}. This characteristic can be expressed by a voltage controlled current source. However, the collector current rapidly decreases in the region where V_{CE} is lower than about 0.3V. This region is called a saturation region. Normally, this saturation region should not be used as the operation region of the bipolar transistor.

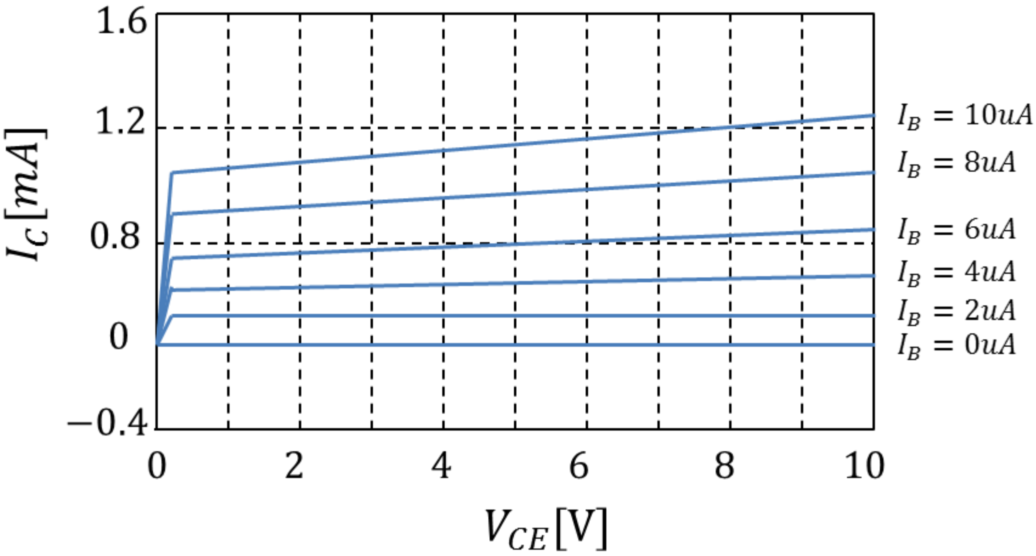

Fig. 3.2 Collector-emitter voltage and collector current

It can be seen that the collector current I_C changes with a change in the collector-emitter voltage V_{CE}, although it is slight. This effect is called the Early effect. Considering the Early effects, we have the followings:

$$I_C = I_S e^{\frac{qV_{BE}}{kT}}\left(1 + \frac{V_{CE}}{V_A}\right) \tag{3.3}$$

The MOS transistor has a gate formed on a semiconductor with an insulator such as silicon dioxide SiO2 and a metallic material such as polysilicon. When the substrate is a p-type semiconductor, the drain-source region is formed of an n-type semiconductor. Consider that a positive voltage V_{DS} is applied between the drain and source, and a voltage V_{GS} is applied between the gate and source. Then the current I_D flows between the drain and source when the voltage V_{GS} is higher than a certain voltage, and when the voltage V_{GS} is lower than a certain voltage, the current I_D does not flow.

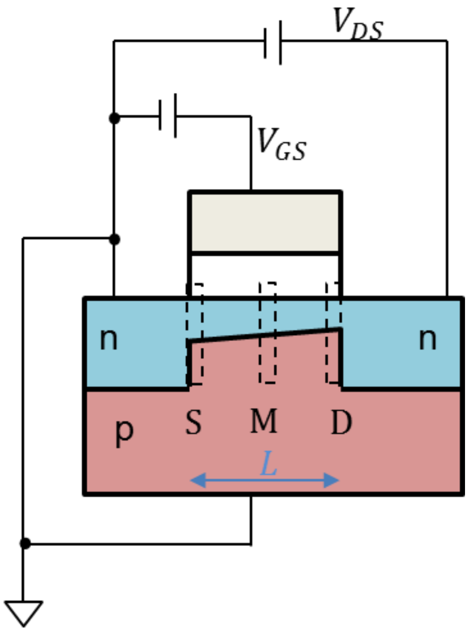

Fig. 3.3 Channel in the linear region. ***L***= the channel length.

A path through which carriers flow is called a channel. As shown in Fig.3.3, a carrier is induced across the entire region between the drain and the source forming a channel by the gate, and a linear region is formed. Drain current is expressed as:

$$I_D = \mu C_{ox}\frac{W}{L}(V_{GS} - V_T - \frac{V_{DS}}{2})V_{DS} \tag{3.4}$$

Here, W is the channel width, L is the channel length, V_T is the threshold voltage.

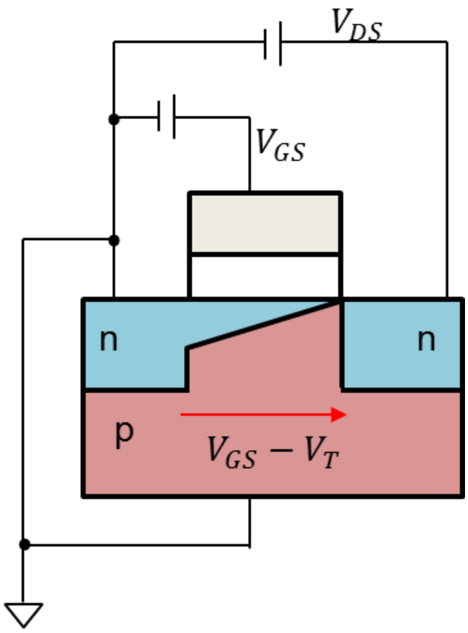

Fig. 3.4 Channel in saturation region.

When $V_{DS} > V_{GS} - V_T$, the charge induced in the channel near the drain disappears as shown in Fig.3.4. Drain current is obtained as:

$$I_D = \frac{\mu C_{ox}}{2}\frac{W}{L}(V_{GS} - V_T)^2 \tag{3.5}$$

The drain current I_D is determined by the gate-source voltage V_{GS} and it does not depend on the drain-source voltage V_{DS}. Such a region is called a saturation region, and often is used as the operating region of MOS transistors.

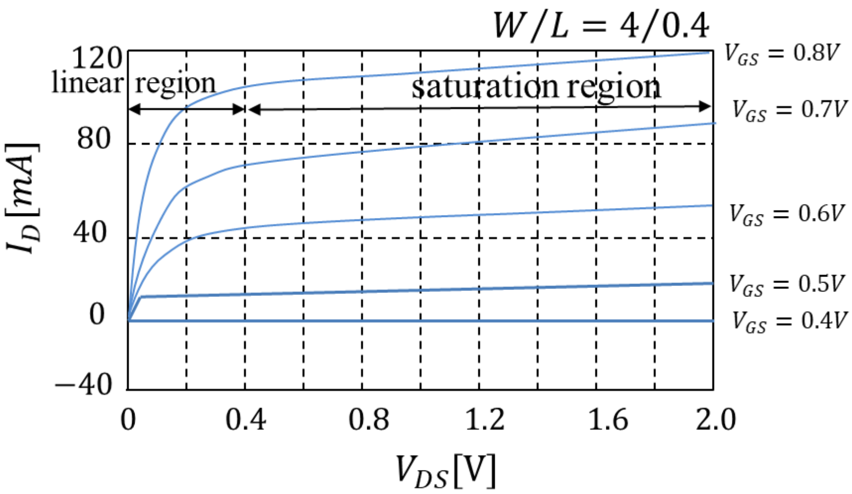

Fig. 3.5 Voltage-current characteristics in saturation region. W= the channel width, L= the channel length.

Fig.3.5 shows the characteristics of the drain current I_D with respect to the drain-source voltage V_{DS} when the gate-source voltage V_{GS} is used as a parameter. In an actual MOS transistor, when the drain voltage changes even in the saturation region, the drain current I_D changes. One reason for this is a change in the depletion layer thickness between the channel and the drain. This is called a channel length modulation effect. Considering the channel length modulation effect, the drain current I_D is:

$$I_D = \frac{\mu C_{ox}}{2}\frac{W}{L}(V_{GS} - V_T)^2(1 + \frac{V_{DS}}{V_A}) \tag{3.6}$$

Here, V_A is a voltage representing the channel length modulation effect and is called as Early voltage. Fig. 3.6 shows the voltage-current relationship of bipolar transistors, and Fig. 3.7 shows voltage-current relationship of MOS transistors.

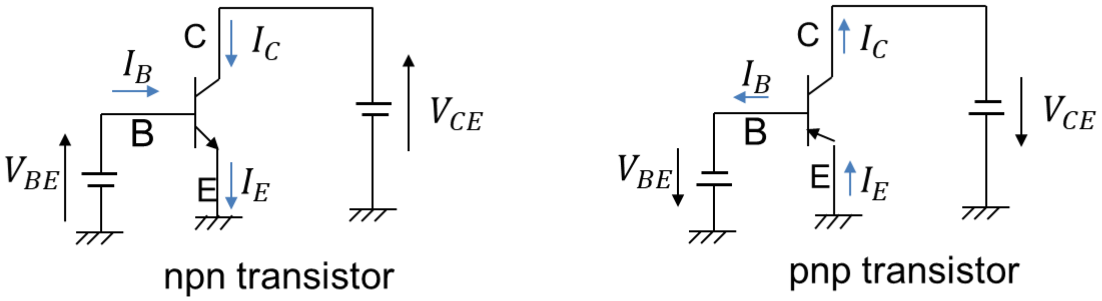

Fig. 3.6 Voltage-current relationship of bipolar transistors

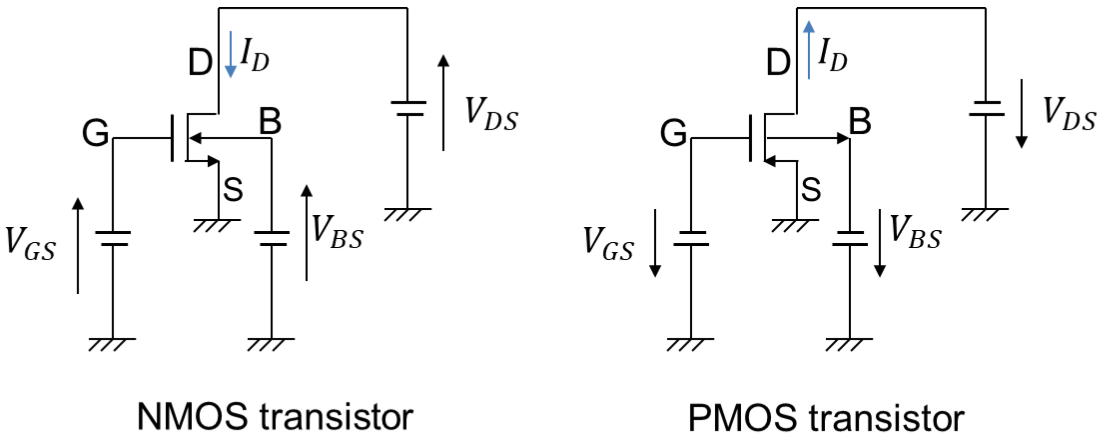

Fig. 3.7 Voltage-current relationship of MOS transistors

3.1.2 Small signal equivalent circuit of transistor

Signal amplification is possible by using bipolar transistors and MOS transistors. For this purpose, it is necessary to obtain a change in the output signal voltage when the transistor is kept in an appropriate operating state in terms of DC, and the input signal voltage is changed around the operating point. What is required in circuit design is a response to a small signal, which is a slight change in voltage, not the voltage value itself. A small voltage change is an input and the output voltage change is taken out as an output. Therefore, characteristics of the output change with respect to the input change are required, and a small signal equivalent circuit that is a circuit focused only on the signal change is required.

In the bipolar transistor circuit, the collector current I_C is a function of the base-emitter voltage V_{BE} and the collector-emitter voltage V_{CE}.

$$I_C = I_C(V_{BE}, V_{CE}) \tag{3.7}$$

Taylor expansion of Eq. (3.7) is given by:

$$I_C + \Delta I_C = I_C(V_{BE}, V_{CE}) + \frac{\partial I_C}{\partial V_{BE}}\Delta V_{BE} + \frac{\partial I_C}{\partial V_{CE}}\Delta V_{CE} \tag{3.8}$$

Proportional coefficient of collector current I_C change ΔI_C to base-emitter voltage V_{BE} change ΔV_{BE} is called as transconductance:

$$\frac{\partial I_C}{\partial V_{BE}} = g_m = \frac{I_c}{U_T} \tag{3.9}$$

Proportional coefficient of collector current I_C change ΔI_C to collector-emitter voltage V_{CE} change ΔV_{CE} is called as collector conductance:

$$\frac{\partial I_C}{\partial V_{CE}} = g_o = \frac{1}{r_o} \tag{3.10}$$

Proportional coefficient of base current I_B change ΔI_B to base-emitter voltage V_{BE} change ΔV_{BE} is called as input conductance:

$$g_\pi = \frac{\Delta I_B}{\Delta V_{BE}} = \frac{g_m}{\beta_F} \tag{3.11}$$

Small signal equivalent circuit of the bipolar transistor is as shown in Fig. 3.8. The parameter r_b is base spreading resistance, when the current flows through the base, the voltage applied to the base-emitter junction decreases.

$$r_o = \frac{1}{g_o}, r_\pi = \frac{1}{g_\pi} \tag{3.12}$$

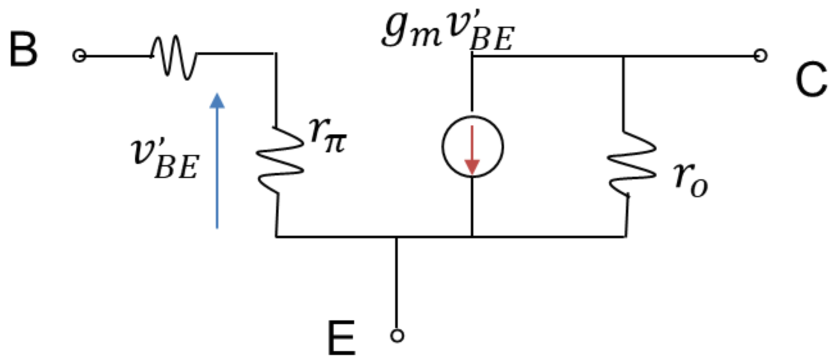

Fig. 3.8 Small signal equivalent circuit of bipolar transistor

In the small signal equivalent circuit of the MOS transistor as shown in Fig. 3.9, it is necessary to consider the back gate effect. Since the drain current I_D is a function of the gate-source voltage V_{GS}, the drain-source voltage V_{DS}, and the body-source voltage V_{BS}, it is expressed as follows:

$$I_D = I_D(V_{GS}, V_{DS}, V_{BS}) \tag{3.13}$$

The state when the gate-source voltage V_{GS}, the drain-source voltage V_{DS}, and the body-source voltage V_{BS} change slightly is expressed as follows by Taylor expansion:

$$I_D + \Delta I_D = I_D(V_{GS0}, V_{DS0}, V_{BS0}) + \frac{\partial I_D}{\partial V_{GS}}\Delta V_{GS} + \frac{\partial I_D}{\partial V_{DS}}\Delta V_{DS} + \frac{\partial I_B}{\partial V_{BS}}\Delta V_{BS} \tag{3.14}$$

$$\frac{\partial I_D}{\partial V_{GS}} = g_m, \ \frac{\partial I_D}{\partial V_{GS}} = g_D, \ \frac{\partial I_D}{\partial V_{BS}} = g_{mb} \tag{3.15}$$

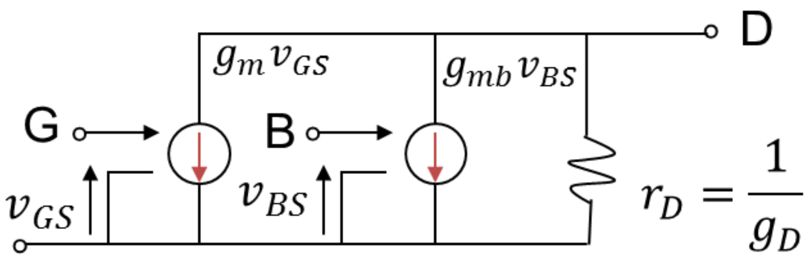

Fig. 3.9 Small signal equivalent circuit of MOS transistor

3.2 Small signal model

The operational amplifier is a high gain amplifier originally used in an analog electronic computer, and performs addition / subtraction, calculus, and other operations. With the progress of integrated circuit technology, operational amplifiers have also been integrated, and very high performance operational amplifiers have become available at low cost. By using an operational amplifier, various operational amplifiers including an amplifier circuit can be easily realized with high performance. Sometimes a simpler and better circuit is obtained than when individual components are used.

This section shows several examples of operational amplifiers and applications of the proposed stability criterion to them.

3.1.2 Two-pole operational amplifier with C compensation.

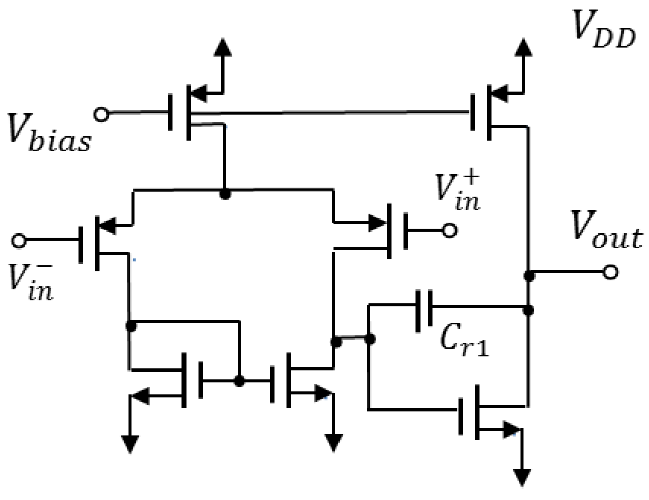

(a) Transistor level circuit.

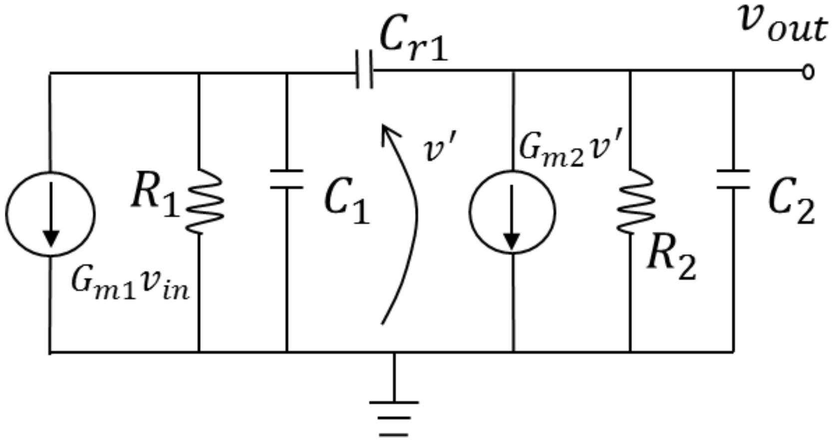

(b) Small-signal model.

Fig. 3.10 Two-pole amplifier with inter-stage capacitance. $\boldsymbol{R_1}, \boldsymbol{R_2}$= equivalent resistors, $\boldsymbol{C_1}, \boldsymbol{C_2}$= equivalent capacitances, $\boldsymbol{G_{m1}}, \boldsymbol{G_{m2}}$= transconductances, and $\boldsymbol{C_{r1}}$= compensation capacitance.

Consider the two-pole amplifier in Fig. 3.10 whose open-loop transfer function is given by:

$$G(s) = K\frac{1+b_1 s}{1+a_1 s+a_2 s^2}. \tag{3.16}$$

Here, $b_1 = -\frac{C_{r1}}{G_{m2}}$, $K = G_{m1}G_{m2}R_1R_2$,

$$a_1 = R_1C_1 + R_2C_2 + (R_1 + R_2 + R_1G_{m2}R_2)C_{r1},$$

$$a_2 = R_1R_2C_2\left[C_1 + \left(1 + \frac{C_1}{C_2}\right)C_{r1}\right] \tag{3.17}$$

Fig. 3.11 (b) (c) show feedback amplifiers using the operational amplifier in Fig. 3.10(a), and their closed-loop transfer function is obtained as follows:

$$\frac{G(s)}{1+fG(s)} = \frac{K(1+b_1 s)}{1+fK+(a_1+fKb_1)s+a_2 s^2} \tag{3.18}$$

Here $f = \frac{R_2}{R_1+R_2}$ for Fig. 3.11 (b) and $f = 1$ for Fig. 3.11 (c).

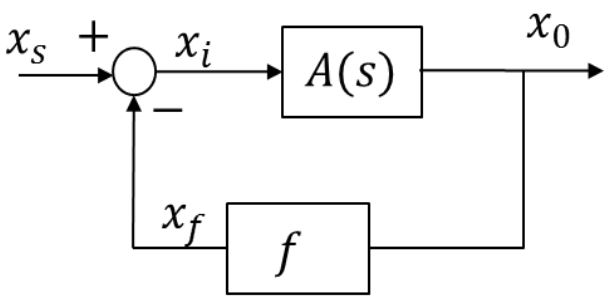

(a) Block diagram

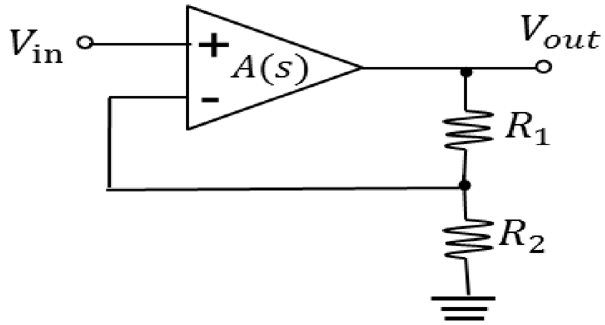

(b) Circuit example 1 with $f = R_2/(R_1 + R_2)$.

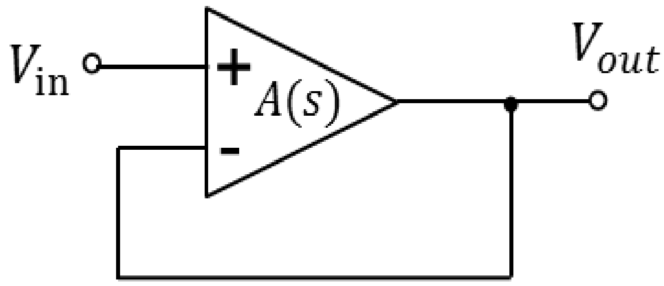

(c) Circuit example 2 with $f = 1$ voltage follower

Fig. 3.11 Feedback systems

Application of the proposed criterion

Then we set a parameter θ as follows:

$$\theta = a_1 + fKb_1 \tag{3.19}$$

Using Eq. (3.17), the parameter θ is obtained as follows

$$\theta = R_1C_1 + R_2C_2 + (R_1 + R_2)C_{r1} + (G_{m2} - fG_{m1})R_1R_2C_{r1} \tag{3.20}$$

Based on the R-H stability criterion, we can obtain the following as the necessary and sufficient condition for the operational amplifier feedback circuit stability:

$$\theta > 0 \tag{3.21}$$

Note that the explicit stability condition in Eq. (3.20), Eq. (3.21) cannot be found out in any analog circuit design book [6-13], to the best of our knowledge. We can see from Eq. (3.20), Eq. (3.21) which parameter values should be increased or decreased to obtain the feedback stability.

3.2.2 Two-pole operational amplifier with R, C compensation.

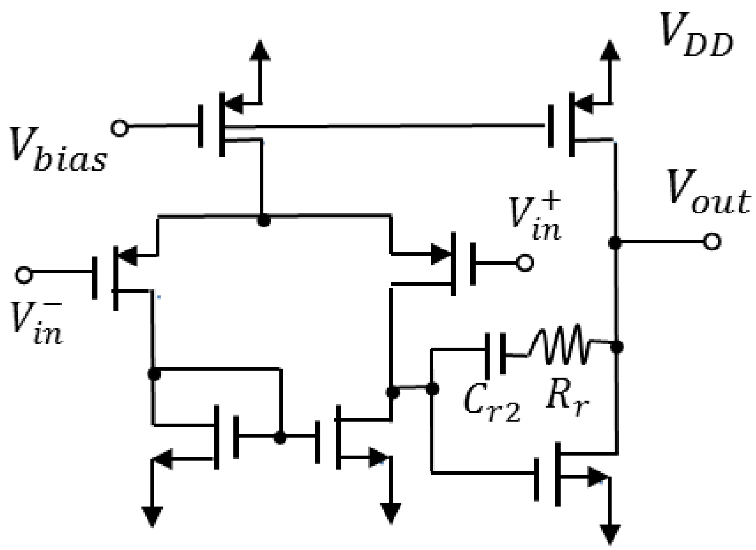

(a) Transistor level circuit.

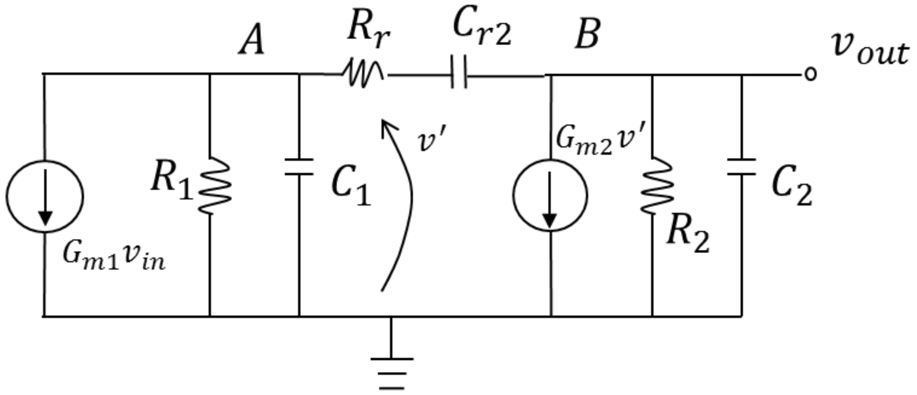

(b) Small-signal model

Fig. 3. 12 Two-pole amplifier with compensation of Miller right-half-plane zero. $\boldsymbol{R_1}, \boldsymbol{R_2}$= equivalent resistors, $\boldsymbol{C_1}, \boldsymbol{C_2}$ = equivalent capacitances, $\boldsymbol{G_{m1}}, \boldsymbol{G_{m2}}$= transconductances, $\boldsymbol{C_{r1}}$= compensation capacitance, and $\boldsymbol{R_r}$= compensation resistor.

The closed-loop transfer function of the feedback amplifier using the operational amplifier in Fig. 3.12 is given by

$$\frac{G(s)}{1+fG(s)} = \frac{K(1+b_1 s)}{1+fK+(a_1+fKb_1)s+a_2 s^2} \tag{3.22}$$

Here, $b_1 = -\left(\frac{C_{r2}}{G_{m2}} - R_r C_{r2}\right)$,

$$K = G_{m1}G_{m2}R_1R_2,\ a_3 = R_1R_2R_rC_1C_2C_{r2},$$
$$a_1 = R_1C_1 + R_2C_2 + (R_1 + R_2 + R_r + R_1R_2G_{m2})C_{r2},$$
$$a_2 = R_1R_2(C_2C_{r2} + C_1C_2 + C_1C_{r2}) + R_rC_{r2}(R_1C_1 + R_2C_2) \tag{3.23}$$

Then we can obtain the parameter α_1 as follows:

$$\alpha_1 = (a_1 + fKb_1) = R_1C_1 + R_2C_2 + (R_1 + R_2 + R_r)C_{r2} + (G_{m2} - fG_{m1} + fG_{m1}G_{m2}R_r)R_1R_2C_{r2}. \tag{3.24}$$

and the Routh table's parameter β_1 is given by

$$\beta_1 = \frac{(a_1 + fKb_1)a_2 - a_3(1 + fK)}{a_2}$$

$$= R_1C_1 + R_2C_2 + (R_1 + R_2 + R_r)C_{r2} + (G_{m2} - fG_{m1} + fG_{m1}G_{m2}R_r)R_1R_2C_{r2} - \frac{R_1R_2C_1C_2R_rC_{r2}(1+fG_{m1}G_{m2}R_1R_2)}{R_1R_2(C_2C_{r2}+C_1C_2+C_1C_{r2})+R_rC_{r2}(R_1C_1+R_2C_2)} \tag{3.25}$$

The stability condition is as follows:

$$\alpha_1 > 0, \qquad \beta_1 > 0 \tag{3.26}$$

Again, the explicit stability condition in Eq. (3.24), Eq. (3.25), Eq. (3.26) cannot be found out in any analog circuit design book [6-13], to the best of our knowledge, and we understand from Eq. (3.24), Eq. (3.25), Eq. (3.26) which parameter values should be increased or decreased to obtain the feedback stability.

3.2.3 Three-pole operational amplifier.

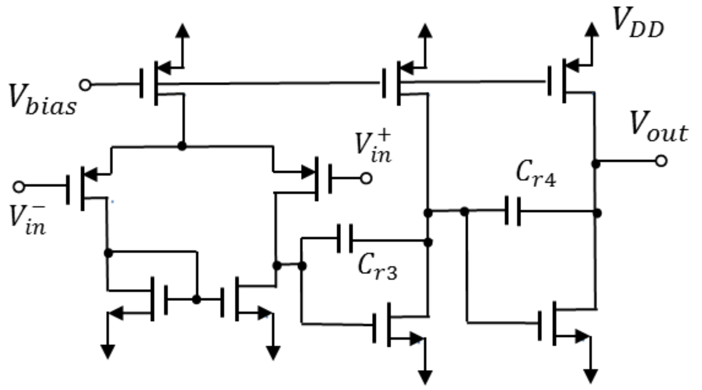

(a) Transistor level circuit.

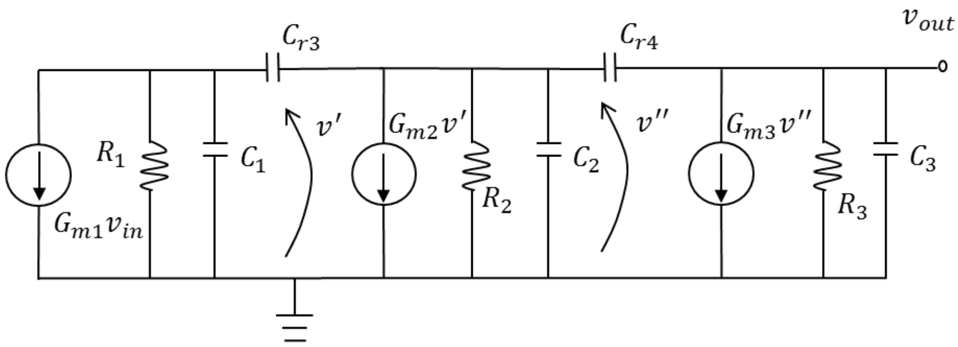

(b) Small-signal model

Fig. 3.13 Three-pole amplifier with inter-stage capacitance. $\boldsymbol{R_1}, \boldsymbol{R_2}, \boldsymbol{R_3}$= equivalent resistors, $\boldsymbol{C_1}, \boldsymbol{C_2}, \boldsymbol{C_3}$= equivalent capacitances, $\boldsymbol{G_{m1}}, \boldsymbol{G_{m2}}, \boldsymbol{G_{m3}}$= transconductances, and $\boldsymbol{C_{r3}}, \boldsymbol{C_{r4}}$= compensation capacitances.

The closed-loop transfer function of the feedback amplifier using the operational amplifier in Fig. 3.13 is given by

$$\frac{G(s)}{1+fG(s)} = \frac{K(1+b_1 s+b_2 s^2)}{1+fK+(a_1+fKb_1)s+(a_2+fKb_2)s^2+a_3 s^3}. \tag{3.27}$$

Where, $K = G_{m1}G_{m2}G_{m3}R_1R_2R_3$,

$b_1 = -(\frac{C_{r3}}{G_{m2}} + \frac{C_{r4}}{G_{m3}})$, $\quad b_2 = \frac{C_{r3}C_{r4}}{G_{m2}G_{m3}}$,

$a_1 = C_{r3}(R_1 + R_2 + G_{m2}R_1R_2) + C_{r4}(R_2 + R_3 + G_{m3}R_2R_3) + R_1C_1 + R_2C_2 + R_3C_3$.

$a_2 = C_{r3}(G_{m2}R_1R_2R_3C_3 + (R_1+R_2)R_3C_3 + R_1R_2(C_1 + C_2)) + C_{r4}(G_{m3}R_1R_2R_3C_1 + (R_2+R_3)R_1C_1 + R_2R_3(C_2 + C_3)) + C_{r3}C_{r4}\big((G_{m2} + G_{m3})R_1R_2R_3 + R_1R_2 + R_2R_3 + R_1R_3\big) + R_1R_2C_1C_2 + R_2R_3C_2C_3 + R_1R_3C_1C_3$.

$$a_3 = R_1R_2R_3[C_{r3}(C_2C_3 + C_1C_3) + C_{r2}(C_1C_2 + C_1C_3) + C_{r1}C_{r4}(C_1 + C_2 + C_3) + C_1C_2C_3]. \tag{3.28}$$

Then we can obtain the parameter ∂_2:

$$\partial_2 = a_1 + fKb_1 = C_{r3}(R_1 + R_2 + G_{m2}R_1R_2) + C_{r4}(R_2 + R_3 + G_{m3}R_2R_3) + R_1C_1 + R_2C_2 + R_3C_3 - fG_{m1}G_{m2}G_{m3}R_1R_2R_3(\frac{C_{r3}}{G_{m2}} + \frac{C_{r4}}{G_{m3}}). \quad (3.29)$$

and the Routh table's parameter β_2:

$$\beta_2 = \frac{(a_1+fKb_1)(a_2+fKb_2) - a_3(1+fK)}{a_2+fKb_2} \quad (3.30)$$

The stability condition is as follows:

$$\alpha_2>0, \qquad \beta_2 > 0. \quad (3.31)$$

Again, the explicit stability condition in Eq. (3.29), Eq. (3.30), and Eq. (3.31) cannot be found out in any analog circuit design book [6-13], to the best of our knowledge.

In this section, we select three circuit configurations as examples for deducing the explicit stability condition based on proposed method. For other circuit configuration, the R-H method would can be applied at the condition that if we can derive its characteristic equation of closed-loop transfer function and Routh table.

3.3 Summary

A circuit that amplifies a signal voltage and/or current whose amplitude is sufficiently smaller than the DC device voltage and current is called a small signal amplifier. In the small signal amplifier, the DC device voltage, current and the signal voltage, and the current can be calculated separately, and the signal component can be analyzed by a linear equivalent circuit. In this chapter, we introduce the transistor and its small signal equivalent circuit. Combining with practical examples, we deduce the small signal model of several examples of operational amplifiers, we will explore the relationship that between R-H stability criterion with Nyquist stability criterion using these small signal models in the next chapter.

CHAPTER IV THEORETICAL DEMONSTRATION

In the research of science and engineering, we lay emphasis on the calculation and analysis of simulation and experimental data, but the theoretical part of the research is also important. Formula derivation and numerical analysis are the premise and guarantee of experiment. The theoretical feasibility can help us better analyze the experimental results and make our experimental data more convincing.

This chapter shows the equivalency between the Nyquist stability criterion and the R-H stability criterion in some conditions and the relationship between R-H parameters and phase margin, as the verification of theoretical part for this dissertation. For finding out if there is a connection between R-H stability criterion and Nyquist stability criterion, we deduce the stability conditions based on the R-H stability criterion and Nyquist stability criterion respectively, and then we compare and judge these stability conditions. We analysis three transfer function examples from simple to complex of the pole and zero. For finding out the relationship between R-H parameters and stability index phase margin, we have also conducted corresponding data analysis using examples.

4.1 Equivalence at mathematical foundations

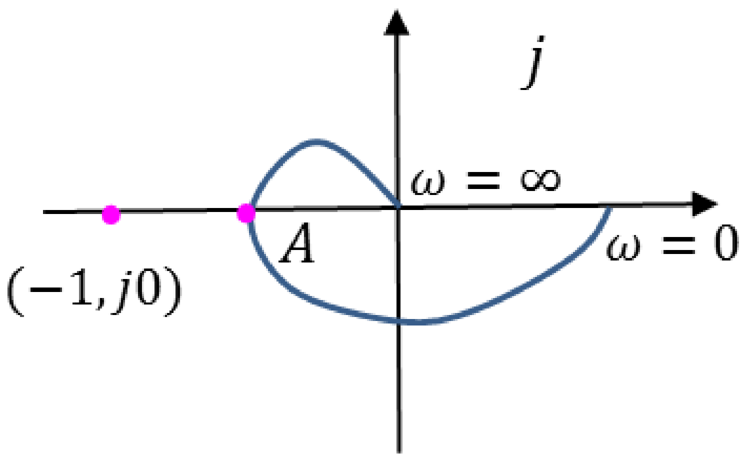

(a) Sketch of Nyquist plot

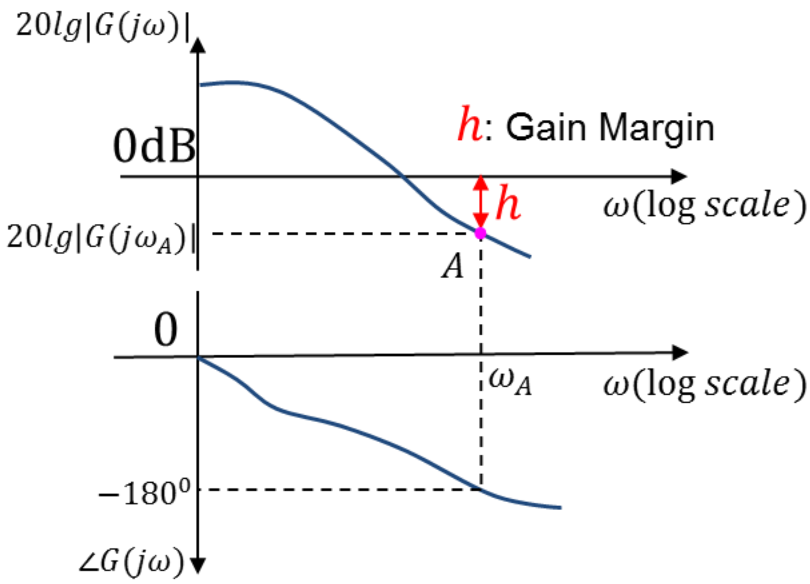

(b) Sketch of Bode plot

Fig. 4.1 Sketch diagram

Example 1: Select one amplifier whose open-loop transfer function is given by

$$G(s) = \frac{K(1+b_1 s)}{1+a_1 s+a_2 s^2} \tag{4.1}$$

Fig. 3.11 (c) shows a feedback amplifier (voltage follower) using this operational amplifier, and its closed-loop transfer function can be obtained as follows:

$$H(s) = \frac{G(s)}{1+G(s)} = \frac{K+Kb_1 s}{1+K+(a_1+Kb_1)s+a_2 s^2} \tag{4.2}$$

Based on the R-H stability criterion, we can also deduce the stability condition as following:

$$1+K>0,\ a_1+Kb_1>0,\ a_2>0 \tag{4.3}$$

We can obtain stability condition:

$$K < -\frac{a_1}{b_1}, \text{ in case } b_1<0$$

$$K > -\frac{a_1}{b_1}, \text{ in case } b_1>0 \tag{4.4}$$

In frequency domain, Eq. (4.1) is represented as:

$$G(j\omega) = \frac{K\big(1+b_1(j\omega)\big)}{1+a_1(j\omega)+a_2(j\omega)^2}$$

$$= \frac{K\,(1-a_2\omega^2+b_1a_1\omega^2)+jK(b_1\omega-a_1\omega-a_2b_1\omega^3)}{(1-a_2\omega^2)^2+a_1^2\omega^2} \tag{4.5}$$

According to the explanation of Nyquist plot that has been introduced in previous chapter, and based on the sketch Nyquist plot as shown in Fig. 4.1(a), we can find out that if the open-loop system is stable ($P=0$), the Nyquist plot must not encircle the plot $(-1, \mathrm{j}0)$. So the stability condition is given as follows:

$$\angle G(j\omega_2) = -\pi \tag{4.6}$$

$$|G(j\omega_2)| < 1 \tag{4.7}$$

Here, ω_2 is the frequency at point A.

Also according to the explanation of Bode plot that has been introduced in the previous chapter, and based on the sketch bode plot as shown in Fig.

4.1(b), we can find out that if the open-loop system is stable, the Bode plot should satisfy the following conditions:

$$\angle G(j\omega_1) = -\pi \tag{4.8}$$

$$\mathrm{GM} = 0 - 20lg|G(j\omega_1)| > 0 \tag{4.9}$$

By simple derivation, we can found out the stability condition that respective based on Nyquist plot and Bode plot as shown in Eq. (4.6), Eq. (4.7) and Eq. (4.8), Eq. (4.9) is actually identical.

Considering that Eq. (4.5), Eq. (4.6) and Eq. (4.8), we can obtain:

$$\omega_2^2 = \frac{1}{a_2}(1 - \frac{a_1}{b_1}) \tag{4.10}$$

Hence, the amplitude value of the point A is:

$$|G(j\omega_2)| = \left|\frac{K(1-a_2\omega_2^2 + b_1 a_1 \omega_2^2)}{(1-a_2\omega_2^2)^2 + a_1^2\omega_2^2}\right| = \frac{K\left|\frac{a_1}{b_1} + \frac{a_1}{a_2}(b_1 - a_1)\right|}{\left|(\frac{a_1}{b_1})^2 + \frac{a_1 a_1}{a_2 b_1}(b_1 - a_1)\right|} = K\left|\frac{b_1}{a_1}\right| \tag{4.11}$$

Based on calculation of Eq. (4.11) and condition Eq. (4.7) and Eq. (4.9), we can obtain the following inequality expression ultimately:

$$\begin{aligned} -\frac{a_1}{b_1} < K < \frac{a_1}{b_1}, &\quad \text{in case } a_1 b_1 > 0 \\ \frac{a_1}{b_1} < K < -\frac{a_1}{b_1}, &\quad \text{in case } a_1 b_1 < 0 \end{aligned} \tag{4.12}$$

Clearly, inequality expressions Eq. (4.4) and Eq. (4.12) are equivalent under some conditions. So, we can say that mathematical foundations of Nyquist and R-H stability criteria are equivalent.

Example 2: Select one amplifier whose open-loop transfer function is given by

$$G(s) = \frac{K(1+b_1 s)}{1+a_1 s+a_2 s^2+a_3 s^3} \tag{4.13}$$

Fig. 3.11 (c) show a feedback amplifier (voltage follower) using this operational amplifier, and the closed-loop transfer function is obtained as follows:

$$H(s) = \frac{G(s)}{1+G(s)} = \frac{K+Kb_1 s}{1+K+(a_1+Kb_1)s+a_2 s^2+a_3 s^3} \tag{4.14}$$

Based on the R-H stability criterion, we also can deduce the stability condition as following:

$$1+K>0,\ a_1+Kb_1>0,\ a_2>0,\ a_3>0,$$
$$\frac{a_2(a_1+Kb)-a_3(1+K)}{a_2}>0 \tag{4.15}$$

We can obtain stability condition:

$$K > \frac{a_3-a_1a_2}{a_2b-a_3},\quad \text{in case}\ \ a_2b-a_3>0$$
$$K < \frac{a_3-a_1a_2}{a_2b-a_3},\quad \text{in case}\ \ a_2b-a_3<0 \tag{4.16}$$

In frequency domain, Eq. (4.14) is represented as:

$$G(j\omega) = \frac{K\big(1+b_1(j\omega)\big)}{1+a_1(j\omega)+a_2(j\omega)^2+a_3(j\omega)^3}$$
$$= \frac{K[(1-a_2\omega^2+a_1b_1\omega^2-a_3b\omega^4)+j(b_1\omega-a_2b_1\omega^3-a_1\omega+a_3\omega^3)]}{(1-a_2\omega^2)^2+(a_1\omega-a_3\omega^3)^2} \tag{4.17}$$

According to the explanation of Nyquist plot that has been introduced in the previous chapter, and based on the sketch Nyquist plot as shown in Fig. 4.1(a), we can find out that if the open-loop system is stable ($P=0$), the Nyquist plot should not encircle the plot $(-1, \mathrm{j}0)$, so the stability condition is given as follows:

$$\angle G(j\omega_3) = -\pi \tag{4.18}$$
$$|G(j\omega_3)| < 1 \tag{4.19}$$

Here, ω_3 is the frequency at the point A.

Also according to the explanation of Bode plot that has been introduced in the previous chapter, and based on the sketch bode plot as shown in Fig. 4.1(b), we can find out that if the open-loop system is stable, the Bode plot should satisfy the following conditions:

$$\angle G(j\omega_1) = -\pi \tag{4.20}$$
$$\mathrm{GM} = 0 - 20lg|G(j\omega_1)| > 0 \tag{4.21}$$

By simple derivation, we can found out the stability condition that respective based on Nyquist plot and Bode plot as shown in Eq. (4.18), Eq. (4.19) and Eq. (4.20), Eq. (4.21) is actually identical.

Considering Eq. (4.17), Eq. (4.18) and Eq. (4.20), we can obtain:

$$\omega_3^2 = \frac{a_1 - b_1}{a_3 - a_2 b_1} \tag{4.22}$$

Hence, the amplitude value of the point A is:

$$|G(j\omega_3)| = \left|\frac{K(1 - a_2\omega_3^2 + a_1 b_1 \omega_3^2 - a_3 b_1 \omega_3^4)}{(1 - a_2\omega_3^2)^2 + (a_1\omega - a_3\omega_3^3)^2}\right| = K\left|\frac{a_3 - a_2 b_1}{a_3 - a_1 a_2}\right| \tag{4.23}$$

Based on calculation of Eq. (4.23) and condition Eq. (4.19) and Eq. (4.21), we can obtain the following inequality expression ultimately:

$$\frac{a_3 - a_1 a_2}{a_2 b - a_3} < K < \frac{a_3 - a_1 a_2}{a_3 - a_2 b}, \text{ in case } (a_3 - a_1 a_2)(a_3 - a_2 b) > 0$$
$$\frac{a_3 - a_1 a_2}{a_3 - a_2 b} < K < \frac{a_3 - a_1 a_2}{a_2 b - a_3}, \text{ in case } (a_3 - a_1 a_2)(a_3 - a_2 b) < 0 \tag{4.24}$$

Clearly, inequality expressions Eq. (4.24) and Eq. (4.16) are equivalent under some conditions. So, we can say that mathematical foundations of Nyquist and R-H stability criteria are equivalent.

Example 3: Select one amplifier whose open-loop transfer function is given by

$$G(s) = \frac{K(1+b_1s+b_2s^2)}{1+a_1s+a_2s^2+a_3s^3} \tag{4.25}$$

Fig.3.11(c) show a feedback amplifier (voltage follower) using this operational amplifier, and the closed-loop transfer function is obtained as follows:

$$H(s) = \frac{G(s)}{1+G(s)} = \frac{K+Kb_1s+Kb_2s^2}{1+K+(a_1+Kb_1)s+(a_2+Kb_2)s^2+a_3s^3} \tag{4.26}$$

Based on the R-H stability criterion, we also can deduce the stability condition as follows:

$$(a_2 + Kb_2)(a_1 + Kb_1) - a_3(1 + K) > 0 \tag{4.27}$$

Let set one function:

$$\begin{aligned} f(K) &= (a_2 + Kb_2)(a_1 + Kb_1) - a_3(1 + K) \\ &= K^2b_1b_2 + Ka_1b_2 + Ka_2b_1 - Ka_3 + a_1a_2 - a_3 \end{aligned} \tag{4.28}$$

- Domain of definition $K \in (0, +\infty)$
- Initial value:

$$f(0) = a_1a_2 - a_3 \tag{4.29}$$

- Derived function:

$$f'(\mathrm{K}) = 2Kb_1b_2 + a_1b_2 + a_2b_1 - a_3 \tag{4.30}$$

For getting to the stability condition Eq. (4.27), the following conditions should be satisfied:

$$f(0) \geq 0, \text{and } f'(\mathrm{K}) > 0 \tag{4.31}$$

Thus, the stability condition yields to the following:

$$2Kb_1b_2 + a_1b_2 + a_2b_1 - a_3 > 0 \tag{4.32}$$

at condition: $a_1a_2 - a_3 > 0$.

In frequency domain, Eq. (4.25) is represented as:

$$G(j\omega) = \frac{K(1 + b_1(j\omega) + b_2(j\omega)^3)}{1 + a_1(j\omega) + a_2(j\omega)^2 + a_3(j\omega)^3} =$$

$$\frac{K\,(1-a_2\omega^2-b_2\omega^2+a_2b_2\omega^4+a_1b_1\omega^2-a_3b_1\omega^4)+jK(a_3\omega^3-a_1\omega+a_1b_2\omega^3-a_3b_2\omega^5+b_1\omega-a_2b_1\omega^3)}{(1-a_2\omega^2)^2+(a_1\omega-a_3\omega^3)^2} \tag{4.33}$$

According to the explanation of Nyquist plot that has been introduced in the previous chapter, and based on the sketch Nyquist plot as shown in Fig. 4.1(a), we can find out that if the open-loop system is stable ($P = 0$), the Nyquist plot must not encircle the plot $(-1, \mathrm{j}0)$, so the stability condition as follows:

$$\angle G(j\omega_4) = -\pi \tag{4.34}$$
$$|G(j\omega_4)| < 1 \tag{4.35}$$

Here, ω_4 is the frequency at point A.

Also according to the explanation of Bode plot that has been introduced in the previous chapter, and based on the sketch Bode plot as shown in Fig. 4.2(b), we can find out that if the open-loop system is stable, the Bode plot should satisfy the following conditions:

$$\angle G(j\omega_1) = -\pi \tag{4.36}$$
$$\mathrm{GM} = 0 - 20lg|G(j\omega_1)| > 0 \tag{4.37}$$

By simple derivation, we can find out the stability condition that respective based on Nyquist plot and Bode plot as shown in Eq.(4.34), Eq.(4.35) and Eq.(4.36), Eq.(4.37) is actually identical.

Considering Eq. (4.33), Eq. (4.34) and Eq. (4.36), we can obtain:

$$a_3\omega_4^3 - a_1\omega_4 + a_1b_2\omega_4^3 - a_3b_2\omega_4^5 + b_1\omega_4 - a_2b_1\omega_4^3 = 0. \quad (4.38)$$

After transformation, we can obtain:

$$1 - a_2\omega_4^2 = \frac{(1-b_2\omega_4^2)(a_1-a_3\omega_4^2)}{b_1} \quad (4.39)$$

Hence, the amplitude value of point A is:

$$|G(j\omega_4)| = \left|\frac{K1-a_2\omega_4^2-b_2\omega_4^2+a_2b_2\omega_4^4+a_1b_1\omega_4^2-a_3b_1\omega_4^4}{(1-a_2\omega_4^2)^2+(a_1\omega_4-a_3\omega_4^3)^2}\right| = \cdots = \frac{Kb_1}{|a_1-a_3\omega_4^2|} \quad (4.40)$$

From Eq. (4.38), we have

$$a_3b_2\omega_4^4 + (a_2b_1 - a_1b_2 - a_3)\omega_4^2 + a_1 - b_1 = 0 \quad (4.41)$$

Solution of Eq. (4.41):

$$\omega^2 = \frac{a_3+a_1b_2-a_2b_1 \pm \sqrt{(a_2b_1-a_1b_2-a_3)^2-4a_3b_2(a_1-b_1)}}{2a_3b_2} \approx \frac{a_3+a_1b_2-a_2b_1}{2a_3b_2} \quad (4.42)$$

From Eq. (4.42), Eq. (4.40) and condition Eq. (4.27):

$$|G(j\omega_4)| = \frac{K|b_1|}{|a_1-a_3\omega_4^2|} = \frac{K|b_1|}{\left|a_1-a_3\frac{a_3+a_1b_2-a_2b_1}{2a_3b_2}\right|} = \frac{K|2b_1b_2|}{|a_1b_2+a_2b_1-a_3|} < 1 \quad (4.43)$$

By calculation we can obtain the following inequality expression ultimately:

$$a_3 - a_1b_2 - a_2b_1 < 2Kb_1b_2 < a_1b_2 + a_2b_1 - a_3$$

in case $a_1 b_2 + a_2 b_1 - a_3 > 0$

$$a_1 b_2 + a_2 b_1 - a_3 < 2K b_1 b_2 < a_3 - a_1 b_2 - a_2 b_1$$
$$\text{in case } a_1 b_2 + a_2 b_1 - a_3 < 0 \quad (4.44)$$

Clearly, inequality expressions Eq. (4.32) and Eq. (4.44) are equivalent under some conditions. So, we can say that mathematical foundations of Nyquist and R-H stability criteria are equivalent.

4.2 Relationship between R-H parameters and phase margin

Example1: Consider the two-pole amplifier as shown in Fig. 3.10. Accordingly, Fig. 3.11 (b) shows a feedback amplifier using this operational amplifier, and its closed-loop transfer function is shown in Eq. (3.18). Based on the R-H stability criterion, we can obtain the explicit stability condition is shown in Eq. (3.21).

Table. 4.1 Data collection

f=0.01										
C_{r1} [fF]	10	20	30	40	50	60	70	80	90	…
θ [uS]	0.11	0.18	0.25	0.32	0.39	0.46	0.53	0.60	0.67	…
PM [degree]	16	19	22	24	27	29	31	33	34	…
GM [dB]	9.1	7.6	7.0	6.6	6.4	6.3	6.2	6.0	6.0	…
F_{gm} [GHz]	4.5	3.4	2.9	2.6	2.3	2.1	2.0	1.9	1.8	…
F_{pm} [GHz]	2.6	2.1	1.8	1.5	1.4	1.2	1.1	1.0	9.4	…

We define the R-H parameter θ as one time dimension parameter. Using the parameter values of short-channel CMOS devices, and calculating the values of parameter θ and the corresponding operational amplifier system phase margin (PM), gain margin (GM), F_{gm} and F_{pm} at various feedback factor f conditions, using MATLAB. F_{gm} is the frequency where the gain margin is measured, which is a -180^o phase crossing frequency in Bode plot, and F_{pm} is the frequency where the phase margin is measured, which is a 0dB gain crossing frequency in Bode plot. For example, when feedback factor $f = 0.01$, we can obtain the values as Table. 4.1.

Using the polyfit function of MATLAB, we can obtain the fitted curve which can indicate the relationship between parameter θ with phase margin as shown in Fig. 4.2 in variation feedback factor conditions. In feedback factor $f = 0.01$ condition, we can obtain the fitted curve as shown in Fig. 4.3, and its corresponding relation function is given as follows:

$$PM = 2.601e^{28}\theta^5 - 5.616e^{23}\theta^4 + 4.683e^{18}\theta^3 - 1.915e^{13}\theta^2 + 4.076e^{28}\theta + 13.38 \tag{4.45}$$

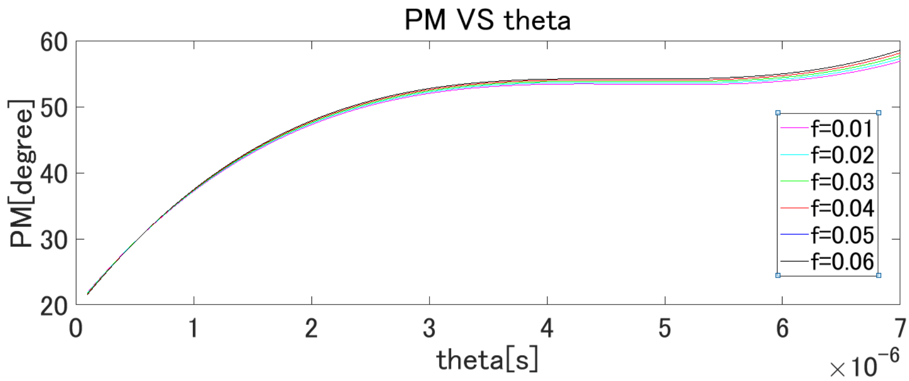

Fig. 4.2 Relationship between PM and parameter **θ** in various feedback factor conditions. PM= phase margin, theta= parameter **θ**.

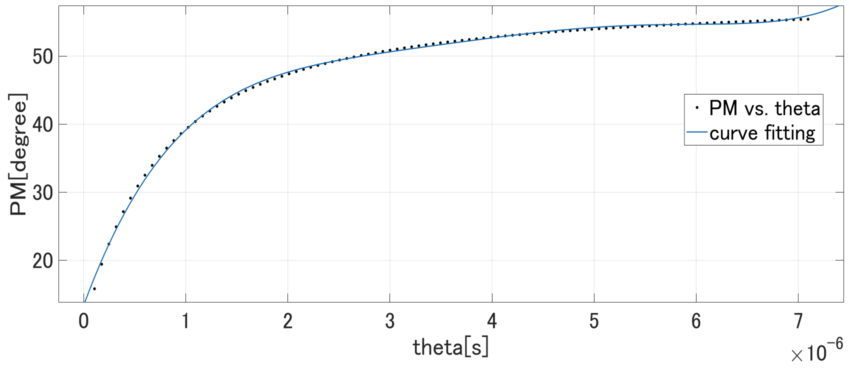

Fig. 4.3 Relationship between PM and parameter $\boldsymbol{\theta}$ at feedback factor $\boldsymbol{f} = \mathbf{0.01}$ condition. PM= phase margin, theta= R-H parameter $\boldsymbol{\theta}$.

As shown in Fig. 4.2 and Fig. 4.3, the PM and the R-H parameter θ have the monotonic relationship, following with increase of the parameter value, the phase margin increases, in other words, the feedback system becomes more stable.

We can calculate the required value of the compensation capacitor, for a given operational amplifier PM, based on the calculated value of the parameter θ.

Example2: Consider the two-pole amplifier as shown in Fig. 3.12, whose open-loop transfer function is given by

$$G(s) = \frac{K(1+b_1 s)}{1+a_1 s+a_2 s^2+a_3 s^3} \tag{4.46}$$

Accordingly, Fig. 3.11 (b) shows a feedback amplifier using this operational amplifier, and its closed-loop transfer function is shown as Eq. (3.22). Based on the R-H stability criterion, we can obtain the stability condition is shown as Eq. (3.26).

We also define the R-H parameter α_1, β_1 as time dimension parameters. Using the parameter values of short-channel CMOS devices, and calculating the values of parameters α_1, β_1 and the corresponding feedback system PM, in variation feedback factor f conditions by MATLAB. In feedback factor $f = 0.01$ condition, we can obtain the relation function in Fig. 4.4, when parameters α_1, β_1 as independent variables and PM as dependent variable by using interpolation function in curve fitting tool of MATLAB.

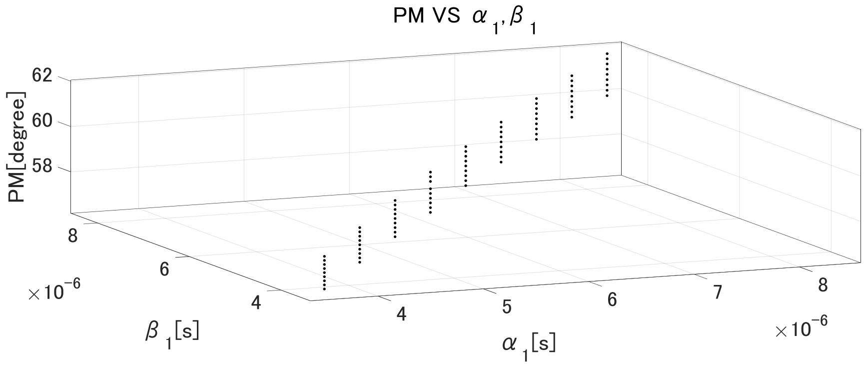

Fig. 4. 4 Relationship between PM with parameter $\boldsymbol{\alpha_1, \beta_1}$ in feedback factor $\boldsymbol{f = 0.01}$ condition. PM= phase margin, $\boldsymbol{\alpha_1, \beta_1}$= R-H parameters.

As shown in Fig. 4.4, the relationship between R-H parameter α_1, β_1 with PM is monotonic one, and following with increase of the parameter value, the phase margin increases, in other words, the feedback system becomes more stable.

4.3 Summary

During our derivation using various examples, we can find out that the inequality expressions respective based on Nyquist and R-H stability criteria are equivalent under some conditions. So, we can say that mathematical foundations of Nyquist and R-H stability criteria are equivalent. Through the analysis of the data in the software we found that the relationship that between R-H parameter with phase margin is monotonic one, and following with increase of the parameter value, the phase margin increases, in other words, the feedback system becomes more stable.

CHAPTER V
VERFICATION WITH SPICE SIMULATION

In this chapter, we describe the verification of our theoretical analysis and derivation results obtained in the previous chapter. The simulation is performed with LTspice (Linear Technology Simulation Program with Integrated Circuit Emphasis) software which is one of SPICE simulators for free.

5.1 Equivalence verification

Table. 5.1 Parameter values of the amplifier 1

	Parameter values							R-H criterion	Bode plot
case	R_1	C_1	R_2	C_2	G_{m1}	G_{m2}	C_{r1}	θ	SPICE simulation
(1)	$50k$	$10f$	10k	$0.1p$	0.01	$8m$	$1p$	< 0	unstable
(2)	$50k$	$1f$	10k	$10f$	0.01	$8m$	$0.1p$	< 0	unstable
(3)	$100k$	$100f$	$10k$	$1f$	$9m$	$4m$	$0.1p$	< 0	unstable
(4)	$100k$	$5f$	$90k$	$3f$	$8m$	$7.5m$	$0.9p$	≈ 0	critical stable
(5)	$100k$	$3f$	$50k$	$1f$	$8.5m$	$8m$	$0.5p$	≈ 0	critical stable
(6)	$1meg$	$6f$	$500k$	$0.5f$	$80u$	$70u$	$1f$	≈ 0	critical stable
(7)	$50k$	$10f$	100	$0.1p$	0.01	$8m$	$1p$	> 0	stable
(8)	$100k$	$5f$	$90k$	$3f$	$80u$	$70u$	$0.9p$	> 0	stable
(9)	$150k$	$6f$	$100k$	$1.5f$	$80u$	$70u$	$0.5p$	> 0	stable

We calculate the values of the parameters θ, α_1, β_1 as shown in Eq. (3.20), Eq. (3.24), Eq. (3.25) and depict Bode plots using SPICE for judging stability of the amplifier with the voltage follower configuration (Fig. 3.11(c)) for amplifiers 1, 2 . See Table. 5.1, Figs. 5.1, 5.2, 5.3 as amplifier 1, Table. 5.2, Figs. 5.4, 5.5, 5.6 as amplifier 2.

Table. 5.2 Parameter values of the amplifier 2

	Parameter values								R-H criterion		Bode plot
case	R_1	C_1	R_2	C_2	G_{m1}	G_{m2}	R_r	C_{r2}	∂_1	β_1	SPICE simulation
(1)	$115k$	$5f$	$100k$	$80f$	$9m$	$8m$	5	$0.5p$	< 0	< 0	unstable
(2)	$50k$	$5f$	$10k$	$10f$	$9m$	$8m$	2	$0.2p$	< 0	< 0	unstable
(3)	$150k$	$5f$	$100k$	$10f$	$9m$	$8m$	1	$0.8p$	< 0	< 0	unstable
(4)	$110k$	$10f$	$10k$	$3f$	0.01	$8m$	5	$0.5f$	≈ 0	≈ 0	critical
(5)	$115k$	$10f$	$100k$	$3f$	0.01	$8m$	5	$0.5f$	≈ 0	≈ 0	critical
(6)	$150k$	$8f$	$100k$	$50f$	$7m$	$8m$	10	$0.6p$	> 0	> 0	stable
(7)	$100k$	$8f$	$80k$	$50f$	$6m$	$8m$	5	$0.6p$	> 0	> 0	stable
(8)	$200k$	$5f$	$150k$	$10f$	$5m$	$7m$	2.5	$0.6p$	> 0	> 0	stable

Then we show analysis between their simulation results and the parameter values of θ, α_1 and β_1. We found out the following: when θ, α_1 and β_1 are greater than 0, less than 0 and approximate to 0, then the corresponding amplifier with the voltage follower configuration in Fig. 3.11 (b) is stable, unstable and critical stable respectively.

We can distinctly find that the amplifier stability depends on the parameters $\theta, \alpha_1, \beta_1$, and the feedback system is stable if and only if the parameters θ, α_1 and β_1 are positive.

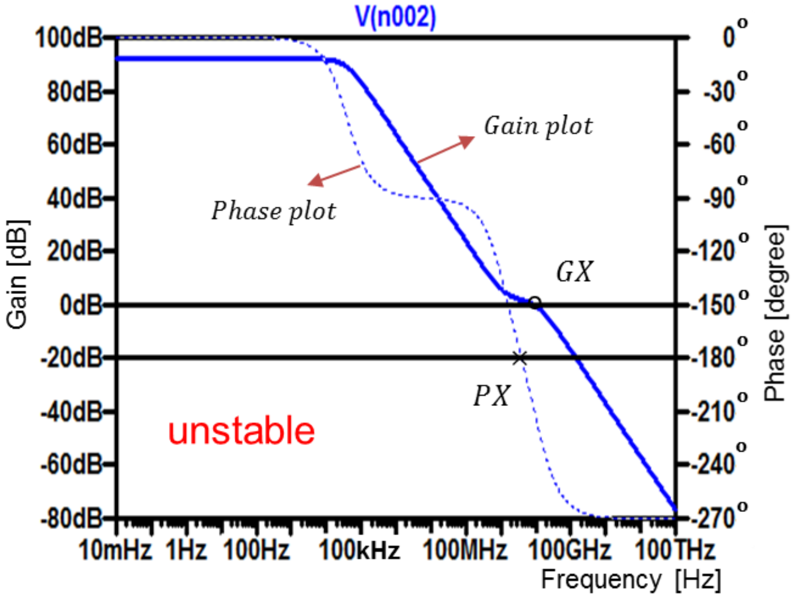

Fig. 5.1 Bode plots for case (1) of unstable amplifier 1. GX= gain crossover point, PX= phase crossover point.

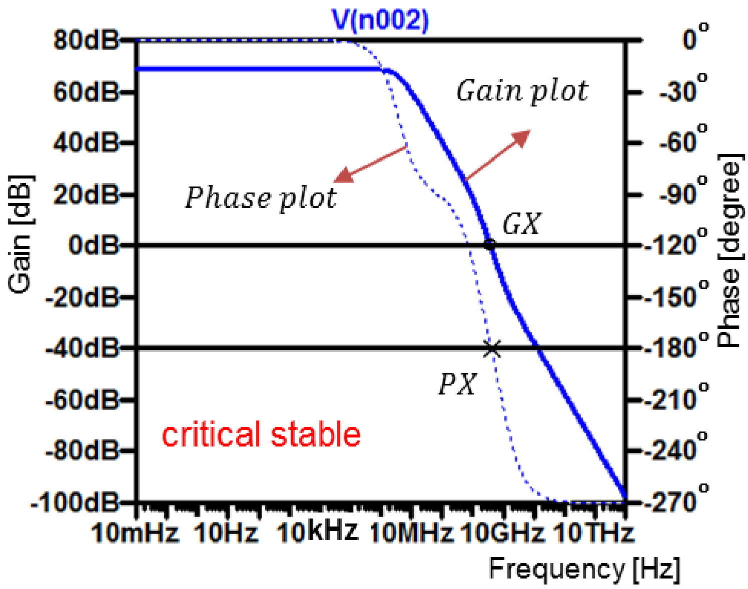

Fig. 5.2 Bode plot for case (6) of critical stable amplifier1. GX= gain crossover point, PX= phase crossover point.

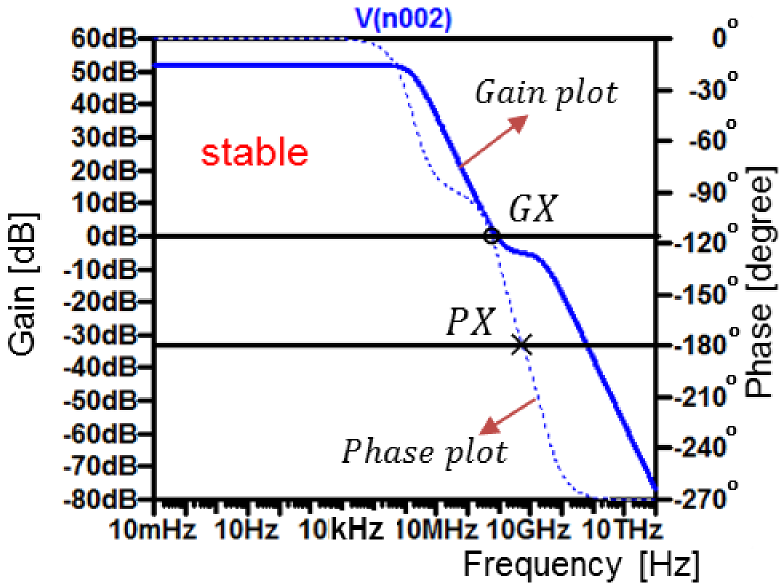

Fig. 5.3 Bode plot for case (7) of stable amplifier 1. GX= gain crossover point, PX= phase crossover point.

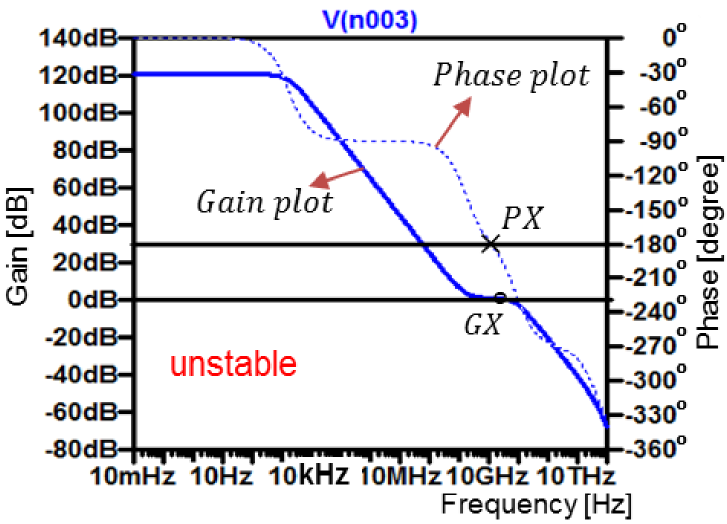

Fig. 5.4 Bode plot for case (3) of unstable amplifier2. GX= gain crossover point, PX= phase crossover point.

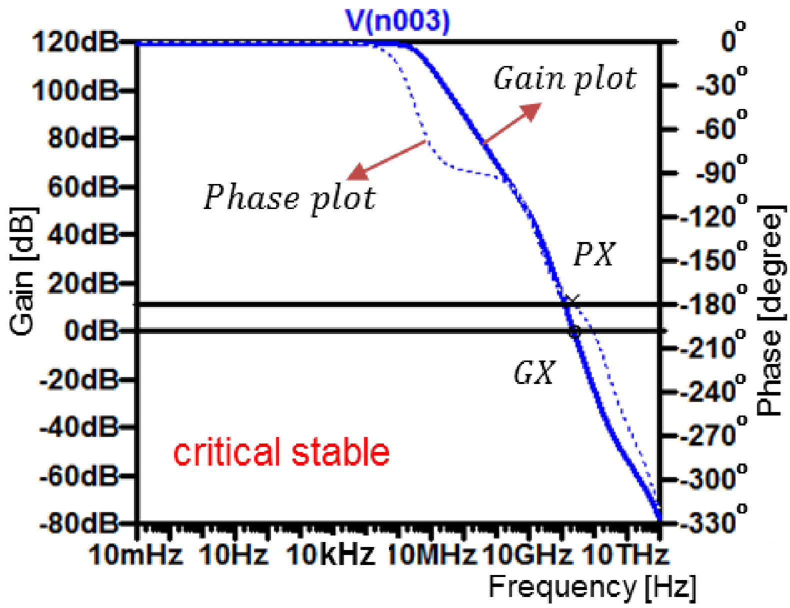

Fig. 5.5 Bode plot for case (5) of critical stable amplifier 2. GX= gain crossover point, PX= phase crossover point.

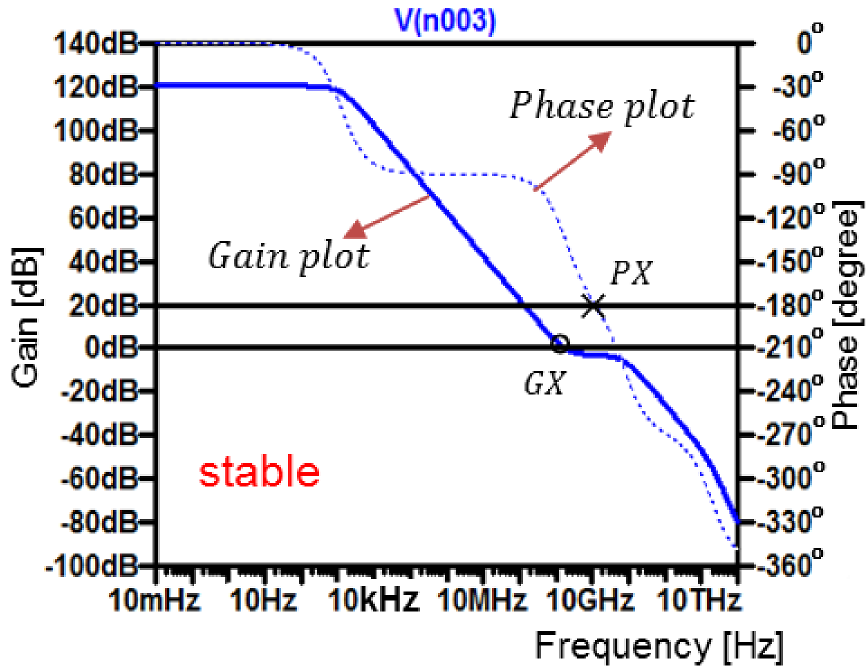

Fig. 5.6 Bode plots for case (8) of the stable amplifier 2. GX= gain crossover point, PX= phase crossover point.

5.2 Application verification

Using the parameter values of short-channel CMOS devices (Appendix), and calculating inequality expressions Eq. (3.21) and Eq. (3.26), we can obtain the value range of the compensation capacitor C_{r1} :

$$C_{r1} > 79.57\text{fF} \tag{5.1}$$

We also obtain the following inequality expression:

$$3.5 \times 10^{-8} + 3.7 \times 10^{10} C_{r2} + R_r C_{r2} + 831.7 R_r > \frac{4.3\times10^{-8} R_r C_{r2}}{5.1\times10^{-17} + 4.3\times10^{-3} C_{r2} + 3.5\times10^{-8} R_r C_{r2}} \tag{5.2}$$

Let,

$$X = 3.5 \times 10^{-8} + 3.7 \times 10^{10} C_{r2} + R_r C_{r2} + 831.7 R_r$$
$$Y = \frac{4.3\times10^{-8} R_r C_{r2}}{5.1\times10^{-17} + 4.3\times10^{-3} C_{r2} + 3.5\times10^{-8} R_r C_{r2}} \tag{5.3}$$

We select several values of the parameters in Eq. (5.1), Eq. (5.2) and depict their Bode plots using SPICE (LTspice) for judging stability of the amplifier with the voltage follower configuration. See Table. 5.3, Fig. 5.7~Fig. 5.12 as amplifier 3, Table. 5.4, Fig. 5.13~Fig. 5.18 as amplifier 4. The frequency in these transient analysis simulations is 1×10^5Hz.

Table. 5.3 Parameter values of the amplifier 3

case	C_r	SPICE
(1)	2.4pF	stable
(2)	79.57fF	critical stable
(3)	10fF	unstable

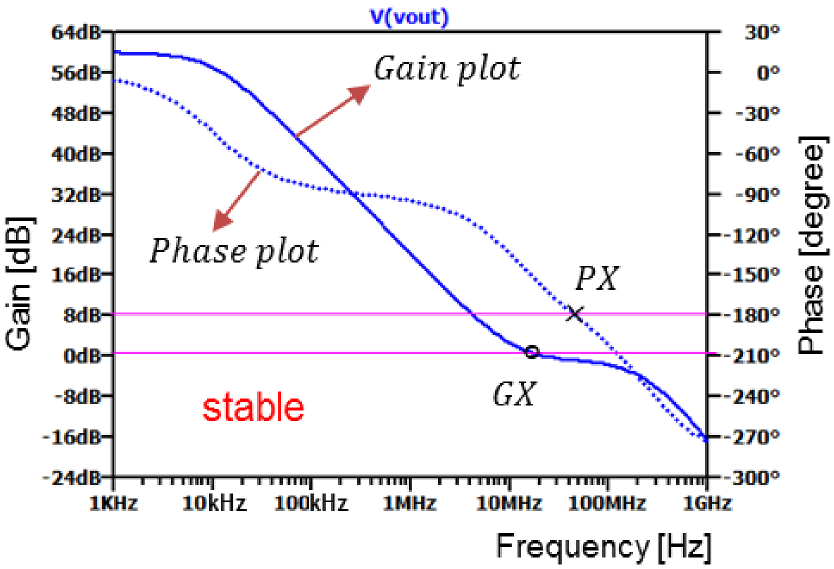

Fig. 5.7 Bode plot for case (1) of the stable amplifier 3. GX= gain crossover point, PX= phase crossover point.

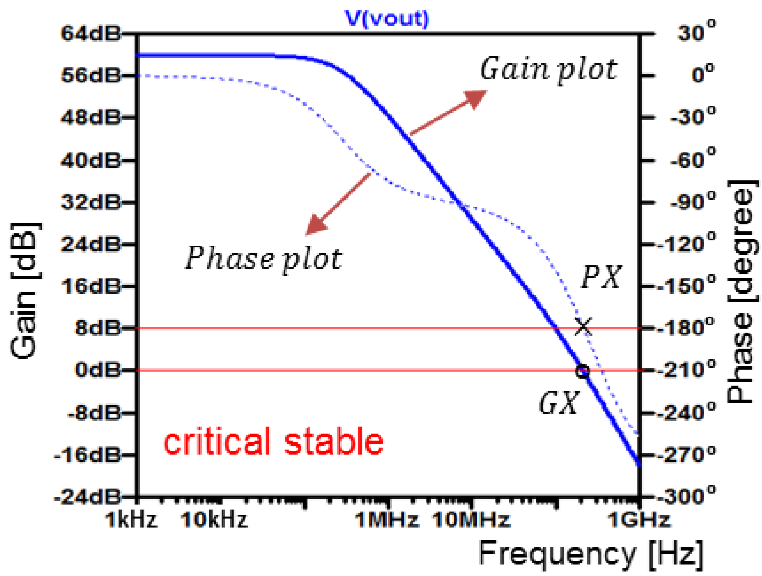

Fig. 5.8 Bode plot for case (2) of the critical stable amplifier 3. GX= gain crossover point, PX= phase crossover point.

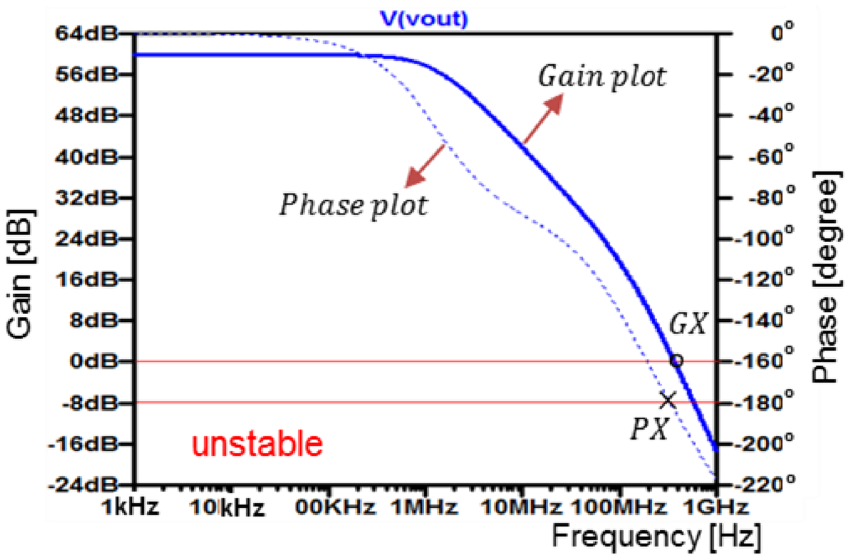

Fig. 5.9 Bode plot for case (3) of the unstable amplifier 3. GX= gain crossover point, PX= phase crossover point.

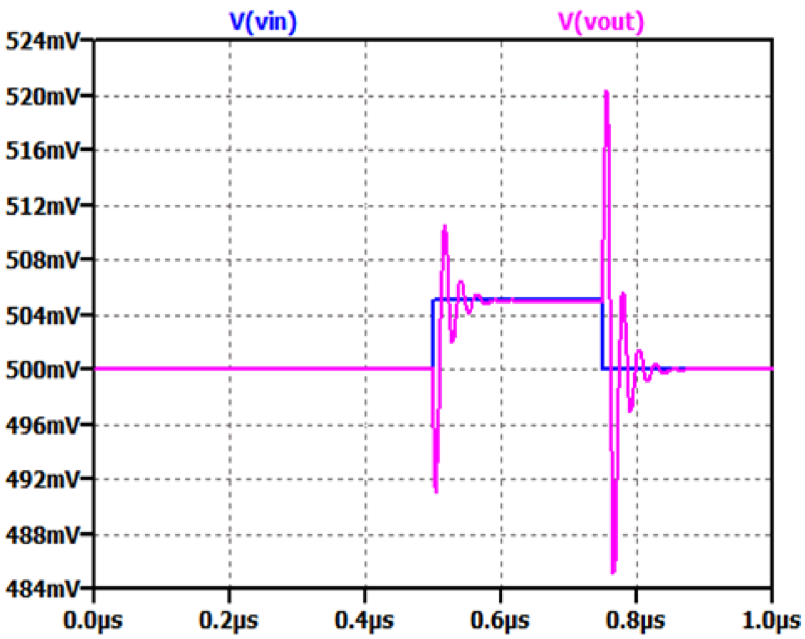

Fig. 5.10 Pulse response for case (1) of the stable amplifier 3

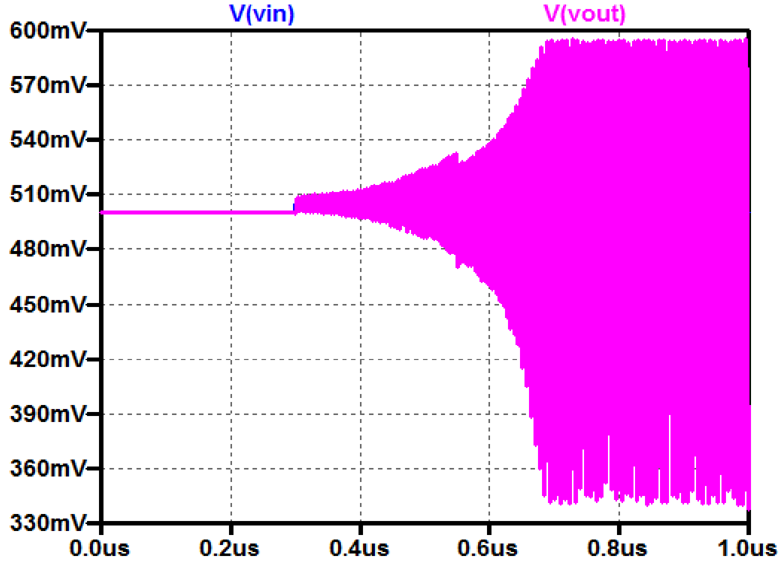

Fig. 5.11 Pulse response for case (2) of the critical stable amplifier 3

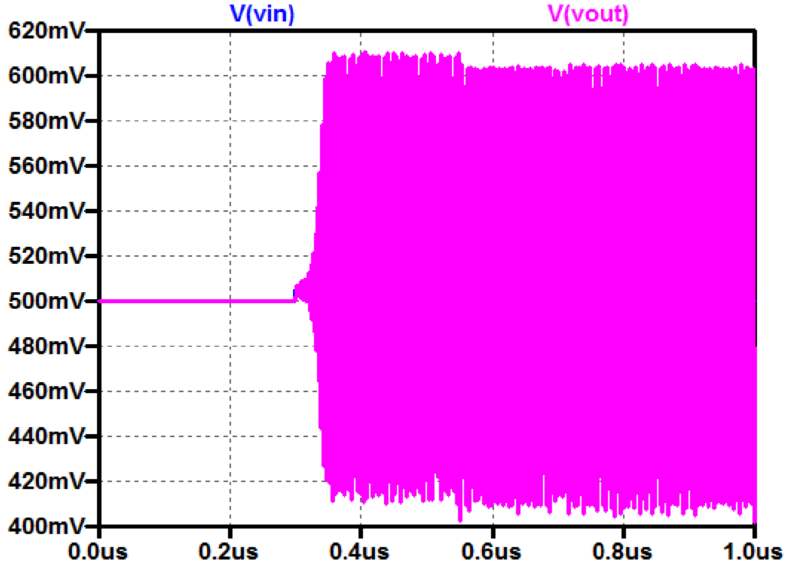

Fig. 5.12 Pulse response for case (3) of the unstable amplifier 3

Table. 5.4 Parameter values of the amplifier 4

	Parameter values				R-H criterion	Bode plot
Case	R_r	C_r	X	Y		SPICE simulation
(1)	6.5k	2.4p	1.41×10^{-5}	6.13×10^{-8}	$X > Y$	stable
(2)	1	2.4p	1.10×10^{-6}	9.94×10^{-12}	$X > Y$	stable
(3)	7k	10f	9.8×10^{-8}	3.10×10^{-8}	$X \approx Y$	critical

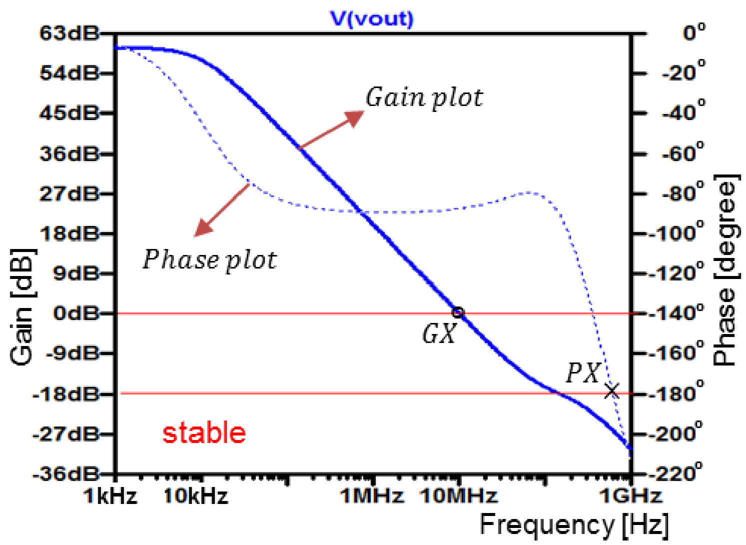

Fig. 5.13 Bode plot for case (1) of the stable amplifier 4. GX= gain crossover point, PX= phase crossover point.

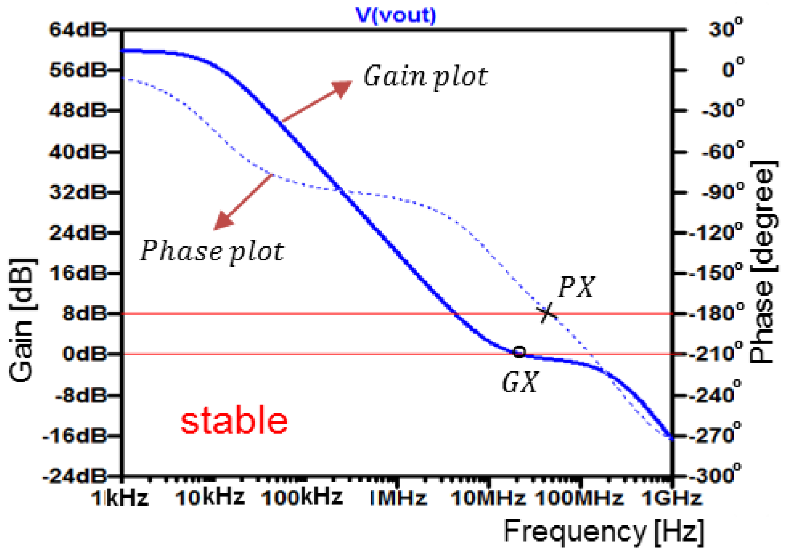

Fig. 5.14 Bode plot for case (2) of the stable amplifier 4. GX= gain crossover point, PX= phase crossover point.

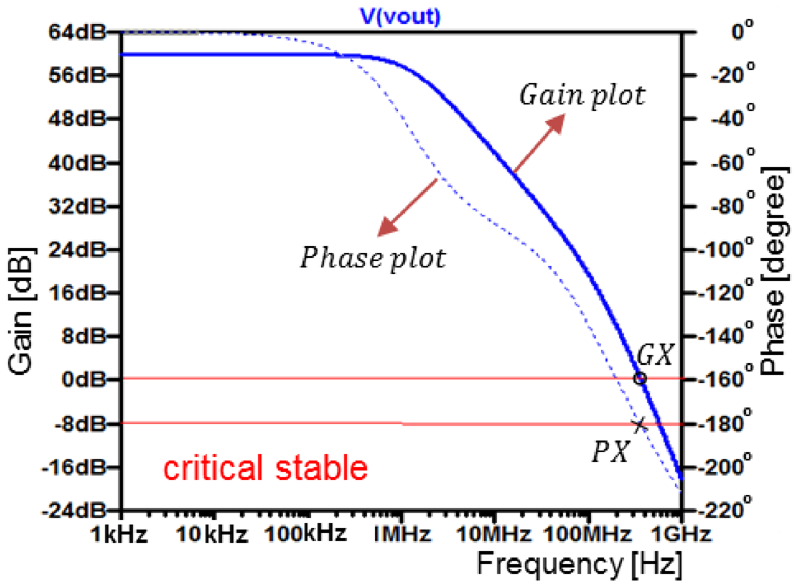

Fig. 5.15 Bode plot for case (3) of the critical stable amplifier 4. GX= gain crossover point, PX= phase crossover point.

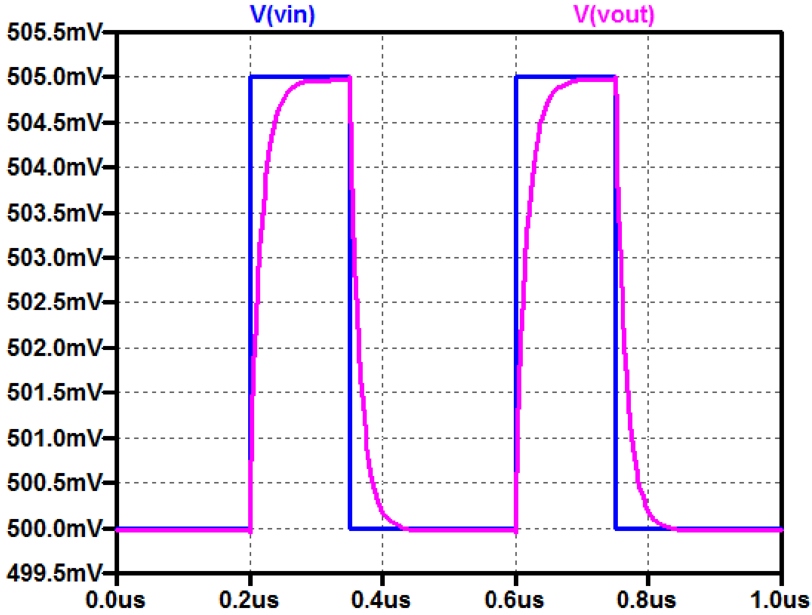

Fig. 5.16 Pulse response for case (1) of the stable amplifier 4

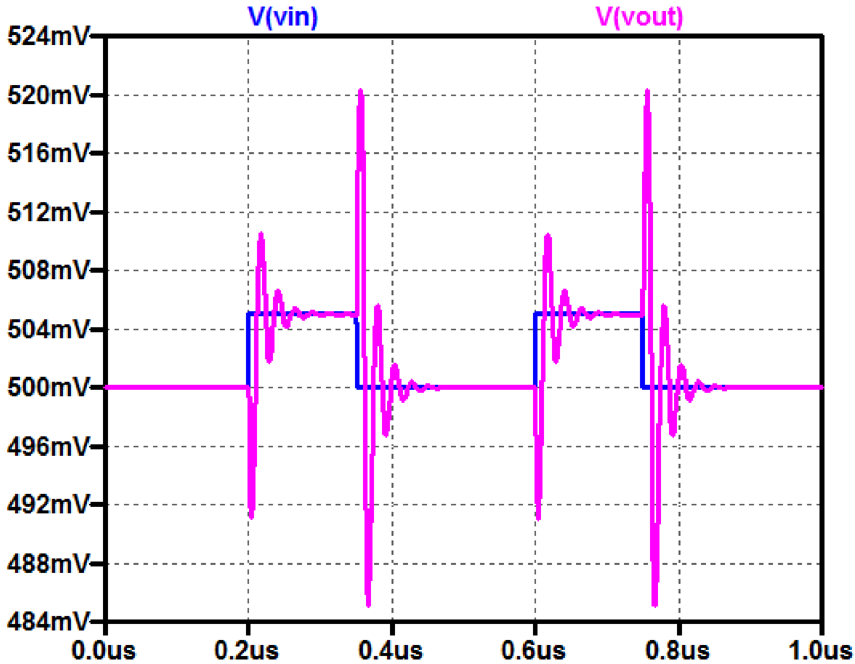

Fig. 5.17 Pulse response for case (2) of the stable amplifier 4

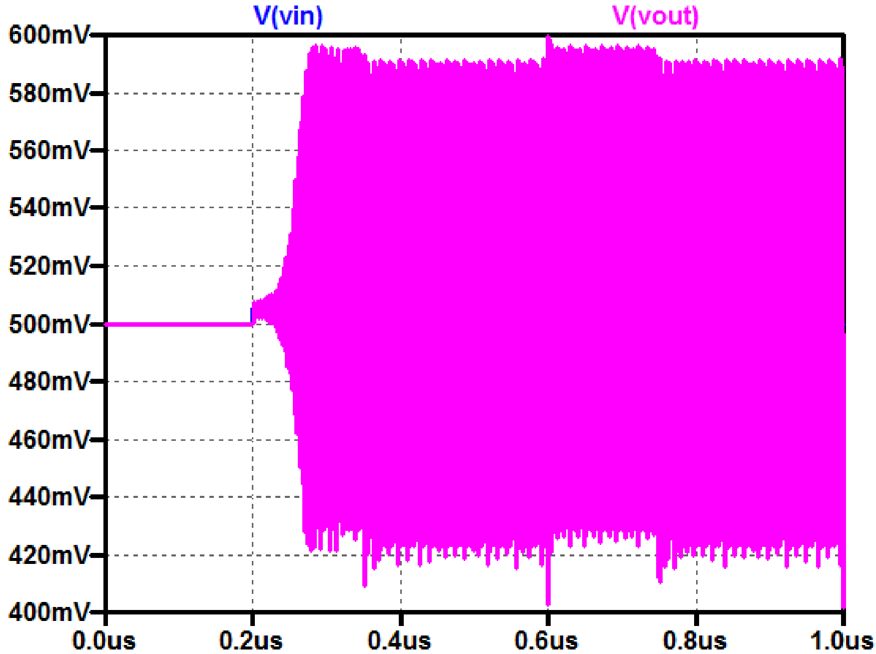

Fig. 5.18 Pulse response for case (3) of the critical stable amplifier 4

Consider the two-pole amplifier in Fig. 5.19. Based on the principle and processing represented in the previous chapter, we obtain the parameter θ as shown in Eq. (3.20). We can calculate the required value of the compensation capacitor, for a given operational amplifier phase margin (PM), based on the calculated value of the parameter θ. Using the polyfitt function, we can obtain the curves which can indicate the relationship between capacitor C_{r1} and phase margin as Fig. 5.20.

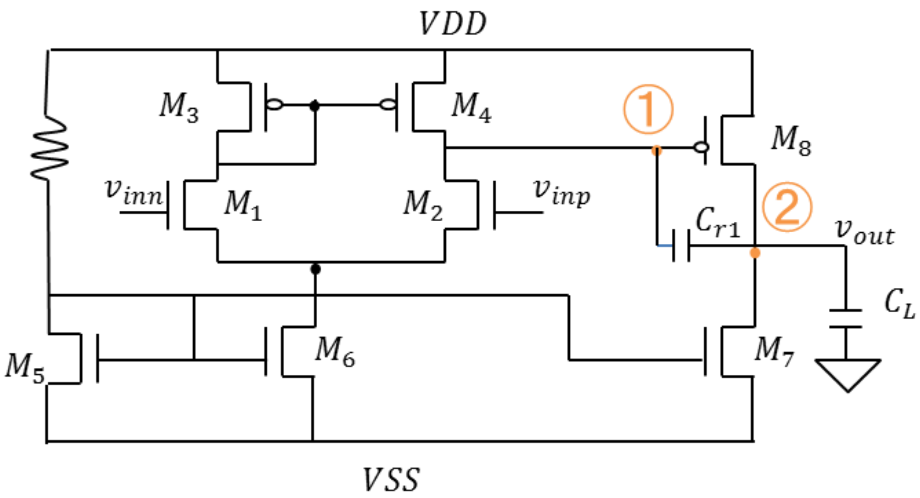

(a) Transistor level circuit

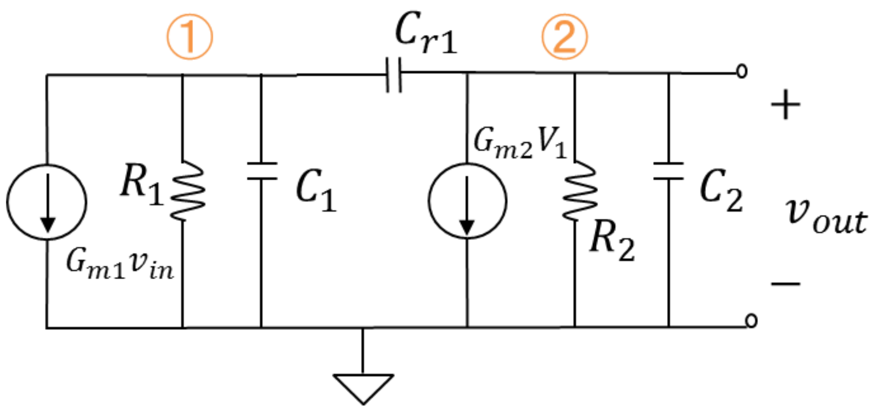

(b) Small-signal model

Fig. 5.19 Two-pole amplifier with inter-stage capacitance. R_1, R_2= equivalent resistors, C_1, C_2= equivalent capacitances, G_{m1}, G_{m2}= transconductances, and C_{r1}= compensation capacitance.

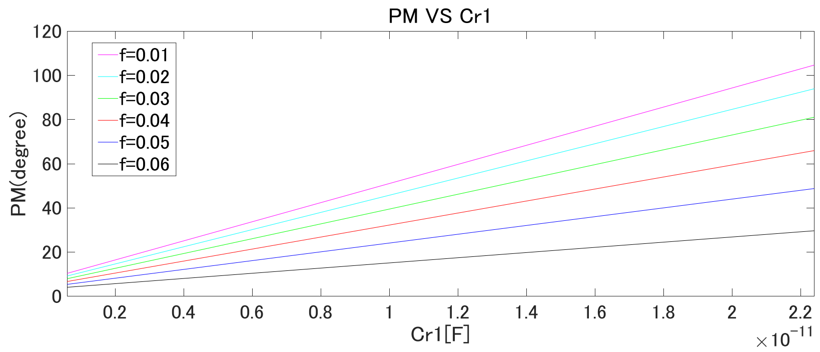

Fig. 5.20 Relationship between PM with compensation capacitor C_{r1} in variation feedback factor f conditions.

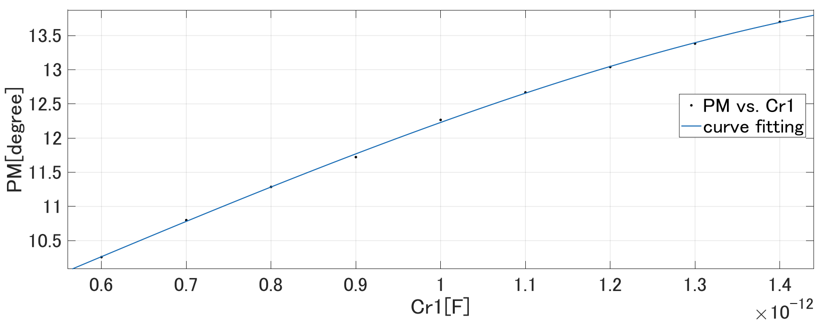

(a) Compensation capacitor C_{r1} as independent variable and PM as dependent variable.

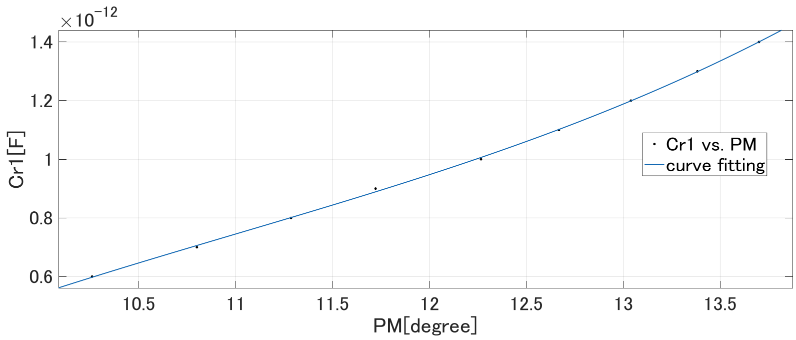

(b) PM as independent variable and compensation capacitor C_{r1} as dependent variable.

Fig. 5.21 Relationship between PM with compensation capacitor C_{r1} at feedback factor $f = 0.01$ condition.

In feedback factor $f = 0.01$ condition, we can obtain the fitted curve as Fig. 6.21 and the relation function between PM with capacitor as following:

$$PM = -1.026e^{36}{C_{r1}}^3 + 1.52e^{24}{C_{r1}}^2 + 4.488e^{12}C_{r1} + 7.24 \qquad (5.4)$$

$$Cr1 = 6.343e^{-15}PM^3 - 2.091e^{-13}PM^2 + 2.493e^{-12}PM - 9.822e^{-12} \qquad (5.5)$$

If we want to obtain 45^{o} phase margin, the needed corresponding capacitor value is $0.25694\mathrm{nF}$ by calculation from function Eq. (5.5).

For verifying this result, we have performed simulation using amplifier circuit shown in Fig. 5.19, the feedback system circuit shown in Fig. 3.11(b) when the feedback factor $f = 0.01$, and compensation capacitance is 0.25694nF. The simulation result is shown in Fig. 5.22. The phase margin result is $180^{\circ} - 133^{\circ} = 47^{\circ}$ obtained from LTspice simulation, and it is similar to the result $45^{\circ}$from function Eq. (5.5).

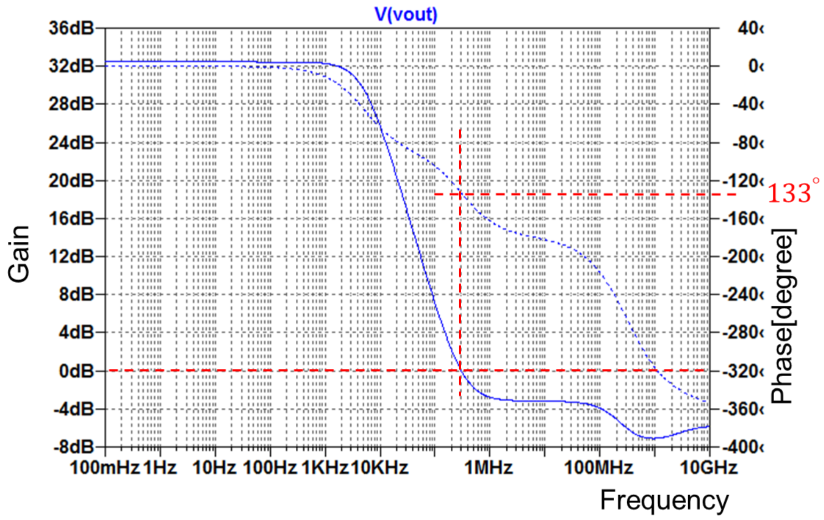

Fig. 5.22 LTspice simulation result with conditions: feedback factor $\boldsymbol{f} = \mathbf{0.01}$, compensation capacitor of $\mathbf{0.25694nF}$.

Although the relationship between Cr1 and the phase margin (corresponding to Fig. 5.19) can be obtained by using the small equivalent circuit which can indicate the variation tendency of stability following the circuit parameter variation. But as we see, this relationship only can reflect the impact from single circuit parameter on stability. The advantages of the proposed method are through the explicit stability condition Eq. (3.21), Eq. (3.26), Eq. (3.31) and relationship between parameter and phase margin (corresponding function Eq. (4.54) and Fig. 4.3), we can overall consider consideration multiple circuit parameters one time as well as the trade-off analysis between the influences on system stability from every single circuit parameter.

5.3 Summary

In this chapter, we have performed simulation to verify our theoretical analysis and derivation results obtained in previous chapter. By observing our simulation results, we can clearly see that the conclusion of the R-H method is the same as that of the traditional Bode plot method.

CHAPTER VI
CLOSED-OPEN CONVERSION

The operational amplifier is an important circuit that plays a central role in analog circuits, and it is a high gain amplifier originally used in an analog electronic computer, and performs addition / subtraction, calculus, and other operations. With the progress of integrated circuit technology, operational amplifiers have also been integrated, and very high performance operational amplifiers have become available at low cost. By using an operational amplifier, various operational circuits including an amplifier circuit can be easily realized with high performance. Sometimes a simpler and better circuit is obtained than when individual components are used.

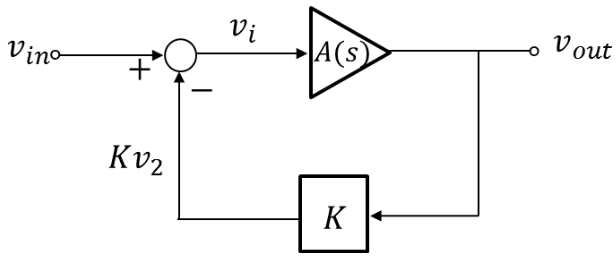

Fig. 6.1 Feedback control system

In this chapter we propose an idea to obtain the open loop characteristics by using corresponding closed loop results. We explain its principle and select operational amplifiers for verifying the proposed method, and compare with conventional method including LPF (Low pass filter) method and null double injection method. Our simulations have verified the effectiveness of the proposed method by comparison with the conventional methods. The proposed method can be accurate because the open loop gain around the frequency where phase and gain margins are evaluated would not be very high. When this method reveals that the phase margin is not sufficient for the designed operational amplifier, some parameter values are increased or decreased based on the results obtained by the Routh-Hurwitz method described in previous chapters so that its enough phase margin should be gained. In addition, we discuss the application of Nyquist plot for judging the stability which is not often used by circuit designer, including discussion on its advantages and disadvantages.

6.1 Closed loop characteristic locus in open loop Nyquist plot

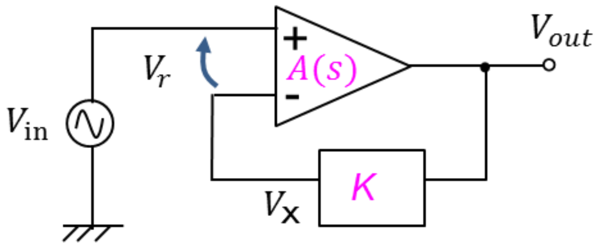

Fig. 6.2 Inverting operational amplifier

Examining the stability of operational amplifier circuits has been a concern since the negative feedback circuit was invented. In control theory, the system is stable if the poles of the closed-loop transfer function are all on the left plane of the complex plane. There are many difficulties when this stability criterion be applied to circuits, for example, knowing the positions of the poles and zeros is difficult because the questions of equivalent circuit and numerical calculation. As a method for practically dealing with this problem, the frequency characteristic of the transfer function is widely used. From the viewpoint of stability, the input signal V_{in} can be regarded as a disturbance factor of the loop, and the error signal V_r indicates the reverberation when it returns around the loop. The expression of error signal V_r is given by

$$V_r = \frac{1}{1+KA(s)} V_{\text{in}} \tag{6.1}$$

Since the coefficient $1 + KA(s)$ is an important factor indicating the quantitative relationship, let's call it a stability factor. Another problem when applying the stability theorem to circuits is that it is difficult to find the stability factor by simulation. Because the error signal V_r does not exist in practical circuit, Eq. (6.1) cannot be used. Also V_r can be obtained as a difference between the real signals V_{in} and V_{X}. However, in real circuits the input offset inevitably exists and generates an error.

We propose an idea to obtain the open loop characteristics $KA(s)$ with corresponding closed loop results and we call this operation as a closed-open conversion method. The reason why the closed-open conversion method has not been used so far is that the numerical error greatly affects the result because the gain of operational amplifier is large. Considering the feedback control system, and the transfer function of closed-loop is as follows:

$$\frac{V_{out}}{V_{in}} = W(s) = \frac{A(s)}{1+KA(s)} \tag{6.2}$$

By calculation we can obtain the transfer function of open loop:

$$A(s) = \frac{1}{1/\text{W(s)-K}} \tag{6.3}$$

As we know, the gain of opamp $|A(s)|$ is very large in the low frequency region, so $W(s) \approx 1/\text{K}$ in Eq. (6.2). Therefore, the resulting $A(s)$ will largely change with a small error in $W(s)$, since $1/W(s)$ is so close to K that the denominator of Eq. (6.3) becomes very small in magnitude. Simulations yield precision results even in the low-frequency region, however, this is not true for the measurement results, and this leads to the erroneous result for $A(s)$.This is why the closed-open conversion method has not been used, because the gain of the opamp is too large, especially for low frequencies.

However, which has an effect on stability is that the Nyquist diagram is close to the origin point, and at this moment, the gain is much smaller. In a portion on the Nyquist plot places where the gain is small, the numerical accuracy of the closed-open transformation increases, making the proposed closed-open conversion method practical, and it may be used for measurement results. The low frequency gain is almost independent of stability. As the operational amplifier gain decreases at high frequencies, it approaches the -1 point (Nyquist diagram). Around this point, the closed-loop gain is also small, so that it is easy to obtain the accuracy of mutual conversions.

An error signal can be obtained in a region where the stability is meaningful by using the actual signal of the operational amplifier.

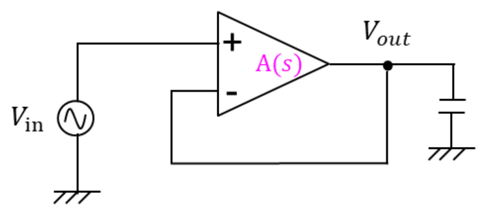

Fig. 6.3 Buffer configuration

This time, we select the unity gain buffer connection configuration (feedback factor is $K = 1$) as shown in Fig. 6.3 to introduce our proposed closed-open conversion method. The buffer connection is the easiest to see when looking at the open loop characteristics from the closed loop, and when the gain is 1, the system is most likely to be unstable. Generally, $KA(s)$ is used as the open loop characteristics, and is instead of $A(s)$ in this condition. The closed loop characteristics is as follows:

$$\frac{V_{out}}{V_{in}} = W(s) = \frac{A(s)}{1+KA(s)} \tag{6.4}$$

and by calculation, we can obtain the open loop characteristics:

$$A(s) = \frac{W(s)}{1-W(s)} \tag{6.5}$$

Since the transfer function depends on the load, discussion on the loop stability should be considered as a round transfer function including the load condition. $W(s)$ can be easily obtained by AC analysis. If AC analysis is performed with an actual load on the buffer, it is not necessary to change the load conditions for simulation.

Fig. 6.4 shows the Bode plot which is often used for judging the stability, and the frequency domain which is encircled by the green border. In this area, we can obtain the phase margin and gain margin to determine the stability [6].

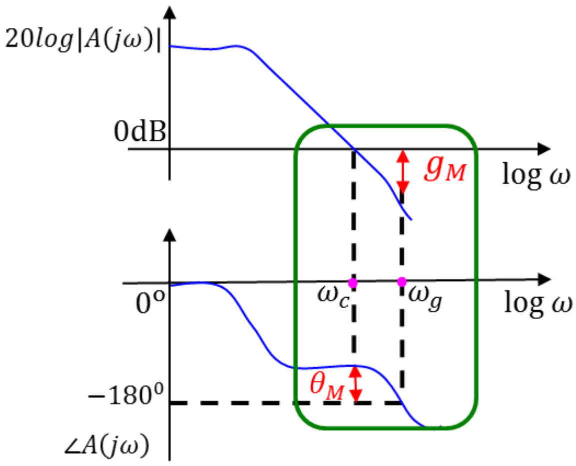

Fig. 6.4 Bode plot and effect area on stability

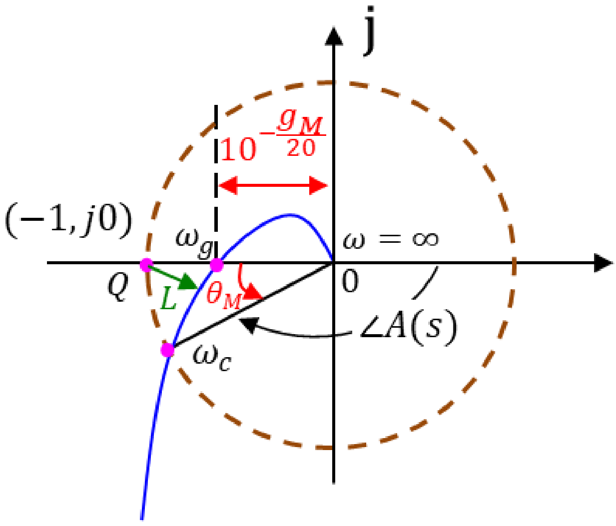

Fig. 6.5 Nyquist plot

Fig. 6.5 shows the Nyquist plot in the high frequency domain corresponding the green border area in Fig. 6.4. Stability is defined by characteristics at around the unit circle (brown broken line), where $|A(s)|$is small. Nyquist diagram also can show phase margin and gain margin, and minimum distance to -1 point is a better indicator to determine stability [14]. In order to introduce and verify this theory, we select one operational feedback amplifier whose configuration is as shown in Fig. 6.3 and the transfer function of the operational amplifier is given by

$$A(s) = \frac{10}{(1+s)(1+0.3s)(1+0.06s)} \tag{6.6}$$

Depict the Nyquist plot of open loop transfer function $KA(s)$ by using Mathematica software at different feedback factor conditions, as shown in Fig. 6.6. Fig. 6.7 shows the Bode plot of stability factor $1/(1+KA(s))$,

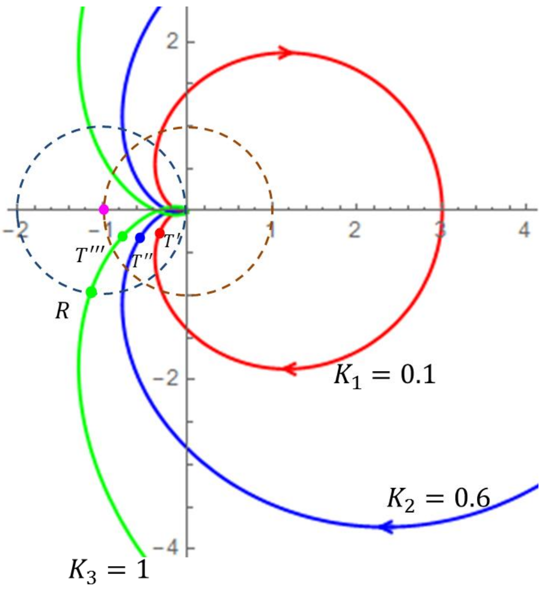

Fig. 6.6 Nyquist plots with different feedback factor K

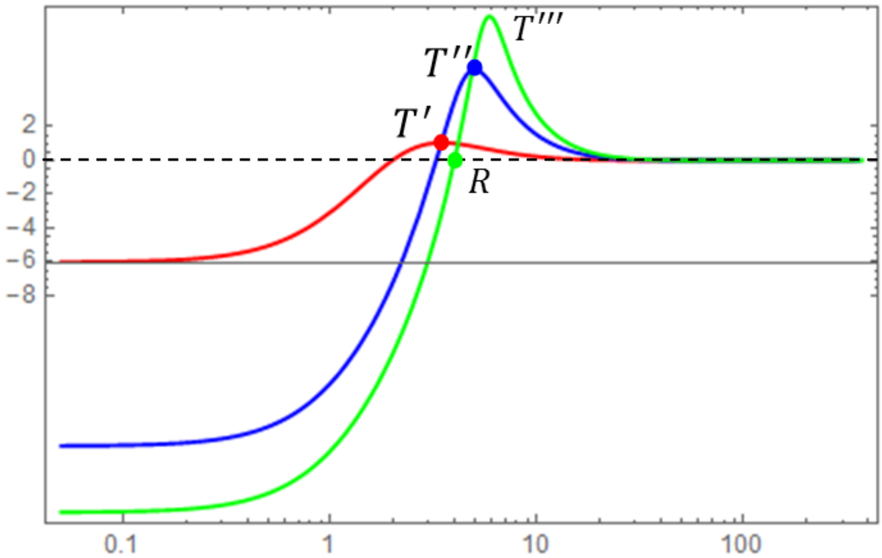

Fig. 6.7 Bode plot of stability factor $\mathbf{1/(1+KA(s))}$

By comparison of Fig. 6.6 and Fig. 6.7, we can find out that the closest points T', T'', T''' with the -1 point appear as peak in the Bode plot of the stability factor, and the magnitude is the reciprocal of the closest approach distance. The stability factor peak value is a direct stability index rather than a gain margin or a phase margin.

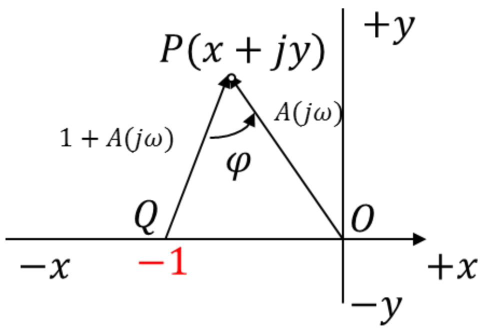

Fig. 6.8 Nyquist plane of open loop transfer function $\boldsymbol{A(j\omega)}$

Fig. 6.8 shows a complex plane where $A(j\omega)$ is represented and point P shows the Nyquist locus of the open loop transfer function. Also the length of vector OP indicates the absolute value of $A(j\omega)$, and the inclination angle indicates the phase angle of $A(j\omega)$. If we choose the point Q at $-1+j0$, the vector QP represents $1+A(j\omega)$. The closed loop transfer function is given by

$$W(j\omega) = \frac{A(j\omega)}{1+1*A(j\omega)} = \frac{\overrightarrow{OP}}{\overrightarrow{QP}} = Me^{j\varphi} \tag{6.7}$$

The squared of the length of $W(j\omega)$ is expressed by:

$$M^2 = \frac{|\overrightarrow{OP}|^2}{|\overrightarrow{QP}|^2} = \frac{x^2+y^2}{(x+1)^2+y^2} \tag{6.8}$$

By rearranging Eq. (6.8), we can obtain the trajectory equation of M as follows:

$$\{x + \frac{M^2}{M^2-1}\}^2 + y^2 = (\frac{M}{M^2-1})^2 \tag{6.9}$$

This is a circumference equation with a center at $(-M^2/(M^2-1)+j0)$ on the real with radius $M/(M^2-1)$. Fig. 6.9 shows a circle group of $M = const.$ with a solid line. The locus of $\varphi = const.$ is an arc passing through the origin O and the point Q. This is clear from the $\angle QPO = \varphi$ relation and the geometrical theorem that the circumference angle is constant [19].

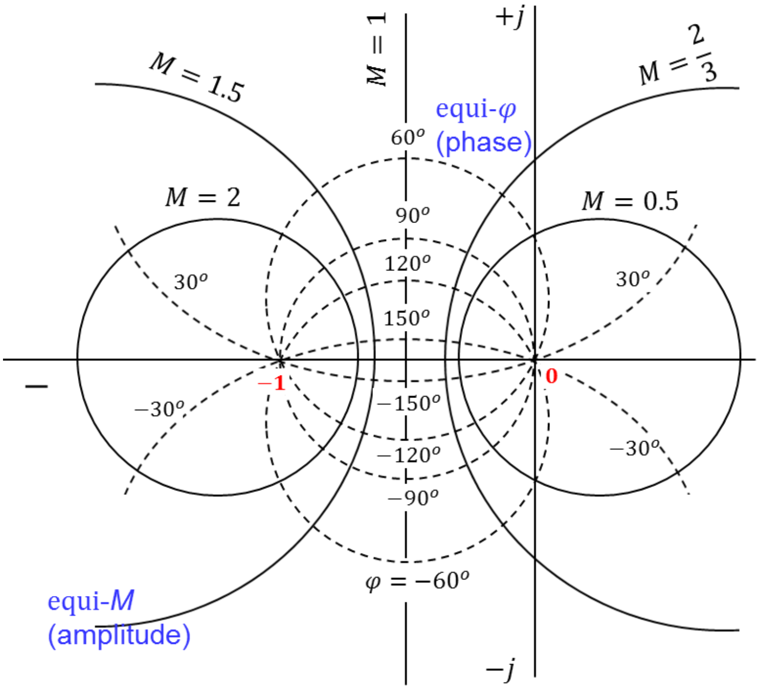

Fig. 6.9 Closed loop $\boldsymbol{M \cdot \varphi}$ locus in open loop Nyquist plot

By using different axes on the same complex plane, closed loop and open loop characteristics become a single plot. M trajectory and φ trajectory are orthogonal. Next, we will talk about why it is orthogonal. At first, consider the reciprocal of the closed-loop transfer function $W(j\omega)$ as follows:

$$\frac{1}{W(j\omega)} = 1 + \frac{1}{A(j\omega)} = \frac{1}{M} e^{-j\varphi} \tag{6.10}$$

When the angular frequency ω is changed from 0 to ∞, the vector locus of $1/A(j\omega)$ is drawn on the complex plane, which is an inverse Nyquist plot as shown in Fig. 6.10.

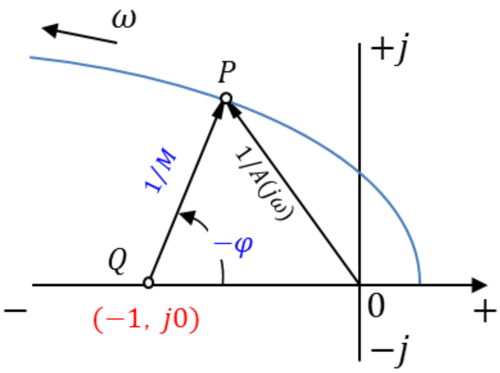

Fig. 6.10 Inversion Nyquist plane of open loop transfer function $\boldsymbol{A(j\omega)}$

Vector OP indicates $1 + A(j\omega)$. If a point with a distance of 1 from the original point is determined on the negative real axis, the vector QP is $1/(1 + A(j\omega))$, and its magnitude is equal to $1/M$, and its phase angle indicates $-\varphi$. If we draw the same circle centered at $(-1,\ j0)$ with radius of $1/M$, it will be a locus of points where $M = constant$. Also, as shown by the dotted line in the figure, when radiation with a tilt angle of $-\varphi$ is drawn from point Q, this is trajectory of $\varphi = constant$.

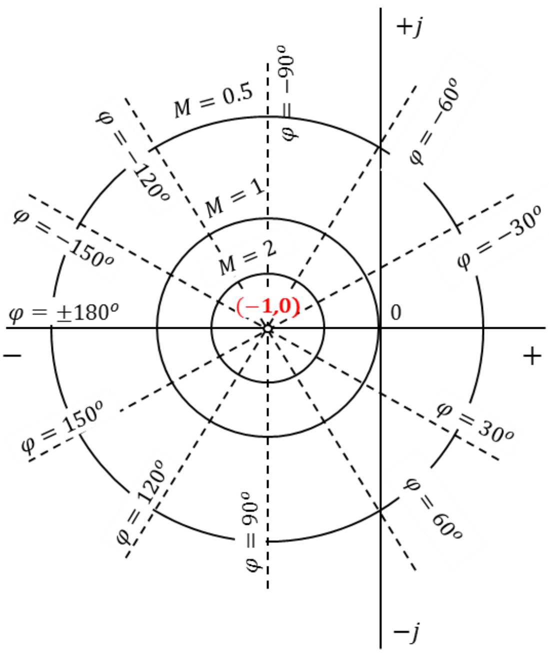

Fig. 6.11 Closed loop $\boldsymbol{M \cdot \varphi}$ locus in open loop inverse Nyquist plot

Obviously, the M locus and φ locus are orthogonal as show in Fig. 6.11.

The Nyquist plot and the inverse Nyquist plot are reciprocal relationship with each other. In the inverse Nyquist plot, $M = constant$ locus is a concentric circle, and the map which obtained by taking the inverse of this circle group is the M locus in the Nyquist plot. Since this locus is an inversion with respect to the origin of the circumference having the center on the real axis, it is also a group of circles having the center on the real axis. The $\varphi = constant$ locus is straight line on the inverse Nyquist plot, but the locus on the Nyquist diagram which is inversion with it, is represented by a circle group. The M locus and the φ locus are orthogonal to each other on the inverse Nyquist plot, so the two locus are also orthogonal to each other on the Nyquist plot, which is an equiangular map.

6.2 Verification and comparison

Conventional low pass filter (LPF) method is often used for checking the open loop characteristics by inserting a LPF with a very low cutoff frequency into the feedback circuit to ensure the DC operating point, the circuit diagram as shown in Fig. 6.12(b). About the LPF method there are two disadvantages: first one is that we need to replace the feedback section with another circuits; this operation is inescapable influence simulation result. Another disadvantage is that we need to measure the transfer characteristics from the positive input due to the loop has been disconnected, but which affects the stability is the transfer characteristic from the negative input.

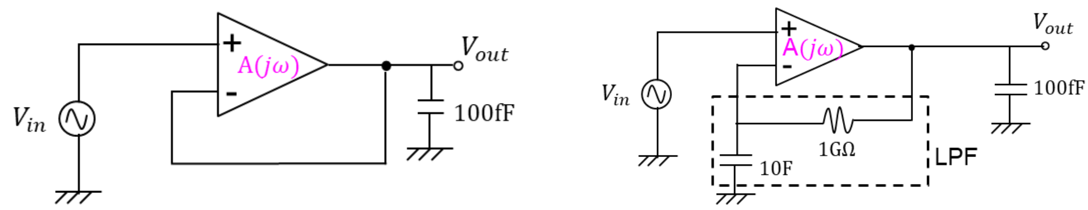

(a) Proposed method (b) LPF method

Fig. 6.12 Closed loop system circuits

The internal circuit of the operational amplifier is as shown in Fig. 6.13[10], and the values of bias voltage V_{bias1} and V_{bias2} are 546.88mV and 366.99mV respectively. At the process of the proposed method, we run the circuit with LTspice and read the output file (text editor) in which the closed loop characteristics are written in a format like {frequency, real part, imaginary part}. Using these data, we can calculate and get open loop characteristics by Eq. (6.5). We also depict the plot using the data from the LPF method for comparison with the proposed method at one same graph.

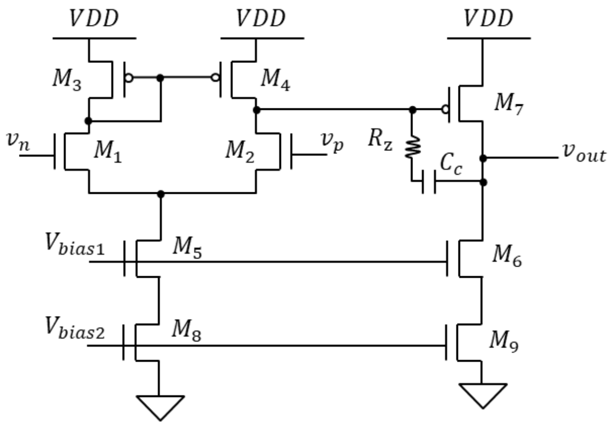

Fig. 6.13 Internal circuit of the opamp

Using the obtained data of the open loop characteristics, we can depict the Bode plot of the open loop transfer function $A(j\omega)$ as the blue line shown in Fig. 6.14. The red line shown in Fig. 6.14 is the simulation result from the LPF method. We also depict the Nyquist plot using the data from two methods as shown in Fig. 6.15, and we can see that two results are consistent.

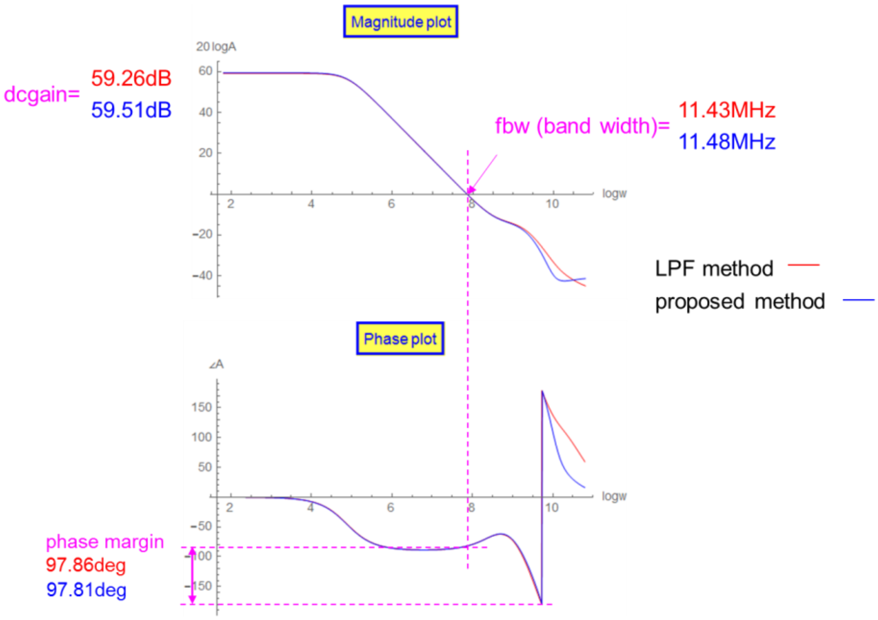

Fig. 6.14 Bode plot of open loop transfer function

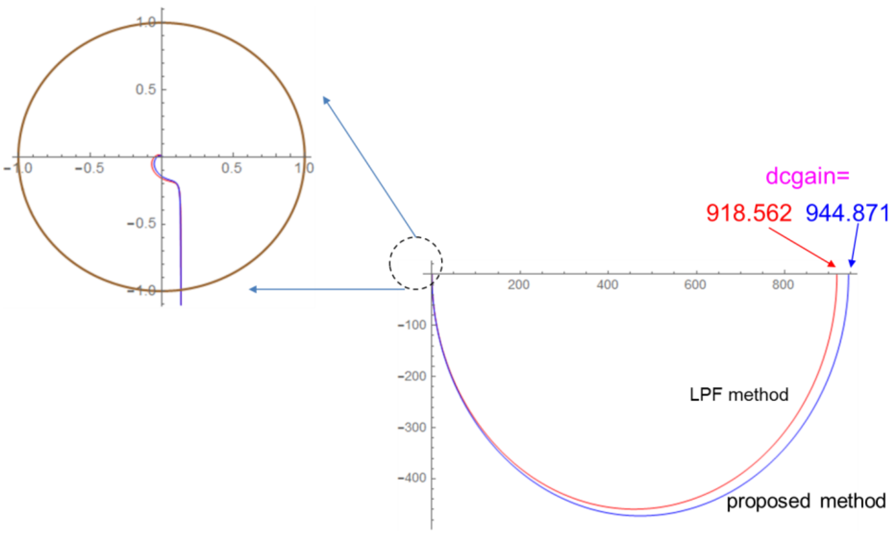

Fig. 6.15 Nyquist plot of open loop transfer function

In the high frequency domain, especially around the unit circle, the simulation results are consistent. In the low frequency region, the difference of DC gain is caused by the difference of operation point.

We also have performed simulations by using "Null double injection" method taken from an article by R. D. Middlebrook, and the circuit is shown in Fig. 6.16 [24]. The loop gain is equivalent to the following:

$$G_v = \frac{v_f}{v_i}, \qquad G_i = \frac{i_f}{i_i} \tag{6.11}$$

Here v_f and i_f denote the feedback signals, while v_i and i_i are the input. G_v is the open loop voltage gain, and G_i is the open loop current gain, and they are related through the following equation:

$$G + 1 = (G_v + 1)||(G_i + 1)$$

$$G = \frac{G_i * G_v - 1}{G_i + G_v + 2} \tag{6.12}$$

As shown in Fig. 6.16(a), we inject two batteries and the independent current source I_1 for measuring the open loop gain. The current source is defined as 'AC 1' so that it will provide a 1A small signal current in the AC analysis. The two batteries are used to measure the current in each direction. They are given a voltage of 0 so that they don't affect simulation results. The battery V_2 measures the current i_i and the battery V_1 measures the current i_f. We inject two batteries and the independent voltage source V_5 for measuring the open loop gain as shown in Fig. 6.16(b). The voltage source is defined as 'AC 1' so that it will provide a 1V small signal voltage in the AC analysis. The batteries are again given a voltage of 0, not to affect the simulation. The circuits need to be analyzed at the same time in order to produce the total gain as the total gain relies on both the open loop current gain and the open loop voltage gain.

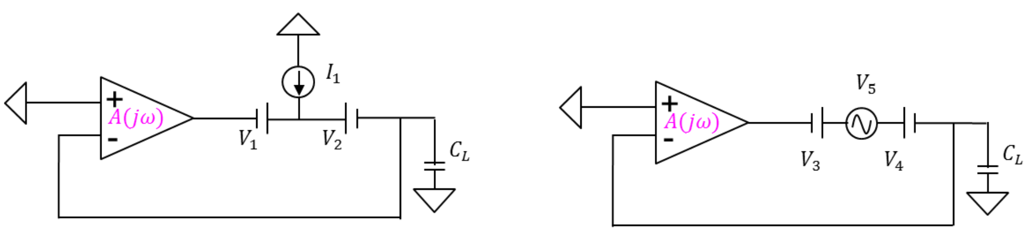

(a) Measurement of current gain (b) Measurement of voltage gain

Fig. 6.16 Null double injection method

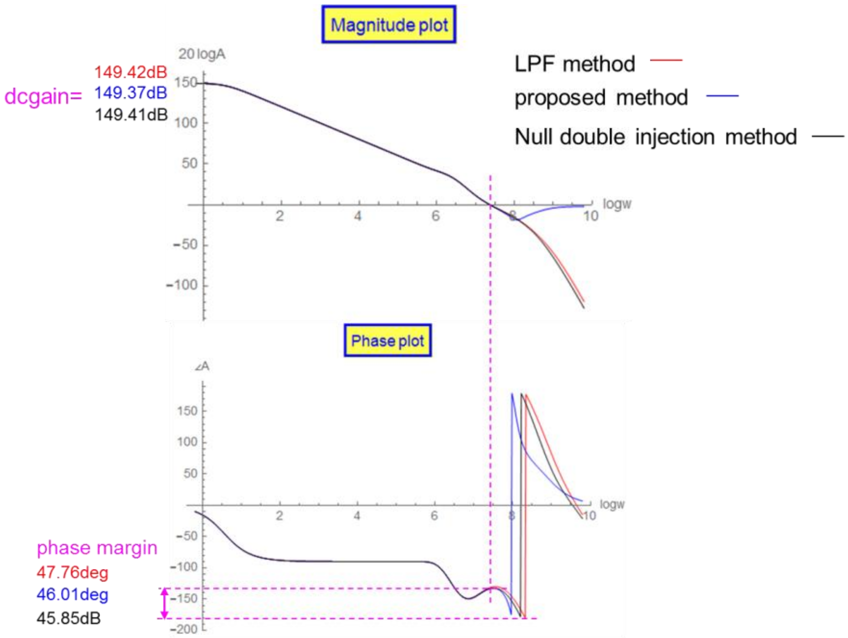

Fig. 6.17 Bode plot of open loop transfer function

We select an LT1128 amplifier, perform its simulations and compare the three simulation results. We depict the Bode plot and Nyquist plot using the data from the proposed method, and traditional method include LPF method and null double injection method for comparison at one same graph as shown in Fig. 6.17 and Fig. 6.18.

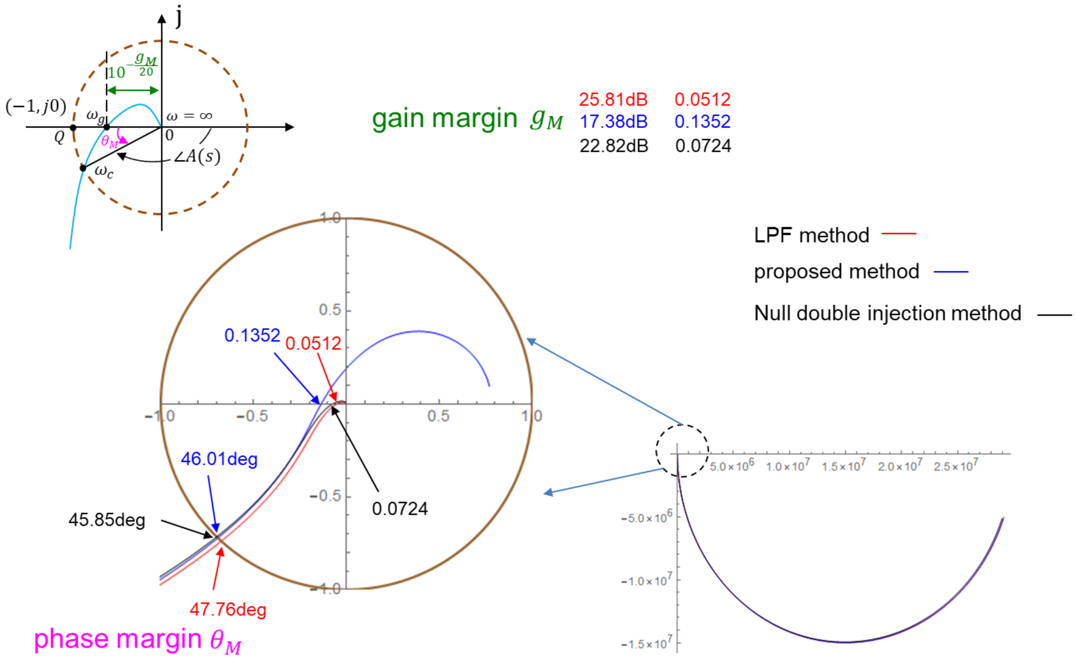

Fig. 6.18 Nyquist plot of the open loop transfer function

By comparison, we can find out that the proposed method can be used for obtaining the open loop characteristics from the closed loop measurement. In the low frequency region, the simulation results are consistent. But in the high frequency domain, especially around the unit circle, the simulation results are not consistent. The LPF method need to open up the loop, and that the DC bias point of the circuit will be altered. Since the circuit is linearized around the DC bias point in AC analysis, this will influence the simulation results. Considering the proposed and null double injection methods which can both make measurement without opening up the loop, the proposal approach is simpler and less time-consuming.

6.3 Summary

In this chapter, we have tried the closed-open conversion method for obtain the open loop characteristics (opamp stability etc.) from closed loop operation results. The effectiveness of this method was demonstrated by practical example. Since the traditional LPF method need to open up the loop, this will influence the simulation results. The null double injection method also does not need opening up the loop although, but compared with the proposed method, the later one is simpler and less time-consuming.

CHAPTER VII
DISCUSSION

7.1 Discussion

In this dissertation, our work can be divided into two parts: application of R-H stability criterion in judging the stability of operational amplifier, and one try of closed-open conversion method that to obtaining open loop characteristics. The former is the main body of this article, we used Chapter 3 and Chapter 4 for introductory principle and simulation respectively. And we talk about the closed-open conversion method in Chapter 5 including principle and simulation result.

According to the above consideration, we have proposed the following for operational amplifier stability analysis and design

- Depict a small signal equivalent circuit for the operational amplifier circuit in open-loop structure.
- Derive its open-loop transfer function.
- Derive its closed-loop transfer function and obtain its characteristic equation.
- Apply the R-H stability criterion and obtain the relation function between the R-H parameter with phase margin. (which is not easy to obtain with Bode plot)
- Then use this relation function for circuit parameters.

The R-H method would be effective especially for multi-stage operational amplifiers (high-order systems).

It may be true that one might ponder the derivation of precise explicit transfer function with polynomials of S is difficult due to many parasitic components in the operational amplifier circuit. However, even if the derived equivalent circuit or transfer function uses only major components and neglects parasitic components, the R-H method provides the information whose major parameter values should be increased or decreased for stability.

Since the coefficients of Routh table are polynomials, the parameter value modification processing would be complicated. Then we can only modify one dominant parameter whereas the other parameters are fixed each time and observe the change of stability brought by the modification.

The R-H method can judge with simple calculation for given parameter values whether the operational amplifier circuit with feedback configuration is stable or not, but it cannot obtain gain and phase margins directly. On the other hand, Bode plot can obtain them. Then the usage of the proposed method together with the Bode plot would be more effective.

Regarding to the closed-open conversion method, although cluster theory analysis shows that our method is feasible, and our simulation also has good results, however there are only slight difference between traditional method and proposed method on the details. Analyzing and finding out what causes these differences is what we should be doing.

7.2 Future work

Although we have achieved good simulation results, there is still a long way to go before it can be well applied to the actual circuit design, and there are still many difficulties to be overcome, as well as many areas to be improved and considered. Validation in more examples and application in real circuits is the next step we want to take. We hope that this method will be familiar and used by more circuit designers, researchers from enterprises, schools and other research institutions. We also want to provide an easy-to-use tool to obtain the open loop characteristics from the closed loop operation results as our target.

CHAPTER VIII
CONCLUSION

This dissertation proposes a stability analysis and design method for the operational amplifier feedback circuit based on the equivalent small signal circuit model of the operational amplifier and the Routh-Hurwitz stability criterion. We summarize our work as the following aspects:

- In terms of innovation.

This proposed method can lead to obtain explicit stability conditions for operational amplifier circuit parameters that have not been described in any operational design book/paper, to the best of our knowledge.

- In the theoretical proof.

We have shown the equivalence between Nyquist and Routh-Hurwitz stability criteria for analysis and design of the operational amplifier stability under some conditions, and have deduced the relationship between Routh-Hurwitz stability criterion parameters with phase margin of the operational amplifier. We have shown that they are monotonic relationship.

- In the verification and simulation parts.

We have confirmed with SPICE simulation that this method is equivalent to the Bode plot method, and satisfactory results have been obtained with LTspice simulations at transistor level circuit. Also the acquisition and application of the relationship between R-H stability criterion parameters with phase margin demonstrate the feasibility of the proposed method on both sides of theory and practice.

- In comparison with the conventional method.

Compared to the conventional Bode plot method which only can judge the stability qualitatively, the proposed method not only can judge the stability but also can further perform quantitative analysis; this clarifies which circuit parameters influence the operational amplifier stability, and we know whether these circuit parameters should be increased or decreased. The R-H method has an advantage of being able to obtain explicit stability condition for circuit parameters; hence the R-H method can be practically used together with the Bode plot method.

- Supplement method.

In the later part of this dissertation, an additional method is proposed to obtain the open loop characteristics directly without opening up the loop and not need to insert any extra circuit element. Our simulation results show the practical usage feasibility of this proposed closed-open conversion method. When this method reveals that the phase margin is not sufficient for the designed operational amplifier, some parameter values are increased or decreased based on the results obtained by the above-mentioned Routh-Hurwitz method so that its enough phase margin should be gained.

PERFERENCES

[1] J. Wang, G. Adhikari, H. Kobayashi, N. Tsukiji, M. Hirano, K. Kurihara, A. Nagahama, I. Noda, K. Yoshii, "Analysis and Design of Operational Amplifier Stability Based on Routh-Hurwitz Method", IEEE 13th International Conference on Solid-State and Integrated Circuit Technology, Hangzhou, China (Oct. 2016).

[2] J. Wang, G. Adhikari, H. Kobayashi, N. Tsukiji, M. Hirano, K. Kurihara, A. Nagahama, I. Noda, K. Yoshii, "Analysis and Design of Operational Amplifier Stability Based on Routh-Hurwitz Method", IEEJ Technical Meeting on Electronic Circuits, ECT-16-025, Tokyo (March 2016).

[3] J. Wang, G. Adhikari, N. Tsukiji, M. Hirano, H. Kobayashi, K. Kurihara, A. Nagahama, I. Noda, K. Yoshii, "Equivalence Between Nyquist and Routh-Hurwitz Stability Criteria for Operational Amplifier Design", IEEE International Symposium on Intelligent Signal Processing and Communication Systems (ISPACS), Xiamen, China (Nov. 2017).

[4] J. Wang, G. Adhikari, H. Kobayashi, N. Tsukiji, M. Hirano, K. Kurihara, A. Nagahama, I. Noda, K. Yoshii, "Equivalence Between Nyquist and Routh-Hurwitz Stability Criteria for Operational Amplifier Design", IEEJ Technical Meeting on Electronic Circuits, ECT-17-403, Tokyo (March 2017).

[5] G. Palumbo, S. Pennisi, Feedback Amplifiers Theory and Design, Springer Science + Business Media New York (2002).

[6] B. Razavi, Design of Analog CMOS Integrated Circuits, McGraw-Hill (2003).

[7] P. Gray, P. J. Hurst, S. Lewis, R. G. Meyer, Analysis and Design of Analog Integrated Circuits, 4th Edition, John Wiley & Sons, Inc. (2001).

[8] D. A. Johns, K. Martin, Analog Integrated Circuit Design, John Wiley & Sons (1997).

[9] J. H. Huijsing, Operational Amplifiers – Theory and Design, Kluwer Academic Publishers (2001).

[10] R. J. Baker, CMOS Circuit Design, Layout and Simulation, 3rd edition, IEEE Series on Microelectronic Systems, IEEE Press (2010).

[11] F. Maloberti, Analog Design for CMOS VLSI Systems, Kluwer Academic Publishers (2001).

[12] A. S. Sedra, K. C. Smith, Microelectronic Circuits, 4th Edition, Oxford University Press (1998)

[13] H. S. Saeed, Automatic Control Systems, pp. 206-207, Delhi Katson Publishers. (2008).

[14] Y. Gendai, “OPAMP Stability Design Using Nyquist Plot”, IEEJ Technical Meeting on Electronic Circuits, ECT-15-046, Yokosuka, Japan (July 2015).

[15] S. S. Hakim, Feedback Circuit Analysis, New York: Wiley, 1966.

[16] H. Kobayashi, J. Wei, M. Murakami, J. Kojima , N. Kushita, Y. Du, J. Wang “Performance Improvement of Delta-Sigma ADC/DAC/TDC Using Digital Technique”, IEEE 14th International Conference on Solid-State and Integrated Circuit Technology, Qingdao, China (Nov. 2018)

[17] Korn, G. A.; Korn, T. M. (1967), Mathematical Handbook for Scientists and Engineers (2nd ed.), McGraw-Hill Companies, ISBN 978-0-07-035370-1

[18] https://en.wikipedia.org/wiki/Laplace_transform#CITEREFKornKorn1967

[19] 福島弘毅「制御工学基礎論」電子・通信・電気工学基礎講座

[20] H. W. Bode, Network Analysis and Feedback Amplifier Design, New York: Van Nostrand, 1945.

[21] S. Rosenstark, Feedback Amplifier Principles, New York: MacMillan, 1986.

[22] R. D. Middlebrook, "The general feedback theorem: a final solution for feedback systems," in IEEE Microwave Magazine, vol. 7, no. 2, pp. 50-63, April 2006. doi: 10.1109/MMW.2006.1634022

[23] S. Rosenstark, "Loop gain measurement in feedback amplifiers", Int. J. Electron., vol. 57, pp. 415-421, 1984.

[24] R. D. Middlebrook, "Measurement of loop gain in feedback systems", Int. J. Electron., vol. 38, pp. 485-512, 1975.

[25] https://en.wikipedia.org/wiki/Laplace_transform#CITEREFKornKorn1967

[26] CMOS Analog Circuit Design Second Edition, Phillip E.Allen, Douglas R.Holberg

[27] The Design of CMOS Radio-Frequency Integrated Circuits, Thomas H. Lee

[28] R. D. MIDDLEBROOK, "Measurement of loop gain in feedback systems," Pages 485-512 | Received 23 Sep 1974, Published online: 23 Feb 2007

[29] R. D. Middlebrook, “Design-Oriented Analysis of Feedback Amplifiers,” Proceedings National Electronics Conference, vol. XX, October 1964, pp. 234-238.

[30] M. A. B. Mohd Yusof , N. Tsukiji, Y. Kobori, A.Kuwana, H. Kobayashi,"A Study on Loop Gain Measurement Method Using Output Impedances in Operational Amplifier", Journal of Technology and Social Science, Vol.2, No.3, pp.19-28 (Nov. 2018)

[31] N. Tsukiji, Y. Kobori, H. Kobayashi,"A Study on Loop Gain Measurement Method Using Output Impedance in DC-DC Buck Converter ",IEICE Trans. Communications, Vol.E101-B,No.9,pp.1940-1948 (Sep. 2018).

[32] P.J. Hurst, "Exact simulation of feedback circuit parameters," pp.1382 – 1389, Nov 1991 ISAN: 4084099, DOI: 10.1109/31.99170, IEEE

[33] M. Tian, V. Visvanathan, J. Hantgan, K. Kundert, "Striving for small-signal stability," pp. 31 - 41 ISAN: 6842801 DOI: 10.1109/101.900125 Publisher: IEEE

[34] J. Wang, Y. Gendai, A. Kuwana, H. Kobayashi (Gunma Univ.) "Obtaining Gain- and Phase-Margin from Closed Loop Measurement of OPamps International Conference on Mechanical, Electrical and Medical Intelligent System 2019 (ICMEMIS2019), Kiryu, Japan (Dec 4-6, 2019)

PUBLICATIONS

JournalPapers

[1] **Jianlong Wang**, Gopal Adhikari, Nobukazu Tsukiji, Haruo Kobayashi, “Analysis and Design of Operational Amplifier Stability Based on Routh-Hurwitz Stability Criterion”,電気学会論文誌（和文誌 C), vol. 138, no. 12, pp.1517-1528 (2018 年 12 月)

[2] **JianLong Wang**, Gopal Adhikari, Haruo Kobayashi, Nobukazu Tsukiji, Mayu Hirano, Keita Kurihara, Akihito Nagahama, Ippei Noda, Kohji Yoshii, "Analysis and Design of Operational Amplifier Stability Using Routh-Hurwitz Stability Criterion", Means and Methods for Measurement and Monitoring, Supplement Book to Advanced Micro-Device Engineering VIII, Applied Mechanics and Materials, vol. 888, pp.1-10 (2019) ISBN: 976-3-0357-1553-8

International Conference Papers

[1] **JianLong Wang**, Gopal Adhikari, Haruo Kobayashi, Nobukazu Tsukiji, Mayu Hirano, Keita Kurihara, Akihito Nagahama, Ippei Noda, Kohji Yoshii, "Analysis and Design of Operational Amplifier Stability Based on Routh-Hurwitz Method," IEEE 13th International Conference on Solid-State and Integrated Circuit Technology, Hangzhou, China (Oct 26, 2016).

[2] **JianLong Wang**, Gopal Adhikari, Nobukazu Tsukiji, Mayu Hirano, Haruo Kobayashi, Keita Kurihara, Akihito Nagahama, Ippei Noda, Kohji Yoshii, “Equivalence Between Nyquist and Routh-Hurwitz Stability Criteria for Operational Amplifier Design,” IEEE International Symposium on Intelligent Signal Processing and Communication Systems (ISPACS), Xiamen, China (Nov. 6-9, 2017).

[3] (Invited) Haruo Kobayashi, Jiang-Lin Wei, Masahiro Murakami, Jun-ya Kojima, Nene Kushita, Yuanyang Du, **Jianlong Wang**, “Performance Improvement of Delta-Sigma ADC/DAC/TDC Using Digital Technique”, IEEE 14th International

Conference on Solid-State and Integrated Circuit Technology, Qingdao, China (Nov. 2018)

[4] **JianLong Wang**, Nobukazu Tsukiji, Haruo Kobayashi, "Design of Operational Amplifier Phase Margin Using Routh-Hurwitz Method", 2nd ICMEMIS, Kiryu, Japan (Nov. 2018) (Award)

[5] **Jianlong Wang**, Gopal Adhikari, Nobukazu Tsukiji, Haruo Kobayashi," Analysis and Design of Operational Amplifier Stability Based on Control Theory" 5th GUMI ＆9th MADE International Symposium of Gunma University Medical Innovation and 9th International Conference on Advanced Micro-Device Engineering, Kiryu City Performing Art Center, Japan (Dec. 2018)

[6] Yuto Sasaki, Kosuke Machida, Riho Aoki, Shogo Katayama, Takayuki Nakatani, **Jianlong Wang**, Keno Sato, Takashi Ishida, Toshiyuki Okamoto, Tamotsu Ichikawa, Anna Kuwana, Kazumi Hatayama and Haruo Kobayashi, "Accurate and Fast Testing Technique of Operational Amplifier DC Offset Voltage in μV-order by DC-AC Conversion",3rd International Test Conference in Asia, Tokyo (Sept. 2019).

[7] Riho Aoki, Shogo Katayama, Yuto Sasaki, Kosuke Machida, Takayuki Nakatani, **Jianlong Wang**, Anna Kuwana, Kazumi Hatayama, Haruo Kobayashi, Keno Sato, Takashi Ishida, Toshiyuki Okamoto, Tamotsu Ichikawa, "Simulation Evaluation of Null Method for Operational Amplifier Testing", 3rd International Conference on Technology and Social Science (ICTSS2019) , Kiryu, Japan (8-10 May, 2019)

[8] Shogo Katayama, Riho Aoki, Yuto Sasaki, Kosuke Machida, Takayuki Nakatani, **Jianlong Wang**, Anna Kuwana, Kazumi Hatayama, Haruo Kobayashi, Keno Sato, Takashi Ishida, Toshiyuki Okamoto, Tamotsu Ichikawa, "Experimental Evaluation of Null Method and DC-AC Conversion for Operational Amplifier Testing"3rd International Conference on Technology and Social Science (ICTSS2019) , Kiryu, Japan (8-10 May, 2019)

[9] **Jianlong Wang**, Yuji Gendai, Anna Kuwana, Haruo Kobayashi (Gunma Univ.)"An Idea to Obtain the Open Loop Characteristics of Opamp by Closed Loop Result"5th Taiwan and Japan Conference on Circuits and Systems (TJCAS 2019 at Nikko) ,Nikko, Tochigi, Japan, August 19-21, 2019

[10] Riho Aoki, Shogo Katayama, Yuto Sasaki, Kosuke Machida, Takayuki Nakatani, **Jianlong Wang**, Anna Kuwana, Kazumi Hatayama, Haruo Kobayashi (Gunma Univ.),Keno Sato, Takashi Ishida, Toshiyuki Okamoto, Tamotsu Ichikawa (ROHM Semiconductor Co., Ltd.)"Accurate and Fast Testing of Operational Amplifier with NULL Method"5th Taiwan and Japan Conference on Circuits and Systems (TJCAS 2019 at Nikko), Nikko, Tochigi, Japan, August 19-21, 2019

[11] Yuto Sasaki, Kosuke Machida, Riho Aoki, Shogo Katayama, Takayuki Nakatani, **Jianlong Wang** (Gunma Univ.),Keno Sato, Takashi Ishida, Toshiyuki Okamoto, Tamotsu Ichikawa (ROHM Semiconductor), Anna Kuwana, Kazumi Hatayama, Haruo Kobayashi (Gunma Univ.), "Very Low Level DC Voltage Measurement Technique by DC-AC Conversion", Best Student Paper Award,5th Taiwan and Japan Conference on Circuits and Systems (TJCAS 2019 at Nikko) ,Nikko, Tochigi, Japan, (August 19-21, 2019).

[12] Riho Aoki, Shogo Katayama, Yuto Sasaki, Kosuke Machida, Takayuki Nakatani, **Jianlong Wang**, Anna Kuwana, Kazumi Hatayama, Haruo Kobayashi, Keno Sato, Takashi Ishida, Toshiyuki Okamoto, Tamotsu Ichikawa, "Evaluation of Null Method for Operational Amplifier Short-Time Testing", 2019 13th IEEE International Conference on ASIC (ASICON 2019),Chongqing, China (Oct. 29-Nov. 1, 2019)

[13] (Invited Paper) **Jianlong Wang**, Yuji Gendai, Anna Kuwana, Haruo Kobayashi (Gunma Univ.) "Obtaining Gain- and Phase-Margin from Closed Loop Measurement of OPamps", International Conference on Mechanical, Electrical and Medical Intelligent System 2019 (ICMEMIS2019), Kiryu, Japan (Dec 4-6, 2019) (Best Presentation Award)

Domestic Papers

[1] **王 建龍**、Adhikari Gopal、小林 春夫、 築地 伸和、平野 繭、栗原 圭汰、長浜 顕仁、野田 一平、吉井 宏治 “Analysis and Design of Operational Amplifier Stability Based on Routh-Hurwitz Method”,電気学会　電子回路研究会, ECT-16-025, 東京都市大学 (2016 年 3 月 7 日).

[2] **王建龍**、Gopal Adhikari、小林春夫「制御理論のオペアンプ安定性設計・解析への応用」 第 63 回システム LSI 合同ゼミ、中央大学（2016 年 6 月 25 日)

[3] **JianLong Wang**, Gopal Adhikari, Nobukazu Tsukiji, Mayu Hirano, Haruo Kobayashi,Keita Kurihara, Akihito Nagahama, Ippei Noda, Kohji Yoshii, 「Equivalence Between Nyquist and Routh-Hurwitz Stability Criteria for Operational Amplifier Design」電気学会　電子回路研究会, 法政大学、東京 (2017 年 3 月 9, 10 日).

[4] **王建龍**、Gopal　Adhikari，築地伸和，平野繭，小林春夫，栗原圭汰，長浜顕仁，野田一平，吉井宏治「Design and Analysis of Operational Amplifier Stability Based on Control Theory」 LSI とシステムのワークショップ 2017, ポスターセッション、東京　(2017 年 5 月 15 日)

[5] **JianLong Wang**, Nobukazu Tsukiji, Haruo Kobayashi「Design of Operational

Amplifier Stability and Phase Margin Using Routh-Hurwitz Method」第８回 電気学会東京支部栃木・群馬支所 合同研究発表会 ETG-18-50, ETT18-50 小山高専（2019 年３月４日, ５日）
[6] 青木里穂, 片山翔吾, 佐々木優斗, 町田恒介, 中谷隆之, **王建龍**, 桑名杏奈, 畠山一実, 小林春夫, 佐藤賢央, 石田嵩, 岡本智之, 市川保「オペアンプ試験技術 Null 法のシミュレーション評価」第 9 回 電気学会東京支部栃木・群馬支所 合同研究発表会 ETG-19-22, ETT-19-22, 小山高専 (2019 年３月４日, ５日)
[7] 片山 翔吾, 青木 里穂, 佐々木 優斗, 町田 恒介, 中谷 隆之, **王 建龍**, 桑名 杏奈, 畠山 一実, 小林 春夫, 佐藤 賢央, 石田 嵩, 岡本 智之, 市川 保「オペアンプ試験技術 Null 法の実験評価」第 9 回 電気学会東京支部栃木・群馬支所 合同研究発表会 ETG-19-41, ETT-19-41 小山高専（2019 年３月４日, ５日）
[8] 町田 恒介 、佐々木 優斗 、中谷 隆之 、佐藤 賢央、石田 嵩 、岡本 智之、市川 保、 **王 建龍** 、桑名 杏奈 、畠山 一実 、小林 春夫、「DC-AC 変換による低レベル DC 電圧測定技術」電気学会 電子回路研究会、東京、(2018 年 12 月）
[9] **JianLong Wang**, Nobukazu Tsukiji, Haruo Kobayashi「Design of Operational Amplifier Stability and Phase Margin Using Routh-Hurwitz Method」第８回 電気学会東京支部栃木・群馬支所 合同研究発表会 ETG-18-50, ETT18-50 於 群馬大学 2018 年 3 月１日（木), 3 月２日（金）
[10] 荻原岳, 片山翔吾, 青木里穂, 中谷隆之, 佐藤賢央, 石田嵩, 岡本智之, 市川保 , **王建龍**, 桑名杏奈, 畠山一実, 小林春夫 「オペアンプ AC 特性の FFT 法による高速試験」電気学会 電子回路研究会, ECT-019-116, 日本大学 理工学部 駿河台校舎タワー・スコラ (2019 年 12 月 19 日）

Awards

[1] Best Presentation Award: International Conference on Mechanical, Electrical and Medical Intelligent System 2018 (ICMEMIS2018), Kiryu, Japan (Nov 4-6. 2018)
[2] Best Presentation Award: International Conference on Mechanical, Electrical and Medical Intelligent System 2019 (ICMEMIS2019), Kiryu, Japan (Dec 4-6, 2019)

APPENDIX

Table I Short-channel COMS parameters

Parameter	NMOS	PMOS
r_{on}, r_{op}	167kΩ	333kΩ
$g_{m\mathrm{n}}$, g_{mp}	150μA/V	150μA/V
C_{gdn}, $C_{\mathrm{gd}p}$	1.56fF	3.7fF
$C_{\mathrm{gs}n}$, $C_{\mathrm{gs}p}$	4.17fF	8.34fF
C_{oxn}, $C_{\mathrm{ox}p}$	6.25fF	12.5fF
W/L	50/2	100/2
V_{GS}, V_{SG}	350mV	350mV
V_{THN}, V_{THP}	280mV	280mV
$V_{DD} = 1V$	Scale Factor=50nm	

(Source from "CMOS Circuit Design, Layout, and Simulation" 3rd Edition, R.JACOB BARKER)

Table II small signal equivalent circuit parameters

$R_1 = r_{on} \vert\vert r_{op} = 111k\Omega$
$R_2 = r_{op} \vert\vert R_{ocasn} \approx r_{op} = 333k\Omega$
$G_{m1} = g_{mn} = 150\, uA/V$
$G_{m2} = g_{mp} = 150\, uA/V$
$C_1 = C_{dg4} + C_{dg2} + C_{gs7} = 13.6fF$
$C_2 = C_L + C_{gd8} \approx C_L + 1.56fF = 101.56fF$ $(C_L = 100fF)$